TRANSPORTATION RESEARCH

RECORD

No. 1348

Pavement Design, Management, and Performance

Pavement Surface Properties: Roughness, Rutting, Skid Resistance, and Surface Distress

A peer-reviewed publication of the Transportation Research Board

TRANSPORTATION RESEARCH BOARD
NATIONAL RESEARCH COUNCIL

NATIONAL ACADEMY PRESS
WASHINGTON, D.C. 1992

Transportation Research Record 1348
Price: $20.00

Subscriber Category
IIB pavement design, management, and performance

TRB Publications Staff
Director of Publications: Nancy A. Ackerman
Senior Editor: Naomi C. Kassabian
Associate Editor: Alison G. Tobias
Assistant Editors: Luanne Crayton, Susan E. Gober, Norman Solomon
Office Manager: Phyllis D. Barber
Production Assistant: Betty L. Hawkins

Printed in the United States of America

Library of Congress Cataloging-in-Publication Data
National Research Council. Transportation Research Board.

Pavement surface properties : roughness, rutting, skid resistance, and surface distress.
p. cm. — (Transportation research record, ISSN 0361-1981 ; 1348)
ISBN 0-309-05210-6
1. Pavements—Testing. 2. Pavements—Skid resistance. 3. Automobiles—Tires. 4. Profilometer. I. Series.
TE7.H5 no. 1348
[TE250]
388 s—dc20 92-25095
[625.8] CIP

Sponsorship of Transportation Research Record 1348

GROUP 2—DESIGN AND CONSTRUCTION OF TRANSPORTATION FACILITIES
Chairman: Charles T. Edson, New Jersey Department of Transportation

Pavement Management Section
Chairman: Joe P. Mahoney, University of Washington

Committee on Pavement Monitoring, Evaluation, and Data Storage
Chairman: Freddy L. Roberts, Louisiana Tech University
Secretary: Don H. Kobi, Paris, Ontario, Canada
A. T. Bergan, Frank V. Botelho, Billy G. Connor, Brian E. Cox, Jerome F. Daleiden, Wade L. Gramling, Jerry J. Hajek, Amir N. Hanna, Andris A. Jumikis, Scott A. Kutz, Kenneth J. Law, W. N. Lofroos, Kenneth H. McGhee, Amy L. Mueller, Edwin C. Novak, Jr., Dennis G. Richardson, Richard B. Rogers, Ivan F. Scazziga, Mohamed Y. Shahin, Robert M. Smith, Roger E. Smith, Herbert F. Southgate, Elson B. Spangler, John P. Zaniewski

Committee on Surface Properties–Vehicle Interaction
Chairman, John Jewett Henry, Pennsylvania State University
Secretary: James C. Wambold, Pennsylvania State University
Robert A. Copp, Steven L. Cumbaa, Gaylord Cumberledge, Kathleen T. Diringer, Stephen W. Forster, Carlton M. Hayden, Brian S. Heaton, Walter B. Horne, David L. Huft, Michael S. Janoff, Khaled Ksaibati, Kenneth J. Law, Jean Lucas, Georg Magnusson, Kenneth H. McGee, James E. McQuirt, Jr., William G. Miley, Thomas H. Morrow, Robert L. Novak, William D. O. Paterson, Jean Reichert, Dennis G. Richardson, Richard B. Rogers, Roger S. Walker, Thomas J. Yager

Frank R. McCullagh, Transportation Research Board staff

Sponsorship is indicated by a footnote at the end of each paper. The organizational units, officers, and members are as of December 31, 1991.

Transportation Research Record 1348

Contents

Foreword

Scofield et al. evaluated the precision of two types of profilograph (electronic and mechanical) on portland cement concrete pavements. Pong and Wambold review four current accelerometer-established inertial profile reference methods and evaluate their computation methods. Lundy et al. investigated the extent that pavement wear due to studded tires has contributed to rut development in Alaska and found that it could not be ignored. They also determined that little information has been collected on studded tire wear and usage since 1975. Huft presents information about numerical filtering algorithms used by computerized profilographs. Comparisons made between manual and computerized profilographs indicate that the filtering algorithm attenuated some profile features.

Henry and Wambold discuss the use of smooth versus ribbed tires for skid testing. Hall et al. describe the history of friction testing equipment development and provide a summary of data of smooth and ribbed friction tests. Yager presents data collected using both the smooth and ribbed tire for friction measurement and discusses the advantages of wet pavement evaluation using the smooth tire. Morrow presents procedures and guidelines recommended by FAA to maintain highly skid resistant runways at civil airports. Acosta et al. describe the development of a low-cost system for video image pavement distress analysis.

Evaluation of California Profilograph

LARRY A. SCOFIELD, SYLVESTER A. KALEVELA, AND MARY R. ANDERSON

The Arizona Department of Transportation evaluates portland cement concrete pavements by testing with mechanical as well as electronic profilographs. The precision of the two types of profilograph was evaluated. More than 100 profilograph runs were conducted on a selected pavement section. The range of replicate readings of pavement profile index could be as much as 2.0 in./mi for a rough pavement. Electronic profilographs adjusted to operate at low filter settings gave lower profile index values than those obtained with the same profilographs at higher filter settings.

The first California profilograph was developed in 1940. During almost 50 years of use, it has seen many changes. The beam length has varied from 10 to 25 ft. It has been a mobile unit and a hand-propelled unit. There have been as many as 16 wheels and as few as 4. It has been constructed of wood, steel, and aluminum, and it has been assembled in three to five sections. The model most prevalent in the industry today resembles the 1962 12-wheel profilograph. During the mid-1980s the recording device was computerized by Cox and Sons, Inc. Both mechanical and computerized versions (automated) are currently available in the industry.

It is reported that California developed and published a 7-in./mi profile index specification between 1958 and 1960 (*1*). The original specification and test procedures are still widely used today. The specification appears to have been established on a limited number of pavement sections built with fixed-form construction, from profiles obtained on the outer wheelpath, in the direction of traffic, with a mobile profilograph.

PROBLEM STATEMENT AND STUDY OBJECTIVES

The California Department of Highways developed the profilograph test equipment and roughness specifications to provide an objective method for ensuring a minimum for ride quality for concrete pavements. These devices and methods, developed more than 30 years ago, were based on subjective ride rating surveys and prepared for convenient and expedient application in the construction environment.

Today, ride-quality specifications have been extended far beyond the intent of the original procedures and specifications. In the past, the 7-in./mi roadway simply represented the minimum ride quality needed. Incentives and disincentives were not used. Incentives today can reach 5 percent of the bid item unit price.

L. A. Scofield, S. A. Kalevela, Arizona Transportation Research Center, Arizona Department of Transportation, 206 South 17th Avenue, Mail Drop 075R, Phoenix, Ariz. 85007. M. R. Anderson, Industrial and Management Systems Engineering Department, College of Engineering and Applied Sciences, Arizona State University, Tempe, Ariz. 85287.

Although the California profilograph and roughness specifications have served the industry well, two questions must be resolved. First, are the test procedure and equipment sufficiently accurate and reproducible to warrant such high percent incentive/disincentive specifications? and second, are the mechanical and computerized profilograph units comparable? Because of these questions, a study was conducted to

- Evaluate the precision of the California profilograph;
- Compare mechanical and automated profilographs;
- Evaluate the effects of data filter settings on profile index readings; and
- Evaluate the effects of trace reading variability on the profile index obtained with the mechanical profilograph.

EXPERIMENTAL DESIGN

To accomplish these objectives three test plans were developed: one to develop a precision statement for profilograph testing, one for analyzing the effect of the data filter settings, and one to determine operator variability in trace reduction.

The main experiment was conducted by using a 4-×-4-×-2 randomized block design with replication, resulting in 64 profilograph runs. The experimental design consisted of four operators, four profilographs (two mechanical and two automated), and two levels of pavement roughness (2.5 and 10 in./mi).

The data filter setting experiment consisted of a 3-×-2-×-2-×-2 randomized block design with replication. The experimental design consisted of three data filter settings (8,000, 6,000, 4,000), two automated devices, two operators, and two roughness levels (2.5 and 10 in./mi). The total number of tests for this experiment was 48.

The trace reduction experiment consisted of a 4-×-2-×-2 randomized block design with replication. The experimental design consisted of four operators, two mechanical devices, and two levels of roughness (2.5 and 10 in./mi). Each operator analyzed eight traces during the first round of reading, and a copy of the same eight traces in the second round.

Test Site Location

The field testing was conducted in Phoenix, Arizona, between September and November 1990. Testing was performed on an undoweled plain jointed concrete pavement 12 in. thick. The concrete pavement was constructed on an aggregate base and used skewed random joint spacing of 13, 15, 17, and 15 ft. The pavement had been constructed approximately 5 months earlier and was not open to the public.

Initially, three levels of roughness were desired to better represent the range of expected roughness levels obtained during construction operations. However, the large number of tests needed for this experiment and the difficulty in finding test sections in proximity for convenient testing resulted in the selection of only two levels of roughness.

Equipment and Operators

Four profilographs were used in this study. Two of the profilographs were mechanical and two were automated (computerized). The automated devices were Cox and Sons, Inc., Model CS8200s. One was a retrofitted McCracken unit and one was an original CS8200 unit. Of the two mechanical units, one was made by Cox and Sons, Inc., and the other was a McCracken device. The oldest of the four profilographs was purchased in 1967, and the newest was purchased in 1989. For this study, the two mechanical devices were identified as M1 and M2 and the two computerized devices were identified as E3 and E4.

The operators used for these experiments represented actual construction operators. Each operator represented a different construction group. Therefore, any real differences in methods or procedures between the groups should be revealed in the variability.

The four operators used in the field testing were not the same as those used for analyzing trace reduction. Problems with personnel availability precluded consistent use of all operators between these two segments of the experiment.

Test Procedures

Precision Experiment (Main Experiment)

The intent of the main experiment was to determine the "actual" field variability as opposed to the "ideal" variability possible with the devices. Therefore, the operators were not instructed on how to conduct the testing; they were only instructed on the run sequences and the manner in which the operators would switch devices to provide randomization. Each operator delivered the device managed by his or her construction unit to the test location. The operators assembled their own devices in their normal manner. Before conducting testing, the research group checked each device after assembly for proper calibration. One-in. calibration blocks were used for checking the vertical calibration for the manual units, and all units were gauged against a presurveyed 528-ft distance calibration check. Each of the measurement wheels was visually checked for eccentricity. It took three separate attempts to accomplish the complete experiment with all devices in satisfactory operating condition. Although the final testing was completed in 8 hr, it took several months to arrange the logistics for mobilizing all four units and operators during the three attempts at conducting the experiment.

Before assembling the profilograph units, a K. J. Law 690DNC profilometer was used to conduct the first series of runs over the test sections. Ten runs were made with the profilometer during the day, representing the time span over which the main experiment was conducted. This provided the ability to evaluate any changes in actual pavement roughness with time of day (i.e., thermal curling). Five runs were made with the profilometer for each of the two test sequences. One test sequence was conducted in the morning and one in the afternoon. Because the profilometer measures the profile in each wheelpath simultaneously, only one run was necessary to obtain both wheelpaths.

Profilograph testing was conducted in two replicates and in a complete randomized block design as much as possible within each replicate. Complete randomization was limited by four operators and four machines tested at about the same time. This allowed continuous testing with all operators and devices while ensuring statistical validity. For each operator and machine combination, testing began on the rough wheelpath in the direction of travel. Upon completion of this run, testing was continued with a subsequent run along the smooth wheelpath in the opposite direction of traffic. This "looping" allowed testing to be conducted without the need for deadheading the equipment. During testing no guides were used to ensure proper tracking.

Trace reduction for the mechanical devices was accomplished using only one individual to minimize trace reduction variability. One of the research engineers at the Arizona Transportation Research Center performed all trace reductions to provide evaluations as consistent as possible.

Data Filter Setting Experiment

Upon completion of the main experiment, the data filter experiment was conducted using two operators and two automated profilographs. As in the main experiment, test sequencing was conducted in a randomized complete block design within replicates, subject to the tests conducted in pairs. This allowed continuous testing with both operators and devices. Again only visual alignment control was used.

Trace Reduction Variability Experiment

Profilograph traces produced with the mechanical devices, M1 and M2, during the first attempt at the main experiment were used in the trace reduction variability experiment. Operators were not instructed regarding trace reduction techniques; they used their own established procedures.

Four operators were each given the same set of eight profilograph traces to interpret. The set consisted of four traces for a smooth pavement surface and four traces for a rough pavement surface. For each pavement type, two traces were obtained with the device M1 and two traces with M2. The eight traces were labeled in random order and given to each operator. After the first trace reductions were completed, a new random order of the same traces was sent to the same operators for reduction. Approximately 1 month passed between reductions. At the time of the first reduction, the operators were not advised about the second set of readings.

All copies of the traces were obtained from the same originals by a Xerox 2080 machine. This machine was selected to alleviate the concern that the final traces would be distorted

when compared with the original traces. This also allowed production of clean, unmarked profiles for each reduction. This precluded any bias that might result from eraser marks on the traces during operator interpretation.

Analysis Procedures and Terminology

Four categories of statistical procedures were applied during data analysis: (a) *F*-test for significance of treatment effects, (b) *t*-test for comparison of two means, (c) Duncan's multiple range tests for multiple comparison of several means, and (d) the standard analysis of response repeatability and reproducibility (*2*). The *F*-test was used to test the significance of treatment effects in the analysis of variance. The Student's *t*-test was used in cases that involved the comparison of two means. Where the desire was to make multiple comparisons of several means, Duncan's multiple range test was used.

For this study, repeatability was defined as the closeness of agreement between mutually independent test results obtained from the same wheelpath within the short time intervals by the same operator with the same device. The smaller the range of the test results, the better the repeatability of the test. Reproducibility was defined as the closeness of agreement between mutually independent test results obtained from the same wheelpath by different operators with the same profilograph.

Because the "true" profile index of each wheelpath of the roadway was not known, it was decided to obtain surrogate reference values. The arithmetic average of all test results for a given wheelpath was taken to be the reference value for that wheelpath. An additional evaluation was made by comparing individual readings to the mean value for each wheelpath of the test roadway.

The terms "track" and "road" have occasionally been used to mean the wheelpath over which profilograph tests were conducted.

EXPERIMENTAL RESULTS

Main Study

The test results of the main study are summarized in Table 1. The analysis of variance for the main study showed that (a) roughness readings produced by the four devices were statistically different at the 1 percent significance level, and (b) different operators produced statistically different profile indexes at a significance level of 7 percent.

In general, the two mechanical devices exhibited slightly better repeatability than the automated devices. That is, for a given combination of operator and device, the mechanical devices provided slightly more consistent results. The results in Table 1 show the repeatability range of each device for the smooth and the rough wheelpaths. All devices were repeatable within 2.0 in./mi on the rough wheelpath and within 1.5 in./mi on the smooth wheelpath. The average repeatability range was 0.75 in./mi for the rough wheelpath and 0.56 in./mi for the smooth wheelpath. This repeatability range is an average computed from the test results produced by the four operators for each device.

The closeness of test results to the means for the smooth and rough wheelpaths is depicted in Figures 1 and 2, respectively.

TABLE 1 PAVEMENT ROUGHNESS DATA OBTAINED WITH PROFILOGRAPHS

		Profile Index Readings (in/mile)					
		Smooth track			Rough track		
Profilograph	Operator	Test 1	Test 2	Difference*	Test 1	Test 2	Difference*
M1	1	4.00	3.50	0.50	10.00	8.50	1.50
	2	3.50	3.50	0.00	8.50	7.50	1.00
	3	5.00	4.00	1.00	7.00	7.00	0.00
	4	4.00	4.00	0.00	7.00	8.00	1.00
	MEAN	4.13	3.75	0.38	8.13	7.75	0.88
M2	1	5.00	5.00	0.00	11.00	11.00	0.00
	2	5.00	6.00	1.00	10.00	11.00	1.00
	3	5.50	6.00	0.50	9.00	9.50	0.50
	4	5.50	5.00	0.50	10.50	11.00	0.50
	MEAN	5.25	5.50	0.50	10.13	10.63	0.50
E3	1	5.00	6.00	1.00	8.50	8.00	0.50
	2	5.00	6.50	1.50	7.50	8.50	1.00
	3	6.00	6.50	0.50	8.00	8.50	0.50
	4	5.50	5.50	0.00	7.50	8.00	0.50
	MEAN	5.38	6.13	0.75	7.88	8.25	0.63
E4	1	6.00	6.50	0.50	11.00	11.00	0.00
	2	7.00	6.00	1.00	9.00	8.50	0.50
	3	7.00	6.50	0.50	8.00	10.00	2.00
	4	6.00	5.50	0.50	10.00	8.50	1.50
	MEAN	6.50	6.13	0.63	9.50	9.50	1.00

* Absolute difference between tests 1 and 2

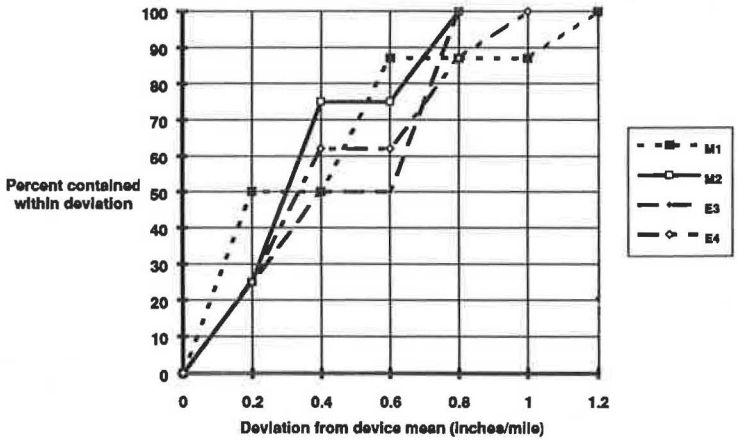

FIGURE 1 Device repeatability depicted in terms of cumulative percentage of device readings within given deviation from device mean on smooth track.

The figures represent, for each device, the percentage of actual test results contained within given deviations from the device mean for the smooth and rough wheelpaths. For example, approximately 100 percent of the test results obtained by all four operators for Device E4 were within a 1-in./mi deviation from the device mean value for the smooth wheelpath. However, only about 60 percent of the test results for Device E4 were within 1 in./mi from the device mean for the rough wheelpath.

The range of roughness values obtained by all operators with each of the devices for the smooth and the rough wheelpath is shown by Figure 3 by solid bars. The mean values for the smooth and the rough wheelpaths are depicted by thick vertical lines. Figure 3 indicates that even though the individual devices may be very repeatable, test results from each of the devices may be significantly different.

The range of test results was between 3.5 and 7.0 in./mi for the smooth wheelpath and between 7.0 and 11.0 in./mi for the rough wheelpath. The quality of these data clearly is not acceptable to administer an incentive/disincentive specification. It should be remembered that the variability could be larger if operator variability in trace reduction were included.

Variability Due to Data Filter Settings

The Cox and Sons Model CS8200 recommends a data filter setting of 8,000. To evaluate the effect of reducing the filter setting, two operators and two automated devices were evaluated at three settings for both the rough and smooth conditions. A total of 48 tests were performed. The results of this testing are given in Table 2. The profile index values for each level of filter setting, given as percentages of the values at the 8,000 filter setting level, are plotted in Figure 4. The values represented in Figure 4 constitute the average of all values obtained at a given filter setting for each track condition. Surprisingly, the overall average values obtained by combining both the smooth and rough track conditions resulted in an almost perfect linear relationship.

As can be seen in Figure 4, at a data filter setting of 4,000 there is approximately a 30 percent reduction in the profile index that would be obtained with the setting at 8,000. A reduction of approximately 7 percent of the 8,000 setting value occurs for every 1,000-unit change in the data filter setting. An analysis of variance indicated that the filter setting had a

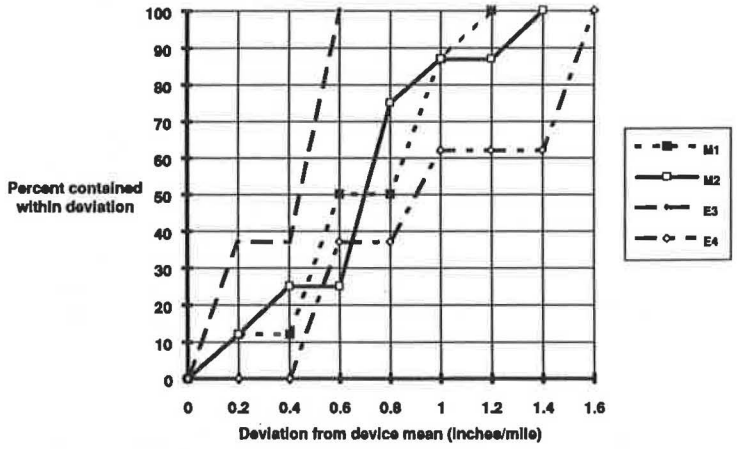

FIGURE 2 Device repeatability depicted in terms of cumulative percentage of device reading within given deviation from the device mean on rough track.

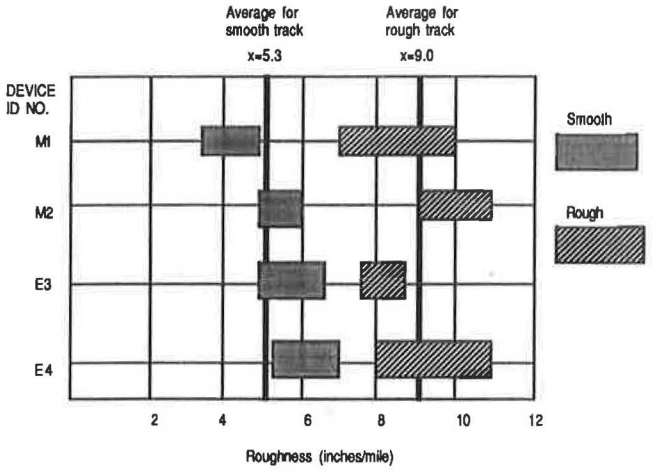

FIGURE 3 Range of roughness readings obtained during testing.

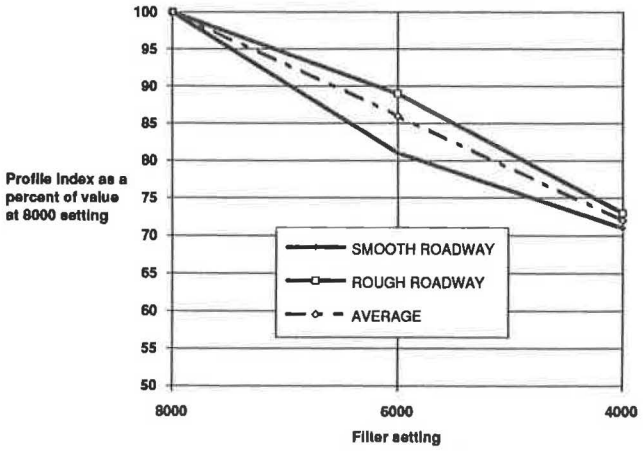

FIGURE 4 Effect of filter setting on profile index values.

significant effect on the roughness value. Duncan's multiple range test confirmed that each setting was distinct at a 1 percent significance level. The variability due to devices was significant at the 1 percent level, and the two operators differed at the 5 percent level. The analysis of variance also indicated significant interactions between operators and road roughness and between operators and devices.

The average difference between operators was 0.61 in.; the average difference between devices was 0.65 in. The difference due to filter setting was almost 1 in. between each setting level (i.e., 8,000 = 7.4 in., 6,000 = 6.4 in., 4,000 = 5.3 in.). One of the problems associated with attempting to determine specific effects from these settings is the strong interactions between operators and road roughness and between operators and devices. For example, although the operators got nearly the same average value on the smooth sections, their average values differed by more than 1 in. for the rough condition. Similarly, whereas the two operators obtained almost the same average readings on Device E4, their average readings for Device E3 differed by more than 1.5 in.

Trace Reduction Variability

Operator variability consists of field variability and trace reduction variability. Field variability is a result of the operators' inability to traverse the same path each time, measure the designated path location, and test at the same speed. It also is affected by test procedures and equipment calibration. The trace reduction variability is produced by the operator with mechanical devices. Once an operator obtains a profile trace from a mechanical device, it must be manually interpreted.

TABLE 2 PROFILE INDEX DATA OBTAINED AT DIFFERENT FILTER SETTINGS OF ELECTRONIC PROFILOGRAPHS

			Profile Index readings (in/mile)					
Filter	Profilograph		Smooth wheel path			Rough wheel path		
Setting	Number	Operator	Test 1	Test 2	Mean	Test 1	Test 2	Mean
8000	E3	1	5.00	5.50	5.25	9.50	11.00	10.25
		2	4.00	4.50	4.25	8.00	8.00	8.00
	E4	1	6.00	6.00	6.00	9.50	11.50	10.50
		2	6.50	5.50	6.00	9.50	8.00	8.75
	Mean		5.38	5.38	5.38	9.13	9.63	9.38
6000	E3	1	4.50	3.50	4.00	8.00	8.50	8.25
		2	4.00	3.50	3.75	8.50	7.50	8.00
	E4	1	4.00	6.00	5.00	9.50	8.00	8.75
		2	4.50	5.00	4.75	8.00	9.00	8.50
	Mean		4.25	4.50	4.38	8.50	8.25	8.38
4000	E3	1	4.50	4.00	4.25	7.00	8.00	7.50
		2	3.50	3.00	3.25	6.00	5.50	5.75
	E4	1	3.00	3.00	3.00	8.50	6.00	7.25
		2	4.50	5.00	4.75	7.00	7.00	7.00
	Mean		3.88	3.75	3.81	7.13	6.63	6.88

TABLE 3 RESULTS OF TRACE REDUCTION BY DIFFERENT OPERATORS

		Profile index readings (in/mile) for different operators							
	Reading	Profile trace number							
Operator	Replicate	1	2	3	4	5	6	7	8
1	1	5.0	9.0	5.5	8.0	8.5	9.0	11.5	12.0
	2	3.0	5.0	3.0	6.0	7.5	8.0	10.0	11.0
	Difference*	2.0	4.0	2.5	2.0	1.0	1.0	1.5	1.0
2	1	3.5	4.5	5.0	6.5	7.0	8.0	9.5	10.5
	2	3.0	3.5	6.0	7.0	7.0	7.5	16.0	11.5
	Difference	0.5	1.0	1.0	0.5	0.0	0.5	6.5	1.0
3	1	1.5	3.0	1.5	2.5	7.0	6.5	8.0	9.0
	2	2.0	2.5	2.5	3.0	7.5	7.0	9.0	6.0
	Difference	0.5	0.5	1.0	0.5	0.5	0.5	1.0	3.0
4	1	1.5	2.5	3.0	3.0	6.5	7.5	9.5	9.5
	2	1.5	3.0	2.0	2.5	7.0	5.5	6.5	8.0
	Difference	0.0	0.5	1.0	0.5	0.5	2.0	3.0	1.5

* Absolute difference

This allows considerable judgment to be exercised in the trace analysis. An example of such a judgment factor would be whether the individual performs "outlining" before evaluating the trace.

The results of the trace reduction experiment are summarized in Table 3. All readings for the smooth wheelpath were within three standard deviations from the mean, which was 3.78 in./mi. For the rough wheelpath, one reading (16.0 in./mi) was out of control or outside the three standard deviation interval for the mean of 8.58. It should be noted that other than the extreme lack of repeatability by Operator 2 on the occasion in which the first and second readings were 9.5 and 16 in./mi, Operator 2 was the most consistent of the operators. His range was 1.0 in. for the other sets of data. The actual calculations by Operator 2 were rechecked and verified against a possible error in calculation or in recording. The extreme of 16 is worthy of concern because it shows that the present system is not adequate to prevent an out-of-control point, even by an excellent operator. A summary of the differences between first and second readings for each operator is given in Table 4.

Measurement error variability due to the difference between the operators and the repeated readings accounted for 67 percent of the product characteristic variability. There was more variability between the average values among operators than there was variability between two readings of a single operator.

Pavement Roughness Variability During Day

To evaluate changes in roughness due to time of day, a K. J. Law 690DNC profilometer was used. Before testing with the profilographs, five tests were conducted with the profilometer at 50 mph. These tests were typically conducted between 7:30 a.m. and 8:30 a.m. on each of the three test days. A second set of five profilometer tests was conducted between 10:00 a.m. and 11:00 a.m. This corresponded with the latter portions of the main profilograph experiment. This 3- to 4-hr window of testing was designed to establish whether the pavement roughness changed during the profilograph testing.

TABLE 4 DIFFERENCES BETWEEN OPERATORS' FIRST AND SECOND TRACE READINGS BASED ON FOUR TRACES FOR EACH TRACK TYPE

	Absolute differences between first and second readings (in/mile)					
Operator	Smooth Track			Rough Track		
Number	Minimum	Maximum	mean	Minimum	Maximum	mean
1	2.00	4.00	2.63	1.00	1.50	1.13
2	0.50	1.00	0.75	0.00	6.50	2.00
3	0.50	1.00	0.63	0.50	3.00	1.25
4	0.00	1.00	0.50	0.50	3.00	1.75
All operators	0.00	4.00	1.13	0.00	6.50	1.53

The K. J. Law 690DNC is an ASTM Class I profile measurement device. Two profile statistics were used in this testing: the Mays roughness index and the international roughness index (IRI). Mays units are expressed as inches per mile and represent the response of the vehicle to the effects of both wheelpaths. IRI units are also expressed in inches per mile. However, IRI represents the response of the vehicle to the effects of a single wheelpath. That is, the IRI unit is computed individually for the right and left wheelpaths. A total IRI can be computed by averaging the values obtained by the right and left wheelpaths.

The roughness measured by the profilometer indicated a decrease in roughness between morning and afternoon readings of 7 to 10 percent for the three test dates. The rate of decrease in roughness was 2 to 3 in./mi/hr. The Mays statistic is used for this comparison. Unfortunately, no direct comparison between the Mays units and profile index was established for this study.

During the morning testing with the profilometer, many tests included a situation termed "lost lock and saturation." This condition can be caused by excessive sunlight entering beneath the shrouds of the test van. This can result in higher-than-actual readings. The profile traces were not processed for these spikes.

An analysis of the profilograph data indicated no statistical difference between readings obtained in the morning and those obtained in the afternoon. Presumably, the large variation in profilograph test results masked the small changes in pavement roughness.

Change in Pavement Roughness With Time

Because the testing was conducted on 3 days over 3 months, an assessment of the change in pavement roughness with time was possible. The pavement increased in roughness by 7 percent for the morning and by 9 percent for afternoon readings. It is surprising that the morning readings had a perfectly linear relationship. The rate in change in roughness was 0.14 in./mi/day and 0.10 in./mi/day for the morning and afternoon conditions, respectively. It should be noted that this increase in roughness occurred at 5 to 8 months after construction.

DISCUSSION OF RESULTS

Historically, the use of profilographs for construction quality control has consisted of evaluating concrete pavement profiles soon after placement. The paved surfaces have typically been assessed in accordance with a maximum acceptable profile index of 7 in./mi. Recently, specifications have evolved from simple acceptance criteria to an incentive/disincentive requirement.

The precision of this device is not acceptable for the administration of incentive/disincentive specifications currently being

applied. Although some controversy currently exists regarding the correlation between mechanical and automated devices that use signal processing techniques, the actual problem is more basic than this recent development. The current specifications simply expect too much from the California profilograph.

Although a detailed statistical analysis was conducted for this study using two levels of roughness, only one section of pavement surface, 1/10 mi long, was used for all testing. This does not represent a spectrum of pavement surface types and roughness. It did, however, allow the effect of the main variables and the interaction of the variables to be clearly seen.

The industry "benchmark" standard of 7 in./mi was established before slip form paving and long before electronic paver controls. Similarly, the relationship between this numerical index and ride quality was based on the operating characteristics of vehicles from the 1950s and earlier. It is difficult to believe that modern-day pavers produce similar quality pavements and that modern vehicles respond similarly to their 1950 counterparts. A clear need exists to reexamine the industry benchmark. The evaluation should consider the quality of pavement available from modern pavers and the response to ride quality provided by modern vehicles.

The industry benchmark may well be reestablished as a function of the roadway classification or use. For example, an urban freeway with extremely high traffic volumes would appear to warrant higher standards of smoothness than rural roadways with significantly less traffic. One benchmark, for all types of roadways, does not appear appropriate for the wide range of pavement conditions found today.

Significant spatial variability exists on pavement surfaces. This variability is not easily accounted for by averaging profile traces obtained in wheelpaths. Currently, little or no information is available to determine if statistical sampling methods need to be developed to properly assess "true" roughness. Although the automated devices have significantly reduced test time, performing multiple runs under current procedures appears impractical. A study should be undertaken to determine the required sampling frequency for proper determination of representative pavement roughness values. Recent research conducted by Janoff suggests that measurement of pavement roughness ". . . can be simplified to be based on profile type roughness measured in only one wheelpath by a far simpler and less costly device than a profilometer" (*3*). This is contrary to the authors' experience.

The change in pavement roughness for both daily cycles and short-term roughness increases is not well documented. Although the phenomenon has been reported for many years, its impact on profilograph testing has not been adequately recognized. This factor should be further defined so that its implications on test timing and methods can be properly evaluated.

A surprising result from this study was the strong statistical interactions between some of the variables. These interactions make it difficult to account for the variability present in profilograph testing with limited experimentation such as with one machine or one operator.

Manual trace reduction appears to have a larger effect on the final answer than commonly believed. The average repeatability established in this study was approximately 0.94 and 1.88 in. Although not rigorously evaluated, other studies found trace interpretation repeatability to be approximately 1 in./mi (*4,5*). It is interesting to note that in one of these studies a computer-generated profilograph trace was supplied to the operator for reduction. The null blanking band was superimposed on the trace by the computer. Therefore, the null band (i.e., the template) was already depicted on the plot. The only variability measured was that of the operator's interpretation. This suggests that operator interpretation alone may approach a variability of 1 in./mi. These results strongly encourage the use of the more efficient computerized profilographs.

As incentive specifications reward contractors for producing ever smoother pavements, consideration should be given to the effects this may have on concrete mix design and resulting concrete quality. Mix designs which promote smooth pavements may produce surfaces with greater attrition and hence lower skid properties with time. Smooth pavement surfaces should be provided in concert with durable concrete pavements and not in lieu of them.

RECOMMENDATIONS

The California profilograph does not appear to have the accuracy necessary to appropriately administer a viable incentive/disincentive specification in view of the smoother and smoother pavements now possible. The industry should move away from the profile index standard and adopt some other summary statistic such as IRI or RMSVA. Using these or other acceptable profile-based statistics would require more accurate measuring equipment. They also provide a cradle-to-grave roughness statistic—that is, the statistic that would be used by the pavement designer could be directly related to the as-constructed roughness and future pavement performance.

Improvements in concrete pavement ride quality appear to have been brought about largely by the adoption of incentive/disincentive specifications and improved construction equipment. These improvements should continue to be encouraged by such specifications. However, devices for acceptance testing must be commensurate in accuracy with the monetary actions represented by these specifications. If this is not possible, specifications that set only a maximum allowable roughness level should be used.

REFERENCES

1. *Six Profilographs Readied for District Use*. California Division of Highways, May 1959.
2. D. C. Montgomery. *Introduction to Statistical Quality Control*. 2nd ed. John Wiley & Sons, Inc., New York, N.Y., 1991, Chapter 6.
3. M. S. Janoff. *NCHRP Report 308: Pavement Roughness and Rideability Field Evaluation*. TRB, National Research Council, Washington, D.C., 1988.
4. R. S. Walker and H.-T. Lin. Profilograph Correlation Study With Present Serviceability Index. In *Transportation Research Record 1196*, TRB, National Research Council, Washington, D.C., 1988, pp. 257–275.
5. M. A. Bower. *An Evaluation of Automated Profile Index Computation for James Cox and Sons, Inc. Model 8200 Profilographs*. Materials Division, Virginia Department of Transportation, Richmond, June 1991

Publication of this paper sponsored by Committee on Surface Properties–Vehicle Interaction.

Evaluation of Computation Methods for Accelerometer-Established Inertial Profiling Reference Systems

MEAU-FUH PONG AND JAMES C. WAMBOLD

Current accelerometer-established inertial profiling reference (AEIPR) methods are reviewed, and their computation methods are evaluated. Four AEIPR were reviewed and computer-simulated to test profile computation. These methods are installed in the K. J. Law Profilometer, the Swedish Road and Traffic Research Institute's (VTI) Laser Road Surface Tester, the University of Michigan Transportation Research Institute/FHWA Road Profiling (PRORUT) system, and the Pennsylvania Transportation Institute profiling vehicle. The South Dakota system was not included when this work started, but it uses a computation method similar to the VTI and PRORUT methods. Seven tests were developed to examine the profiling methods from many angles: amplitude errors, wavelength response, phase shift, transient response, roughness errors, profile reproduction, and computational time.

One of the main concerns of highway agencies is the maintenance and improvement of road surface quality. Highway engineers evaluate pavement conditions to manage maintenance and to support requests for maintenance funds. This evaluation must include (but is not limited to) the factors of safety, pavement performance, pavement distress, and structural capacity (*1*, p. 21). Roughness, a measure of pavement condition, is the main characteristic of the pavement used to describe pavement performance; an effective evaluation requires reliable measurement of road roughness.

ROAD ROUGHNESS AND MEASURING EQUIPMENT

Rough roughness in the United States is measured primarily by two types of equipment: equipment that measures the vehicle's response to roughness, or response-type road roughness meters (RTRRMs), and equipment that measures road profiles, or profiling devices. RTRRMs are not discussed in this paper because they do not measure profiles. Ideally, the road profiling method gives accurate, scaled reproductions of the pavement profile along a reference plane. According to Claros et al., "In practice, the range and the resolution of any profiling device is limited, but within these limits the measurement may be called absolute" (*2*). They also state: "The most universal purpose of these road profile measurements at the present time is to assess the roughness for pavement encountered by motor vehicles" (*3*).

Pennsylvania Transportation Institute, 201 Research Office Building, Pennsylvania State University, University Park, Pa. 16802.

ROAD PROFILE MEASURING DEVICES

Several devices are used to obtain road profiles: rod and level, dipstick, profilograph, straight edge, and accelerometer-established inertial profiling reference (AEIPR) systems. Profiling vehicles other than AEIPR include the French APL system, British HRM system, Canadian ARAN system, and Nevada Automotive Testing Center's DFMV (*4–9*). These devices are not discussed in this paper.

The rod-and-level method is the most time- and labor-consuming way to measure longitudinal profile (*10*). The dipstick is a new product for measuring profile samples at 1-ft intervals. Although the dipstick is more efficient than the rod and level, it still is considered a static, time-consuming instrument when compared with dynamic road profiling devices.

There are three types of profilograph: the California profilograph, the Reinhart profilograph, and the Ames profilograph (*11–13*). Profilographs do not measure road profiles because their responses are not uniform over the wavelength range of interest (*14*, p. 189).

A straight edge is, in theory, the simplest way of measuring road profile (*1,15*). But it is also a slow way, and the wavelengths measured are limited by the length of the straight edge.

An AEIPR system is usually a vehicle installed with instrumentation that measures the elevation of the road surface along the direction of travel. This technology allows highway engineers to measure road profiles with acceptable accuracy more efficiently than any other road profiling method does. A research study of measurements given in Table 1 shows that the profiling vehicle and the dipstick measurement are within 4 percent of each other.

AEIPR Vehicle

The AEIPR model was invented by General Motors Research Laboratory in 1966 (*17*). This early version of an AEIPR vehicle used a pair of accelerometers to measure left and right vertical acceleration, a pair of spring-loaded "road wheels" (in addition to the traveling wheels) to measure the distance between the vehicle and the pavement, and a tachometer to measure the speed of the vehicle. An analog computer was used to compute the road profile. K. J. Law Engineers, Inc., of Novi, Michigan, acquired a patent license from General Motors and is now the commercial source of the Model 690DNC Surface Dynamic Profilometer.

TABLE 1 ROUGHNESS INDEXES OBTAINED BY DIPSTICK AND AEIPR SYSTEM

Site	Dipstick	AEIPR Profiling Device	Difference in Percentage
4	131.0	129.9	0.84%
5	171.3	169.1	1.28%
6	131.4	130.2	-0.91%
11	92.9	94.4	1.61%
13	128.8	130.3	1.16%
14	124.4	123.9	-0.41%
18	231.1	228.1	-1.29%
25	121.4	122.8	1.15%
26	154.3	148.4	-3.82%

Source: Data provided by Pennsylvania Department of Transportation Bureau Bridge and Roadway Technology. (Measurement date: 9/16/1990)

Note: Roughness indices shown are the averages of left and right tracks.

Roughness is given as the International Roughness Index Standard.(16,26)

Other AEIPR vehicles are currently based on the General Motors design, such as the PRORUT system developed by the University of Michigan Transportation Research Institute (UMTRI) for FHWA, the Laser Road Survey Tester developed by the Swedish Road and Traffic Research Institute (VTI), and the South Dakota system (*18–20*). These systems have similar hardware configurations but use a different displacement transducer and different software for signal processing and profile analysis. A special feature of the VTI design is its data acquisition rate: at 32,000 sample/sec, the macrotexture of the pavement can be recorded and analyzed. Each of these systems can measure rutting to a different degree depending on the number of sensors used.

Many different models of AEIPR vehicles have been made available to highway agencies. FHWA invited companies with different profiling vehicles to measure the same sites and compare their results (*3*). Some transducers are more accurate than others; some signal processing units are more delicate than others. The performance of each profiling vehicle equals the combined performance of all its measurement devices, instrumentation, and profile computation methods. Determination of what instrumentation is to be used in the profiling vehicle was not addressed in this research work.

Objective

The objective of this paper is to evaluate the performance of the profiling computation method associated with each AEIPR available. These methods are used in K. J. Law's 690DNC Surface Dynamic Profilometer, UMTRI/FHWA's PRORUT system, VTI's Laser Road Survey Tester, and the Pennsylvania Transportation Institute's (PTI) AEIPR vehicle (*21*). For the South Dakota system and other devices, computation methods are based entirely or partially on these methods. A computer simulation of each profiling method was performed. All of the profiling methods were subjected to a number of tests with the same criteria and then compared for performance.

REVIEW OF AEIPR METHODS

Spangler's Method in K. J. Law 690DNC Surface Dynamics Profilometer

K. J. Law's 690DNC Surface Dynamics Profilometer is commercially available from K. J. Law Engineering, Inc. The computer measurements are triggered by spatial pulses generated by vehicle wheels. This profiling method was designed to give a real-time profile from measurements that are taken every inch and averaged over a 12-in. interval to provide profile samples of a 6-in. interval. This profiling method applied in the 690DNC was developed by Elson Spangler. The system design and the profile computation methods are detailed and illustrated in a U.S. patent (*22*). The profile computation is based on the following equation:

$$P = (W - Y) + \int\int_{x_1}^{x_2} \frac{\ddot{Y}}{V^2}\, ds\, ds \tag{1}$$

where

P = computed profile,
$(W - Y)$ = instantaneous height measurement (distance from vehicle to pavement),
V = vehicle's instantaneous speed measurement,
ds = integration distance interval (set fixed for 6 in. or otherwise),
$\ddot{Y}$ = vertical acceleration measurement, and
x_1, x_2 = distance traveled corresponding to the adjacent samples.

Processing the acceleration signal does not produce the true inertial reference. It produces the highpass-filtered form of the double-integrated acceleration for removing the low-frequency part of the signal, which is usually for wavelengths longer than 300 ft. From the functional block diagram in the patent description, the equation for the inertial reference can be derived into

$$Y_f(S) = \frac{S}{S^3 + T_1S^2 + T_2S + T_3}\, \mathcal{L}\left\{\frac{\ddot{Y}}{V^2}\right\} \tag{2}$$

where

$Y_f(S)$ = vehicle's motion history in Laplace domain,
T_1, T_2, T_3 = filter constants determining the cutoff wavelength,
S = Laplace variable, and
$\mathcal{L}$ = Laplace operator.

Equation 2 shows that Spangler's method contains a third-order filter equation. The profile is obtained by either of the following equations:

$$P = (W - Y) + Y_f \tag{3}$$

$$P = W - (Y - Y_f) \tag{4}$$

These equations produce a calculated profile with the long-wavelength portion removed.

UMTRI/FHWA PRORUT Method

The UMTRI/FHWA PRORUT system measures both longitudinal and transverse profiles (rut). It incorporates laser infrared noncontact displacement sensors, an analog-to-digital converter, anti-aliasing filters, and a PC. Measurement is triggered by a signal from an inductive distance pickup on one of the wheels. The profile is computed after data acquisition. The computation of slope profile involves six to seven steps:

1. The bias in the acceleration measurement is calculated and subtracted to minimize error after integration.
2. The bias-removed acceleration signal is converted from temporal acceleration into spatial acceleration:

$$\ddot{Y}_s(i) = \frac{\ddot{Y}(i)}{V(i)^2} \tag{5}$$

where

$V(i)$ = ith sample of the vehicle's instantaneous speed,
$\ddot{Y}(i)$ = ith sample of vertical acceleration measurement, and
$\ddot{Y}_s(i)$ = ith sample of spatial acceleration.

3. The spatial acceleration signal is integrated once to obtain a first slope signal:

$$S_1(i) = C_f * S_1(i - 1) + \ddot{Y}_s(i) * \Delta s \tag{6}$$

where $S_1(i)$ is the ith sample of first part of slope profile from acceleration measurement and Δs is the distance sampling interval. C_f is given by

$$C_f = 1 - \frac{\Delta s}{\lambda_f} \tag{7}$$

where λ_f is the longest wavelength of interest.
4. The height measurement is differentiated once with a highpass filter to obtain a second slope signal:

$$S_2(i) = \frac{C_f * H(i + 1) - H(i)}{\Delta s} \tag{8}$$

where $S_2(i)$ is the ith sample of the second part of slope profile from height measurement and $H(i)$ is the ith sample of height measurement.
5. The first and the second slope signals are added to obtain slope profile

$$S(i) = S_1(i) + S_2(i) \tag{9}$$

where $S(i)$ is the ith sample of the slope profile.
6. If roughness is the desired result, no further processing of the data is required. The slope profile is used for roughness computation. If the road profile is desired, the slope profile is integrated backward with the same highpass filter so that the phase lag from the previous integration is canceled. Because the profile computation is a postprocessing, the integration can be performed backward. The profile is

$$P(i) = C_f * P(i + 1) + S(i) * \Delta s \tag{10}$$

where $P(i)$ is the ith sample of computed profile.
7. If the road profile is plotted, a highpass filter with moving average algorithm is applied to remove the long-wavelength portion in the profile.

VTI Profiling Method

The VTI method is currently used in the Laser Road Surface Tester (*20,23*). The method is a variation of the Sayers time-domain method used in South Dakota's system (M. W. Sayers, personal communication, June 1989) with a high-order filtering process. The measurements are triggered by a constant frequency of 32,000 Hz while the profilometer is traveling. All the signals are passed through an anti-aliasing filter before the digitizing process begins. The signal processing is described in the following steps:

1. The acceleration signal is integrated and highpassed by a second-order filter. The transfer function of the filter is

$$F_{hp}(S) = \frac{S^2}{S^2 + 2DS + \omega_n^2} \tag{11}$$

where

$F_{hp}(S)$ = filter transfer function in Laplace domain,
D = damping characteristics of the filter,
ω_n = natural frequency of the filter or the cutoff frequency, and
S = Laplace variable.

Combining the integration and filtering process yields

$$VSM(S) = \frac{\mathcal{L}\{\ddot{Y}\}}{S} \cdot \frac{S^2}{S^2 + 2DS + \omega_n^2} \tag{12}$$

where $VSM(S)$ is the vertical velocity of profilometer body in Laplace domain and $\mathcal{L}\{\ddot{Y}\}$ is the Laplace transform of vertical acceleration measurement.
2. The height measurement is differentiated and highpass-filtered

$$HDD(S) = F_{hp}(S) * H(S) \tag{13}$$

$$HD(S) = S * HDD(S) \tag{14}$$

where

$HD(S)$ = highpass-filtered and differentiated height signal in Laplace domain,
$HDD(S)$ = intermediate variable in Laplace domain, and
$F_{hp}(S)$ = highpass filter function in Laplace domain.

3. The profile slope is the combination of time-domain samples of Equations 12 and 14 as follows:

$$YD(i) = \frac{VSM(i) - HD(i)}{V(i)} \tag{15}$$

where $YD(i)$ is the ith sample of profile slope and $V(i)$ is the ith sample of vehicle speed measurement.

4. The time-domain profile slope must be mapped into a spatial domain. This is accomplished by an interpolation process. The distance traveled is given by

$$X(i) = X(i - 1) + V(i) * \Delta t \tag{16}$$

When $j \cdot \Delta s$ falls in the distance interval between $X(i - 1)$ and $X(i)$, the value T can be determined as

$$T = \Delta t \cdot \frac{j\Delta s - X(i - 1)}{X(i) - X(i-1)} \tag{17}$$

The interpolation is given by

$$SP(j) = YD(i - 1) + [YD(i) - YD(i - 1)] \cdot \frac{T}{\Delta t} \tag{18}$$

where

j = sampling index for desired sampling distance interval,
$T < \Delta t$ = time that maps the distance $j\Delta s$ with the traveled distance,
$SP(j)$ = jth sample of spatial profile slope, and
Δs = desired sampling distance.

5. The slope profile is integrated and highpass-filtered by a third-order filtering process. The filter transfer function is defined by

$$F_3(S) = \frac{1}{S + \omega_n} \cdot \frac{S^2}{S^2 + 2DS + \omega_n^2} \tag{19}$$

and the profile is obtained by

$$P(S) = SP(S) * F_3(S) \tag{20}$$

where

$SP(S)$ = slope profile in Laplace domain,
$P(S)$ = profile in Laplace domain, and
$F_3(S)$ = third-order filter transfer function in Laplace domain.

All these filtering and profile computation processes are programmed in a TM32010-RST chip to perform high-speed, real-time signal processing. In this paper, these equations were coded in FORTRAN and computer-simulated.

PTI AEIPR Profiling Method

This profiling method was developed for use at PTI by Pong (*21*). The method was designed to work with off-the-shelf equipment such as the data acquisition A/D board, analog filters, and an IBM-compatible PC; no custom-made instrument is needed. The profile computation algorithm includes a double-integration routine for processing acceleration signals and a highpass filter routine to remove unwanted low-frequency profiles. Two accelerometers are used to acquire left and right vertical acceleration; Selcom noncontact displacement sensors are used to acquire the vehicle's instantaneous height above the pavement surface; and a pulse encoder is used to measure the vehicle's speed. A digital computer installed with an A/D converter records, processes, and stores the signals from all sensors. Analog filters are used to eliminate the unwanted aliasing effects.

Three steps for signal processing were performed. First, acceleration signals were double-integrated over the time period for the vehicle to pass the distance sampling interval. The time period was obtained by dividing the distance interval by the instantaneous speed. In equation form, the three steps are

$$\dot{Y}_i = \ddot{Y}_i \Delta t + \dot{Y}_{i-1} \tag{21}$$

$$Y_i = \dot{Y}_i \Delta t + Y_{i-1} \tag{22}$$

$$\Delta t = \frac{\Delta x}{V_i} \tag{23}$$

where

$\ddot{Y}_i$ = ith sample of vertical acceleration measurement,
Y_i = ith sample of double-integrated acceleration or the inertial reference,
V_i = ith sample of vehicle speed measurement, and
Δx = distance interval.

Second, both the integrated signals and the height signals pass digital highpass filters to remove profiles with wavelengths longer than 300 ft as well as the integration drift and low-frequency noise caused by the analog instrument.

$$Z_i = a_{21}Z_{i-1} + a_{22}Z_{i-2} + b_{20}Y_i + b_{21}Y_{i-1} + B_{22}Y_{i-2} \tag{24}$$

$$G_i = a_{21}G_{i-1} + a_{22}G_{i-2} + b_{20}H_i + b_{21}H_{i-1} + B_{22}H_{i-2} \tag{25}$$

where

Z_i = ith sample of the after-filtered version of signal Y_i,
H_i = ith sample of the before-filtered version of height measurement,
G_i = ith sample of the after-filtered version of signal H_i, and
a, b = filter constants.

Third, the profile is the sum of both the filtered integrated acceleration and height signals. The sum of both signals represents the effect of adding the longer-wavelength portion of the profile measured by accelerometers and the shorter portion measured by height sensors.

$$P_i = Z_i + G_i \tag{26}$$

where P_i is the ith sample of computed profile.

Summary of Profiling Methods

Table 2 summarizes the four profiling methods with regard to their collection of signals, sampling mode, types and orders

TABLE 2 SUMMARY OF FEATURES REGARDING DATA ACQUISITION AND PROCESSING OF AEIPR METHODS

	PRORUT	VTI	Spangler	Pong
Signals Required	A H V	A H V	A H V	A H V
Sampling Base	S	T	S	S
Integration Domain	S	T and S	S	T
Number of Filters[a]	2	2	1	1
Type of Filter	B	B	B	B
Orders of Filters	1 and 1	2 and 3	3	2
Filtering Domain	S	T and S	S	S
Real-Time Profile	No	Yes	Yes	Yes
Special Hardware[b]	No	Yes	Yes	No

Abbreviations:
A: Acceleration
V: Vehicle Velocity
T: Time
H: Height
B: Butterworth
S: Spatial

[a] "Filter" refers to the digital filter to process the digitized signals up to elevation profile. All methods are equipped with the anti-aliasing analog filters before signals are digitized.

[b] "Special hardware" refers to the hardware that is not available from sources other than the profilometer manufacturer.

of digital filters, and whether they are computed in real-time or postprocessed. From this table, the essential features can be seen clearly and referred to for comparing the test results.

EVALUATION OF AEIPR METHODS BY COMPUTER SIMULATION

To establish a reference for comparison, the following items were required: a common set of input data, a computer quarter-car simulation to calculate road profile data into accelerometer as well as height sensor signals, and a set of tests to evaluate their performance.

Preparing Common Data Base

The common data provided for all profiling analysis methods were a road profile with the appropriate distance interval (an array of real numbers with intervals of 0.5 or 1.0 ft). The selection of the profile data was intended to achieve each of the evaluations proposed and explore the performance as well as the weakness of each profiling method.

The common data sets include a single-wavelength sinusoidal profile, a multiwavelength profile, a step, and real sampled road profiles. The single-wavelength sinusoidal profile was used to evaluate precision. The multiwavelength profile was used to find the response function and phase shift of each method to the wavelength range of interest. The step was used to identify the transient response of each method. The actual profile was used to examine how well each method produced the original profile. The actual profile was also used to calculate a roughness index, which was used to evaluate the overall performance.

Quarter-Car Model Simulation

A quarter-car computer model simulation was applied to transfer road profile data into a transducer signal of the vehicle's vertical acceleration and height above the pavement. The method and differential equations for this simulation model are given in ASTM E1170-87.

A computer routine was coded to accept profile data as input. Using an assumed vehicle speed of 40 mph, both the acceleration and height were obtained digitally, with a third-order Runge-Kutta integration algorithm, for use as input to the different computation methods (*23*).

Design of Tests for Evaluating Profiling Methods

Seven tests were prepared to analyze the performance of each profiling method: amplitude errors, frequency response, transient response, phase shift, international roughness index (IRI) error, profile reproduction, and computation time.

Amplitude Errors

The amplitude error test was done to validate the correctness of profiling program coding, to calibrate the orientation of sensors, and to determine if the amplitude error was frequency-dependent. A set of input data generated by simulating the vehicle's bouncing was provided for each method to compute the profile. The bounce test assumed that the profiling vehicle did not travel but vibrated vertically with a certain amplitude and at designated frequencies. In other words, a sinusoidal vertical displacement was imposed on the vehicle body, and the corresponding acceleration was generated accordingly. In this test, the displacement amplitude was 1 in. and the frequencies used were 0.1, 0.25, 0.5, 1, 2, 5, and 10 Hz. The sampling time was selected to set the corresponding speed and sampling distance.

Wavelength Response Function

The purpose of the wavelength response function test was to determine the amplitude ratio (output versus input) of each profiling method as it responded to different wavelengths. A sinusoidal profile with an amplitude of 1 in. and a wavelength range from 10 to 500 ft was provided as input to the quarter-car simulation to generate the necessary sensor's signals. Each profiling method computed a profile based on the same input. The amplitude of the computed profile represented the amplitude ratio. A plot of the wavelength response function was obtained for each profiling method.

Phase Shift

The phase shift test was given to observe the phase changes for profiles of different wavelengths. The phase is the relative phase angle between the original and computed profiles. A series of sinusoidal profiles of 1-in. amplitude with wavelengths from 10 to 500 ft was used. The phase shift was recognized as the time delay or advance of the computed profile with respect to the input of each wavelength. A plot of phase shift angle for various wavelengths was obtained for comparison of the methods.

Transient Response

The transient response test was intended to determine how these profiling methods behave in response to a sudden ele-

vation change. Because all profile computation method incorporate their own highpass filters to remove LWL profile and lowpass filters to eliminate noise (Spangle and PRORUT methods), a sudden elevation change of road profile can cause the filter to overshoot and ring. A step of 1 in. was provided as input to test the behavior of each profiling method. In the computed profile, the amount of overshooting and the distance (or time) required to settle to 5 percent of input amplitude was used as its transient response performance.

IRI Errors and Profile Reproduction

Samples of real profiles obtained by using a dipstick method were used as input for a quarter-car simulation that generated the signals for all profiling methods. The computed profiles were used to calculate the IRIs as well as for comparison to the original profile. For the PRORUT and VTI methods, the IRIs are computed from slope profiles without going through the final elevation profile integrating procedure. The IRIs from the original profile and each computed profile were observed and compared. The profile reproduction was observed by comparing the computed profile with the filtered original profile.

Computation Time

The purpose of this test was to determine the amount of time required to actually compute the profile. The results showed which methods were less time-consuming and more suitable for real-time profiling application. The computation time required for processing 5,280 profile samples was obtained for each method and compared.

Speed Sensitivity

The speed sensitivity test was included in a previous thesis study (*24*). It was found to be unnecessary in the current study because a computer simulation of perfect data preparation has no error due to speed variation. However, in the real profiling system, the speed compensation is variable because of the speed measurement and hardware effects. Therefore, speed sensitivity should be included if the complete profiling system is to be evaluated.

Computer Simulation of Profiling Methods

The four profiling methods were coded into FORTRAN subroutines with an identical input and output parameters format. The programs were coded according to their original programs with minor adaptations so as to be compatible with the Microsoft FORTRAN compiler. Single precision was used. The computation method developers were consulted to verify the correctness of their profiling programs and the results of their method.

The sampling distance was generally set at 0.5 ft, but the VTI method used 0.05 in. because the actual sampling is 32,000 sample/sec, averaging over a number of samples. For Spangler's method, the profilometer's sampling rate was every inch, averaging more than 12 in. For the PRORUT and Pong methods, the user set the sampling distance at 0.5 in. for the final profile report. A main program for each test was coded to call all subprograms to perform the same test on the same data base. The results of all profile computations were to be stored in a file for later plotting and analysis.

Test Results and Findings

The results of the bounce tests were tabulated for easy comparison in Table 3. The error generally increased as the vehicle's bouncing frequency neared the sampling interval. The sum of the absolute error of each frequency is given to identify the overall error. Spangler's and Pong's methods have the least amplitude errors.

The profile wavelength responses of all four methods are plotted with the same scale in Figure 1 for comparison. The VTI method had the steepest roll-off because it has the highest-order filter, which was a cascade of two filters in a series. Spangler's method is the next highest in roll-off. PRORUT's and VTI's responses fall off in the range of 10 to 70 ft, which corresponds with the quarter-car's resonance frequency at 40 mph. This is consistent because both methods were based on the same design. The plot shows a uniform response for the VTI method because it was simulated using a finer interval.

The results of the phase shift are plotted in Figure 2. As expected, the phase shift was found to be proportional to the order of the filtering process. The PRORUT had almost no phase shift.

The results of the step response test are plotted in Figure 3. The amount of overshoot and the settling time in the transient test were found to be proportional to the order of the filter in each method. A quadratic-curve removing process was performed on the PRORUT's step response because of its runaway due to low-order filtering. The PRORUT has the highest fidelity with respect to long wavelength. After the PRORUT method, Pong's method has the least overshooting and fastest settling time, followed by the Spangler and VTI methods.

The percentage roughness errors from the original profile for all sample sites are plotted in Figure 4*a*. A closer comparison was conducted by filtering the original profile to remove the long-wavelength parts and resubmitting the filtered

TABLE 3 AMPLITUDE RATIO OF INITIAL TEST

	Frequency (cycles per second)							
	0.10	0.25	0.50	1.00	2.00	5.00	10.0	Sum of Errors
PRORUT[a]	1.0708	0.8691	1.0251	0.9803	0.9861	0.9976	1.0232	0.0408
VTI-2	1.0074	1.0075	1.0075	1.0077	1.0084	1.0110	1.0323	0.0104
Spangler	1.0000	1.0000	1.0001	1.0002	1.0010	1.0060	1.0242	0.0045
Pong	1.0003	1.0001	0.9999	0.9991	1.0001	1.0065	1.0238	0.0045

Note: Value represents the ratio of the profiles computed by blocking out acceleration or height signal.

[a] PRORUT method does not have high-order lowpass filter to remove the integration runaway; the author had to use statistical methods to purify the post-integrated results for this purpose.

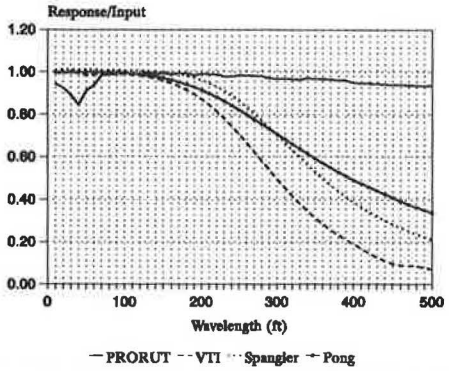

FIGURE 1 Comparison of wavelength response of AEIPR methods using computer simulation at simulation speed of 40 mph.

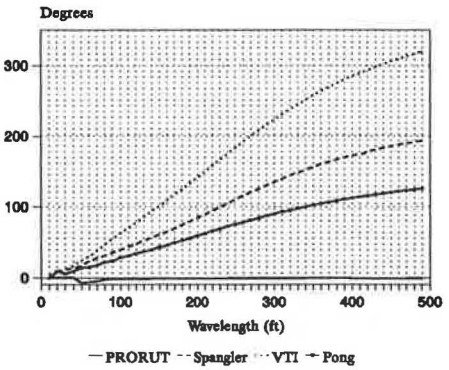

FIGURE 2 Comparison of phase shift of AEIPR methods using computer simulation at simulation speed of 40 mph.

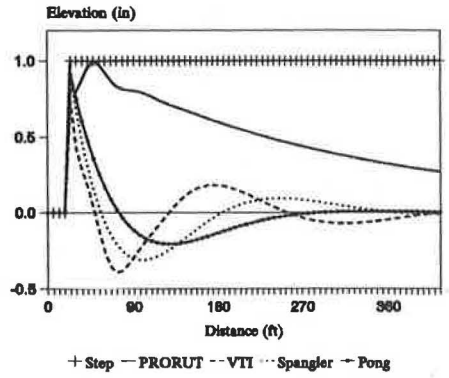

FIGURE 3 Comparison of step response of AEIPR methods using computer simulation at simulation speed of 40 mph.

profile for roughness reproduction. The plots with filtered original profile are given in Figure 4*b*. The difference in error magnitude was due to the removal of the long-wavelength profiles, which contribute a certain amount of roughness.

One test site was chosen as a profile for visual comparison with the reproduced profiles. The original and the reproduced profiles are plotted in Figure 5. The criterion for evaluation was the sum-of-square-error between the reproduced and the

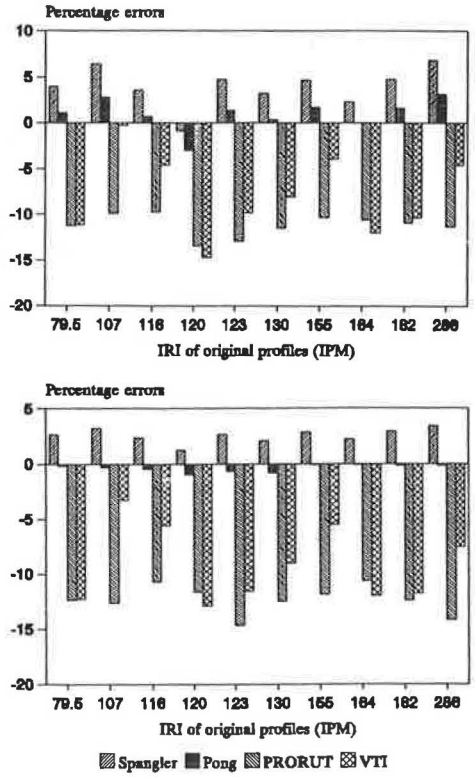

FIGURE 4 Percentage IRI errors of AEIPR methods using as references original profiles as reference, *top*, and highpass-filtered profile, *bottom*.

original profiles. The PRORUT method came the closest to reproducing the original profile, followed by the Pong, Spangler, and VTI methods. It should be noted that the errors are larger if more long-wavelength profiles are removed or distorted from the original profile.

The times required to compute 5,280 profile samples are for Spangler, 2.25 sec; Pong, 2.36 sec, PRORUT, 2.91 sec; and VTI, 6.86 sec. The result was obtained using an Intel 8088 with 8087 processors. Spangler's method is the least time-consuming, and Pong's comes in a close second. Both were

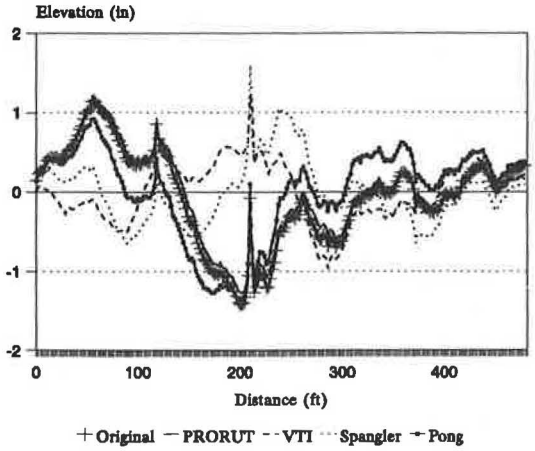

FIGURE 5 Comparison of road profile reproduction by AEIPR methods.

programmed for real-time profiling. VTI's method took the longest, but the VTI commercial system incorporates a real-time digital signal process (DSP) unit to compute profile and requires virtually no time.

Grading of Test Results

Each test result in the evaluation was given a performance index from 1 to 4 (worst to best) based on its ranking. For the amplitude errors test, both the Spangler and Pong methods had the same scores for their absolute error sum. For wavelength response, there was no preference as to how steep the long-wavelength profiles were to be filtered out. The results in this column were better for the lower filter order because filtering is a cutback in measurement fidelity. For phase shift response, the smaller the phase was, the higher the score. For IRI errors, the smaller the error was, the higher the score. The score for the profile reproduction was evaluated by the sum-of-square-error between the reproduced and the original profiles: the smaller the square error, the higher the score. For computation time, the shorter the time, the higher the score. The VTI method was an exception. VTI uses DSP hardware to perform the operation parallel in real-time and took virtually no computer time, which is reflected in the cost of the system.

Two kinds of summary analyses can be conducted: an analysis with equal weight or an analysis with unequal weight. Because the weighted analysis can vary from one to many possible combinations, other researchers can easily perform the analysis with their chosen weight based on these test results. In this paper, two cases were performed in summarizing the scores of the test performance: (a) a summary using equal weight shown in Table 4, and (b) a summary using selected weight. Based on PTI's needs for a profiler, the weight and the weighted scores are listed in Table 5. The sums of the indexes are close for three of the methods. Other users may have different requirements for their profilers and assign different weights for their needs, so these differences are likely to change the evaluation results. For example, if the user puts significant weight on the profile reproduction, the PRORUT system may be chosen. If the weight is on the IRI errors, either the Spangler or the Pong method may stand out. If the user prefers high-speed profiling with texture report, VTI is the only possible method. The profiling devices installed with profiling method of low scores in this evaluation do not necessarily produce unreliable measurements. The quality of a profile measurement also relies on the performance of the overall hardware instrumentation; only a good profiling method combined with precision instrumentation can provide a reliable profile measurement. Choosing the suitable method is as important as choosing the hardware. Once a good method is chosen, high cost-effectiveness will be the reward.

TABLE 4 SUMMARY OF PERFORMANCE RANKING SCORES OF AEIPR COMPUTATION METHODS

	Ampl. Errors	W.L. Resp.	Phase Shift	Step Resp.	IRI Errors	Profile Repr.	Computer Time	Sum of Indices
PRORUT	1	4	4[a]	4[a]	2	4	2	21
VTI	2	1[b]	1	1	1	1	1[c]	8
Spangler	3.5	2	2	2	3	2	4	18.5
Pong	3.5	3	3	3	4	3	3	22.5

[a] PRORUT method does not have a high-order lowpass filter to remove the integration runaway. The results were achieved with a quadratic curve removal procedure for the purpose of comparison.

[b] The result was obtained by setting VTI's sampling distance interval at 0.05 in; all others were set at 0.5 in. If it had been the same interval as the others, the pass band would be similar to PRORUT's.

[c] The VTI system used a Digital Signal Process (DSP) unit to compute the profiles in real time.

TABLE 5 SUMMARY OF PERFORMANCE RANKING SCORES OF AEIPR COMPUTATION METHODS USING PTI SELECTED WEIGHT

	Ampl. Errors	W.L. Resp.	Phase Shift	Step Resp.	IRI Errors	Profile Repr.	Computer Time	Sum of Indices
PTI Weight	1.5	1.1	0.5	0.3	1.5	0.9	0.2	
PRORUT	1.5	4.4	2	1.2	3	3.6	0.4	17.3
VTI	3	1.1	0.5	0.6	1.5	0.9	0.2	7.8
Spangler	5.25	2.2	1	0.3	4.5	1.8	0.8	15.85
Pong	5.25	3.3	1.5	0.9	6	2.7	0.6	20.25

CONCLUSION

In this paper, six computer simulation profiling performance tests were performed using four profile computation methods. The performances of the four methods were compared using a weight of 1 on each comparison. However, each comparison is not equal, and individual users must choose their own relative weights for what is important to them. The best AEIPR method can be identified only when the weights on the tests are chosen. The test results are provided as a reference for those concerned with selecting a profiling method for highway survey or research applications.

REFERENCES

1. J. C. Wambold, L. E. Defrain, R. R. Hegman, K. McGhee, J. Reichert and E. B. Spangler. State of the Art of Measurement and Analysis of Road Roughness. In *Transportation Research Record 836*, TRB, National Research Council, Washington, D.C., 1982.
2. G. J. Claros, W. R. Hudson, and C. E. Lee. *Performance of the Analog and the Digital Profilometer with Wheels and with Non-Contact Transducers*. Research Report 251-3F. Center for Transportation Research, University of Texas, Austin, April 1985.
3. M. W. Sayers and T. D. Gillespie. *The Ann Arbor Road Profilometer Meeting*. Report FHWA/RD-86/100. FHWA, U.S. Department of Transportation, 1986, pp. 1–2.
4. Report of Technical Committee on Slipperiness and Evenness. *Proc., 15th Congress, Permanent Association of Road Congresses*, Mexico City, Mexico, and Paris, France, 1975.
5. R. S. Dickerson and D. G. W. Mace. *A High-Speed Road Profilometer: Preliminary Description*. TRRL Report SR 182UC. U.K. Transport and Road Research Laboratory, Crowthorne, Berkshire, England, 1976.
6. P. B. Still and M. A. Wennett. *Development of a Contactless Displacement Transducer*. TRRL Report LR690. U.K. Transport and Road Research Laboratory, Crowthorne, Berkshire, England, 1975.
7. D. R. C. Cooper, *Measurement of Road Surface Texture by a Contactless Sensor*. TRRL Report LR639. U.K. Transport and

Road Research Laboratory, Crowthorne, Berkshire, England, 1974.
8. *A New Roughness Measurement System*. Highway Product International. R. R. #1. Paris, Ontario, Jan. 1986.
9. S. C. Ashmore and H. C. Hodges, Jr., *Dynamic Force Measurement Vehicle and Its Application to Measuring and Monitoring Road Roughness*. Nevada Automotive Testing Center, 1991.
10. C. B. Breed. *Surveying*, 3rd ed. John Wiley and Sons, Inc., New York, N.Y., 1977, pp. 91–107.
11. J. H. Woodstorm. The California Profilograph. *Proc., ASTM Symposium on Measurement Control and Correction of Pavement Roughness in Construction*, Phoenix, Ariz., Dec. 1982.
12. *Operation of California Profilograph and Evaluation Profiles*. Test Method Calif. 526-E. State of California Department of Public Works, Division of Highways, Sacramento, Oct. 1972.
13. R. S. Walker and H. T. Lin. *Automated Pavement Data Collection Profilograph Correction Study with Present Serviceability Index*. Report FHWA-DP-72-3. FHWA, U.S. Department of Transportation, 1987.
14. B. T. Kulakowski and J. C. Wambold. *Development of Procedures for the Calibration of Profilographs*. Report FHWA-RD-89-110. FHWA, U.S. Department of Transportation, 1989.
15. F. N. Hveem. Devices for Recording and Evaluating Pavement Roughness. *Bulletin 264*, HRB, National Research Council, Washington, D.C., 1960, pp. 1–26.
16. M. W. Sayers, T. D. Gillespie, and W. D. O. Paterson. *The International Roughness Experiment: Establishing Correlation and a Calibration Standard for Measurements*. World Bank Technical Paper 45. Washington, D.C., Jan. 1986.
17. J. R. Darlington and P. Milliman. A Progress Report on the Evaluation and Application Study of the General Motors Rapid Travel Profilometer. In *Highway Research Record* 214, HRB, National Research Council, Washington, D.C., 1968, pp. 50–67.
18. M. R. Hegman and M. W. Sayers. *Reference Manual for the UMTRI/FHWA Road Profiling (PRORUT) System*. Report FHWA-RD-87-004. FHWA, U.S. Department of Transportation, 1987.
19. D. L. Huft. *Description and Evaluation of South Dakota Road Profiler*. Report FHWA-DP89-72-002. FHWA, U.S. Department of Transportation, Nov. 1989.
20. P. W. Arnberg. *The Laser Road Surface Tester (RST): Synopsis of Presentation in Sydney and Melbourne, Australia*. March 1986.
21. M. M. Pong. *The Development of an Extensive-Range Dynamic Road Profile and Roughness Measuring System*. Ph.D. thesis. Department of Mechanical Engineering, Pennsylvania State University, University Park, 1992.
22. E. B. Spangler. Method and System for Measurement of Road Profile. U.S. Patent 4,422,322, issued Dec. 27, 1983.
23. A. J. Cadzow and R. H. Martens. *Discrete-Time and Computer System*. Prentice-Hall, Inc., Englewood Cliffs, N.J., 1970, pp. 383–387.
24. J. J. Lu. *Evaluation of Road Profile Computation Methods*. M.S. thesis. Department of Mechanical Engineering, Pennsylvania State University, University Park, 1989.
25. M. W. Sayers, T. D. Gillespie, and W. D. O. Paterson. *Guidelines for Conducting and Calibrating Road Roughness Measurements*. World Bank Technical Paper 46. Washington, D.C., Jan. 1986.

DISCUSSION

GÖRAN PALMKVIST AND GEORG MAGNUSSON
Swedish Road and Traffic Research Institute, S-581 01 Linköping, Sweden.

It is to be regretted that VTI was not given the opportunity to review this report prior to presentation, although it is said that "The developers were consulted to verify the correctness of their profiling programs and the results of their method." The VTI method for computing IRI and the highpass-filtered profile has thus not been interpreted correctly in the paper.

Already, on April 17, 1989, when VTI commented on the subroutine VTIPROF for the purpose of a similar PTI study by Jiunn-Jye Lu (who came to completely different results), we remarked that ω_n is set to the constant value of 0.25 in the second-order filter in the time domain. In the program used in the paper the cutoff frequency for this filter is set to the frequency corresponding to the cutoff wavelength 300 ft when the simulated speed is 40 mph, that is, $\omega_n = 1.23$. The same cutoff wavelength is also used for the third-order filter in the spatial domain.

An easy test of the function of the measurement method is to perform a so-called bounce test, meaning that the test vehicle will be put in a vertical bouncing mode while stationary. The profile output shall be a straight line. In the paper this test was simulated by blocking out the acceleration or the height signal and the error calculated as the ratio between the two signals thus generated. However, this method does not consider the effect of the phase shift between the signals. A correct bounce test performed at 1-Hz bounce frequency gives the error 0.0008, as compared with 0.0077 in Table 3. At 10 Hz, the error is about 0.005, as compared with the 0.03 found by the authors.

The use of the same cutoff wavelength in the second-order and the third-order filters in effect means that the VTI method is supposed to use a fifth-order filter—or even sixth, as was said at the presentation. This will of course very much influence the wavelength, phase shift, and step response, as illustrated in Figures 1 through 3.

This wrongly calculated highpass-filtered profile is then used for the calculation of IRI, resulting in too low a value, as illustrated in Figure 4. In the Laser RST, the IRI values furthermore are always calculated from the slope profile.

The use of the incorrectly simulated filtering process also has an adverse effect on the profile reproduction, as illustrated in Figure 5. It should also be pointed out that this comparison is meaningless, or at least not fair, because the PRORUT profile is linearly filtered and the VTI and Spangler profiles are not; as for the Pong profile, we do not know. Figure 6 shows that if the VTI profile is linearly filtered, the agreement with a profile established by rod and level or dipstick is excellent.

We do not understand the significance of the calculated time for computing 5280 profile samples. It seems more to be characteristics of the simulation programs used than for the measurement devices studied. About the VTI system, it works in real time and consequently makes the calculations within the time limits required in each case, at measurement speeds up to 90 km/hr. This is also observed by the authors.

CONCLUSION

Our conclusion is that the evaluation of the VTI system as presented is incorrect because the processing of the input data is not in concordance with the actual procedures used in the Laser RST. Although this is only a theoretical analysis of different methods, all divergences from the original procedures must be clearly stated so that the readers will be given the possibility to judge for themselves.

COMMENT

As is pointed out in the paper, the VTI system is a real-time measurement method; it is possible to store the computed slope profiles and also highpass-filtered profiles as a function

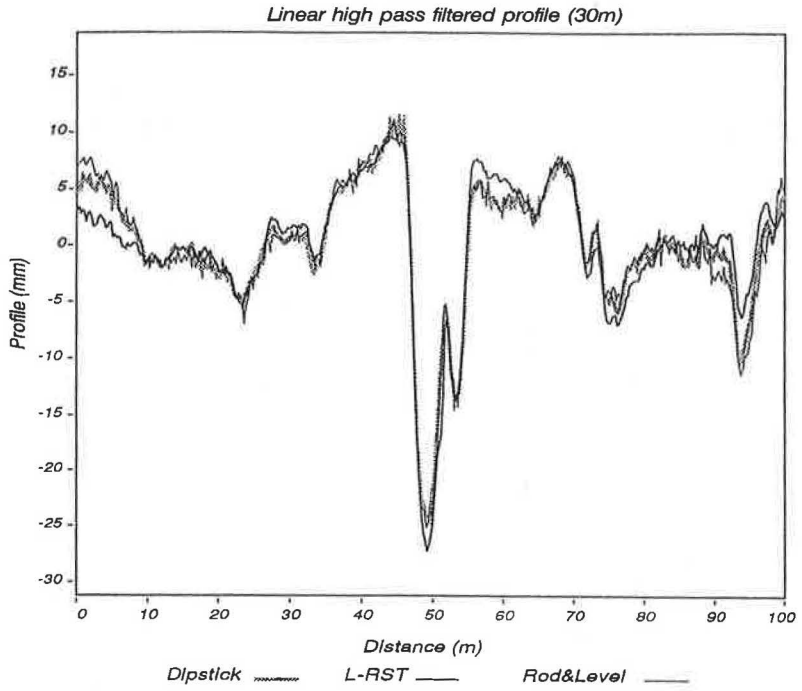

FIGURE 6 Linear highpass-filtered profile (30 m).

of distance. By postprocessing it is subsequently possible, for example, to obtain a linear phase response of the highpass-filtered profile by backward filtering or to choose another filter order or cutoff wavelength for the filter in the spatial domain.

AUTHORS' CLOSURE

The study performed by Jiunn-Jye Lu at PTI in 1989 was found to lack a few installments in the quarter-car simulation model. After the problem was identified and corrected, a second paper was written that also included comments from the readers of the original paper. The VTI-method computer simulation program used in this paper was reviewed and corrected by VTI staff in 1988. We have been using this version since. Unless there were more improvements made in this period, the results presented in the paper should be reliable.

We all know that each road profiling system has different filter. The cutoff wavelength of the filter can always be adjusted to get the best result for wavelength range of interest. In this paper, we wished to make the comparison straightforward by using the same cutoff wavelength for all methods, so a 300-ft wavelength was used. The results presented in the paper matched the order of filter in each method theoretically. VTI used a second- and a third-order (a fifth-order) filter. Please allow me to apologize that I mistakenly called it a sixth-order filter in the presentation. We fully understand that each method could be optimized by choosing the filter cutoff setting, but to compare the methods we used the same for all because we did not know the optimal setting in some cases.

The bounce test was performed using computer simulation. The purpose of blocking out one of the sensors was to avoid any alteration of the original program codings for extracting only one signal. No careful phase-matching procedure was done to any profiling method. The different results that VTI presented in the discussion might be from a different approach. However, the procedures for testing all four methods were identical.

The IRIs in the original paper were calculated from the profile according to the Mike Sayers procedure presented in the World Bank paper. I took time to recalculate the IRIs from the slope profiles according to the original VTI and PRORUT specification. The results showed no significant difference to the original.

The purpose of the profile visual comparison presented in Figure 5 was to show that the amount of profiles of long wavelengths was removed from the original. Theoretically, the VTI method contains a "fifth-order" filter that is the highest of any method and thus attenuates the most when the same cutoff settings are used. The computer simulation shows the proof.

The paper explained exclusively that the computation time was the time requirement for a profiling method to finish 5280 profile samples in a IBM-PC XT with math coprocessor. In the heavily computer-aided engineering stage, computation efficiency is also a factor to be observed. Because all profiling systems are computer-processed, we felt the need to look into this aspect. We had made it clear that VTI use a real-time DSP unit in the paper, regardless of the comparison.

I wish to thank the VTI for pointing out the typing errors in the paper. I have made the correction in the final revision. However, there was no such mistake in the computer simulation program.

CONCLUSION

As I have clearly stated in the paper: the readers should judge for themselves of the evaluation procedures and the results presented in this paper. Readers must perform a final evaluation based on their own needs.

Publication of this paper sponsored by Committee on Surface Properties–Vehicle Interaction.

Wheel Track Rutting Due to Studded Tires

JAMES R. LUNDY, R. G. HICKS, TODD V. SCHOLZ, AND DAVID C. ESCH

The extent of pavement rutting attributable to studded tires was investigated to determine the extent to which pavement wear has contributed to rut development in Alaska. The investigation is based on an extensive literature review as well as a survey questionnaire sent to all highway agencies in the snow zones of North America and Northern Europe. In addition, measurements of studded tire use and wheel track rutting taken at several locations in Alaska during the winter of 1990 provided new information. Very little research has been done since 1975 in this area, except in Scandinavia. Nearly all agencies continue to prohibit or restrict the use period of studded tires, but enforcement of stud use is typically minimal. Very little new information on the percentage of vehicles using studded tires or on tire wear studies is available, except for recent stud use surveys performed in Alaska from 1989 to 1991. At the sites studied, approximately 25 percent of all tires were studded during winter. Factors affecting wear rates are defined, and limited wintertime wear rate measurements in Alaska indicate that pavement wear occurs at a rate of about 0.1 to 0.15 in./million studded tire passes. The contributions of wear from studded tire abrasion in pavement rut development must not be ignored when factors in pavement rutting are analyzed. This analysis will be very difficult in many states because there is almost no information available on actual stud use or on the wear rates from modern vehicles and tire types.

The public has long associated the use of studded tires with improved traction on highways during the winter months when the road surfaces are often icy. However, studded tires also have been shown to increase road wear on both asphalt and portland cement concrete pavements. This paper has been prepared to document the use and effects of studded tires, particularly in terms of producing wheel track ruts.

Specific objectives of this paper are to

1. Quantify the current use of studded tires throughout North America and Northern Europe. This includes data on (a) percentage of vehicles using studded tires, (b) characteristics of the studs (type and number), and (c) periods that studded tires are permitted.
2. Summarize the results of road wear studies (field and test tracks) in each of the following areas: (a) mechanism of pavement wear, (b) rate of pavement wear, and (c) factors affecting the wear rate.
3. Identify the reported consequences and benefits of using studded tires such as (a) increased pavement maintenance to repair ruts, (b) increased safety problems due to splash and spray from rutted pavements, and (c) reduced stopping distance on icy roads.

J. R. Lundy, R. G. Hicks, and T. V. Scholz, Department of Civil Engineering, Oregon State University, Corvallis, Oreg. 97331. D. C. Esch, Alaska Department of Transportation and Public Facilities, Fairbanks, Alaska 99709.

To accomplish the stated objectives, several work activities were undertaken. These included

1. A computer literature search (using Transportation Research Information Services). Many publications identified in this search were reviewed and evaluated in the preparation of this paper.
2. A survey of agency practices. A survey form was developed and mailed to 30 highway agencies in the United States, 11 Canadian provinces and territories, and 4 foreign countries (Norway, Sweden, Finland, and the former West Germany).
3. A telephone survey of selected tire manufacturers to identify the types and number of studs being used.
4. A field survey of studded tire use in Alaska at Fairbanks, Anchorage, and Juneau.
5. Roadway rut depth measurements made in Juneau at four roadway locations. Measurements were taken at fixed points using five dial indicators mounted on rut measurement bar.

STUDDED TIRE PRACTICES

The data presented in this section are the result of an extensive literature review, the survey of selected transportation agencies and selected calls to manufacturers of studded tires. Information was obtained from various agencies in the United States, Canada, and Europe.

Use of Studded Tires

The results of the 1990 survey of snow zone agencies in North America and Northern Europe provided an indication of studded tire use. The results shown in Table 1 indicate that a number of agencies permit their use. When compared with the results of a similar survey from 1975 (*1*), it is seen that three states that allowed studded tires in 1975 now prohibit their use: Arizona, Maryland, and Michigan. Of the agencies surveyed in 1990 that formerly prohibited studded tires, only California has passed legislation allowing their use. It should also be noted that in all cases where studs are permitted, chains are too.

In addition to the increasing number of states prohibiting the use of studded tires, most states restrict their use to winter months. On the basis of the results of the literature review, the periods to which studded tire use is restricted in the United States and Canada is shown in Figure 1 (*1*). Note that in the 1970s 14 states and 2 provinces had no restrictions and that 9 states and 1 province prohibited the use of studded tires.

TABLE 1 AGENCIES PERMITTING THE USE OF STUDDED TIRES (*14*)

United States[a]	Canada[b]	Europe[c]
Alaska	New Brunswick	Sweden
California	Nova Scotia	Norway
Colorado	Quebec	Finland
Connecticut	Saskatchewan	
Delaware		
Idaho		
Indiana		
Iowa		
Kansas		
Maine		
Montana		
Nebraska		
Nevada		
New Jersey		
New York		
North Dakota		
Oregon		
Pennsylvania		
Rhode Island		
South Dakota		
Utah		
Vermont		
Washington		
Wyoming		

[a]Survey forms were sent to 34 states. States not allowing studs: Illinois, Maryland, Michigan, Minnesota, and Wisconsin. New Hampshire, Massachusetts, Ohio, and New Mexico did not respond.
[b]Survey forms were sent to 11 provinces. Provinces not allowing studs: Alberta, NW Territories, and Ontario. British Columbia and Yukon Territory did not respond.
[c]Germany does not allow studded tires.

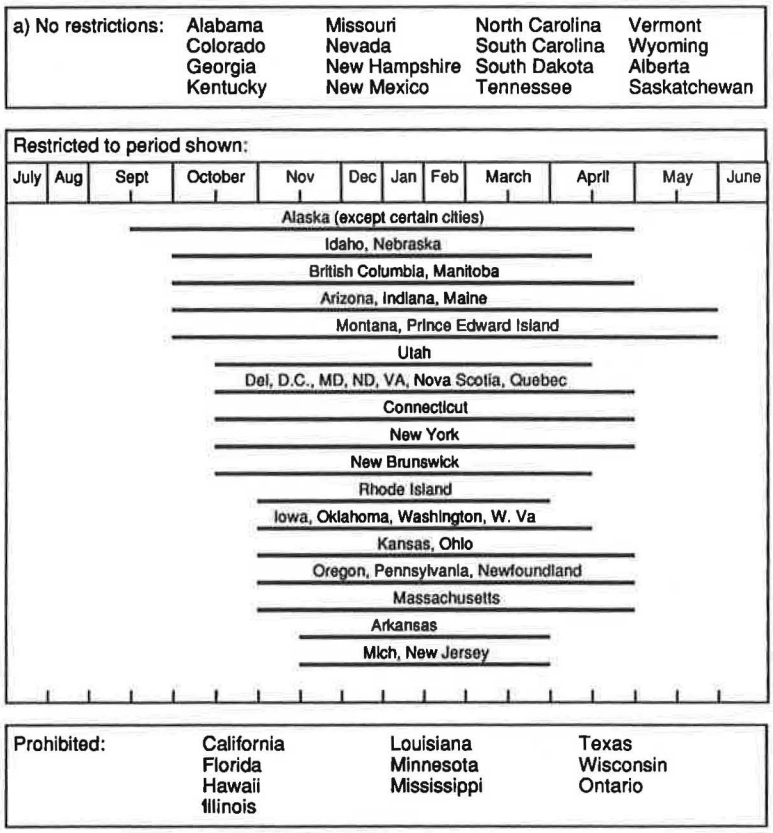

FIGURE 1 Legal restrictions on use of studded tires (*1*).

The remaining states and provinces allow the use of studded tires only during fall, winter, and spring. The results of the 1990 survey (Table 2) showed, for North America, that only three agencies had no restrictions, 25 states or provinces restricted stud use to a given time period, and eight agencies prohibited their use. Of those agencies restricting the use of studs to a specific period, most restrict use to the period from October through April. Similar results from the European countries surveyed are also given in Table 2.

Percentage of Vehicles with Studs

The surveys did not provide much useful information on studded tire use. In fact, only a few agencies were able to provide an estimate of current usage. Therefore, heavy reliance was placed on results from the literature (pre-1980) because the actual use rates are virtually unknown in the United States and Canada.

Historical data on the percentage of studded tire use in the United States and abroad are given in Table 3. These data show studded tire use ranges from 0 to approximately 75 percent of all vehicles. In areas that have harsh winters, it ranges from about 20 to 75 percent. In general, Sweden and Finland have higher rates than most North American agencies. Only Finland had information comparing truck and car use.

A 1990 survey of studded tire use in Alaska is given in Figure 2. As indicated, studded tire use varies by season as well as by year and location. However, it can be seen that wintertime use (through March) by light vehicles is between 20 and 35 percent. It is also noteworthy that between 3 and 6 percent of the surveyed vehicles used studded tires in summer, when Alaska prohibits their use. Data from Anchorage, Fairbanks, and Juneau were averaged, and the studded tires per vehicle pass are shown in Figure 3. Use rates in studded tires passes per vehicle pass range from a low of 0.05 in the summer to about 0.5 during the winter.

Enforcement

The results from the 1990 questionnaire also investigated the role of enforcement during prohibited periods. Generally, the risk of getting caught is considered low to moderate. Only South Dakota, Washington, Illinois, Minnesota, Nevada, Ontario, and Quebec indicated a high risk. Highway agencies in three of these locations (Illinois, Minnesota, and Ontario) do not allow studded tires, eliminating the need for seasonally based enforcement. The cost of being cited also varies considerably; fines range from less than $25 to $500 plus vehicle impoundment.

Characteristics of Studded Tires

A typical studded tire is essentially a normal winter or all-season tire with studs embedded in the tread. Typical specifications for studded tires for passenger cars are shown in Table 4.

Although many types of studs were found in the literature, all have similar parts: a pin (typically tungsten carbide) surrounded by the stud housing or body (typically steel), which has a flange at its base to hold the stud in the tire tread. Four basic stud types have been used; Table 5 summarizes the characteristics of each type. Conversations with tire manu-

TABLE 2 RESTRICTIONS ON USE OF STUDDED TIRES (*14*)

a)	US/Canada			
a)	No restrictions	Colorado Vermont Saskatchewan	Note: Several other states outside the snow zone were not surveyed. These states may or may not restrict the use of studs.	
b)	Restricted to time period shown	Alaska Connecticut Iowa Kansas Maine Nevada New Jersey New York Rhode Island Utah	(September 15 - April 30 (north of latitude 60°N) (October 1 - April 14 (south of latitude 60°N) (November 15 - April 30) (November 1 - April 1) (November 1 - April 5) (October 1 - May 1) (October 1 - April 30) (November 1 - April 1) (October 15 - May 1) (November 15 - April 1) (October 15 - March 15)	
c)	Restricted (period unreported)	California Delaware Idaho Indiana Montana Nebraska	North Dakota Oregon Pennsylvania South Dakota Washington Wyoming	New Brunswick Nova Scotia Quebec
d)	Prohibited	Arizona Illinois Maryland	Michigan Minnesota	Alberta Northwest Territories Ontario
b)	Northern Europe			
a)	No restrictions			
b)	Restricted	Norway Sweden Finland	(Period unreported) (31 October to Easter) (1 November to 31 March)	
c)	Prohibited	Germany		

TABLE 3 HISTORICAL DATA ON USE OF STUDDED TIRES

Agency		% of Vehicles with Studs	Agency	% of Vehicles with Studs
United States (*1*)	Alabama	1	Nevada	6
	Alaska	61	New Hampshire	30
	Arizona	1	New Jersey	20
	Arkansas	1	New Mexico	NA
	California	NA	New York	30
	Colorado	30	North Carolina	2
	Connecticut	25	North Dakota	32
	Delaware	18	Ohio	20
	Florida	NA	Oklahoma	1
	Georgia	NA	Oregon	10
	Idaho	27	Pennsylvania	28
	Illinois	12	Rhode Island	NA
	Indiana	10	South Carolina	3
	Iowa	25	South Dakota	40
	Kansas	7	Tennessee	NA
	Kentucky	12	Texas	0
	Maine	NA	Vermont	60
	Maryland	NA	Virginia	10
	Massachusetts	32	Washington	35
	Michigan	12	West Virginia	10
	Missouri	14	Wisconsin	20
	Montana	60	Wyoming	35
	Nebraska	38		
Canada	Ontario (*15*)			32
	Manitoba (*11*)			20-25
	Quebec (*11*)			50
	Maritime Provinces (*11*)			50+
	Ottawa (*15*)			48
Finland (*16*)	Cars			90-95
	Trucks			40
Sweden (*3*)				60

facturer and distributor personnel revealed that only the controlled protrusion (Type I) stud is currently used in the United States. The principal reason is that as the stud housing or body wears, coinciding with the tread wear, the tungsten carbide pin is pushed deeper into the stud housing, providing a uniform protrusion length throughout the life of the stud. This benefit is not fully realized with the other stud types, because the protrusion length of the stud can vary over time. Figure 4 gives the dimensions for the controlled protrusion stud. The number of studs per tire generally ranges from 64 to 120.

In Sweden it has been long recognized that conventional studs cause excessive pavement wear. In Sweden, therefore, a new ice stud was developed that features low noise and reduced road wear. It weighs only 0.7 g yet reportedly retains ice grip and durability. The reduction in weight is possible because of the use of a new polymer in the stud body (B. Simonsson, personal communication, Aug. 1990).

ROAD WEAR STUDIES

This section of the paper summarizes the results of studies from throughout the world to identify the cause (mechanism) of pavement wear owing to studded tires, the factors that affect the rate of wear, and the rate of pavement wear.

Cause of Pavement Wear

The results of the literature review indicated that the mechanism of wear is primarily by abrasive action. Niemi (*2*) has identified four mechanisms that contribute to pavement wear, as shown in Table 6. Which of the mechanisms is most important is still open to debate. In Alaska it is generally thought

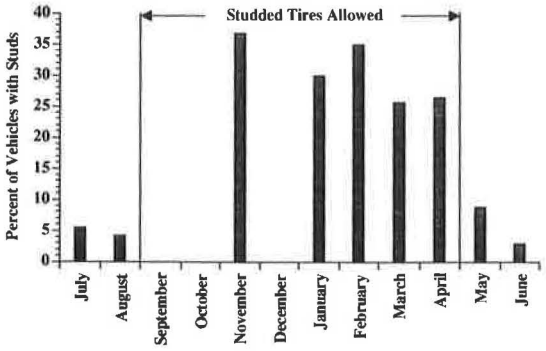

FIGURE 2 Studded tire use survey results from Alaska (*10*).

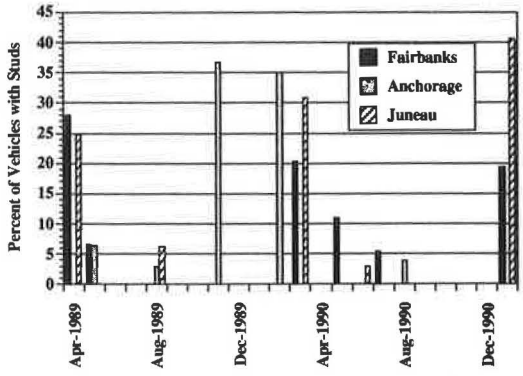

FIGURE 3 Average seasonal studded tire usage patterns in Anchorage, Fairbanks, and Juneau, Alaska (*10*).

TABLE 4 TYPICAL CROSS-SECTIONAL AREA SPECIFICATIONS (*1*)

Nominal Car Size	Tire Data		Tire Stud Data		
	Nominal Size	Typical Tread Surface Area (sq. in.)	Typical Maximum Number of Studs	Typical Cross-Sectional Area (sq. in.)	Percent of Tread Surface Area
Compact	B78x13	250	96	.0314	1.25
Intermediate	F78x14	270	96	.0314	1.10
Full Size	H78x15	312	96	.0314	1.00

that the primary mechanism of studded tire wear is by scraping off the mastic and subsequent abrasion of the aggregate.

Factors Affecting Wear Rate

Several factors have been identified as affecting the rate of pavement wear. Keyser (*3*) has prepared an excellent summary of these factors. As shown in Table 7, Keyser identified the characteristics of the pavement, traffic, and vehicle and tires that affect the rate of wear. In addition, Keyser (*4*) stated the most important factors for bituminous pavement wear were wheel load, stud protrusion, temperature, and humidity.

Figures 5 and 6 show the effect of pavement type on wear rate. The "regular" bituminous pavements consisted of fine-graded mixtures for thin overlays with 85 to 100 penetration asphalts; the "high-type" bituminous pavements contained either rubber or asbestos admixtures and 85 to 100 penetration asphalts. The regular pavements contained a filler, but the high-type pavements did not. For both tests (on a test track and on typical highway pavements), the wear rate was considerably greater for asphalt concrete than for portland cement concrete pavements. Aggregate type also had an effect for the portland cement concrete pavements.

Other factors can also affect the wear rate. For example, the wear rate in acceleration can be 2½ times the wear rate in deceleration that is 2 times the rate at a constant speed (*5*). In addition, temperature affects wear rates for asphalt concrete. The work by Krukar and Cook (*6–9*) shows the lowest wear rate at or near O°C. Increases in pavement wear as pavement temperatures go below O°C are reportedly associated with increased tire hardness and pavement stiffness. As pavement temperature decreases, pavement stiffness increases, as does the force required to push the stud into the stiffer tire so that it is flush with the pavement surface. Thus for a given loading situation, more of the stud will protrude when the temperature is lower, which results in higher stud forces. This combination of high stud force and increased pavement brittleness may result in increased wear rates. Keyser (*3*) reported increases in the rate of wear when the pavement is wet.

Pavement Wear Studies

The number of pavement wear studies is limited. Some agencies have conducted both field and laboratory studies; most studies have not shown good correlation between field and

TABLE 5 CHARACTERISTICS OF STUDS (*6*)

Stud Type	Characteristics
Type I "Controlled Protrusion Stud"	• Carbide pin will move further into stud body if protrusion limit is exceeded • 18 percent lighter in weight than conventional stud • 5 percent smaller flange than conventional stud
Type II "Perma-T-Gripper Stud"	• Pin found in other studs has been replaced with relatively small tungsten carbide chips in a soft bonding matrix enclosed in a steel jacket • Designed to wear within 10 percent of tire wear, thus maintaining a protrusion of approximately 0.020 in. or less
Type III "Conventional Stud"	• Tungsten carbide pin • Stud protrusion will increase with tire wear
Type IV "Finnstop Stud"	• Complete stud of light plastic casing with a tungsten carbide pin • Stud can be adjusted close to the tread rubber eliminating oscillation of the stud • Pin angle contact with road varies little with speed • Plastic housing tends to reduce effect of centrifugal force and heat build-up between rubber and stud • Air cushion can be left under stud to reduce stiffness (floating stud)

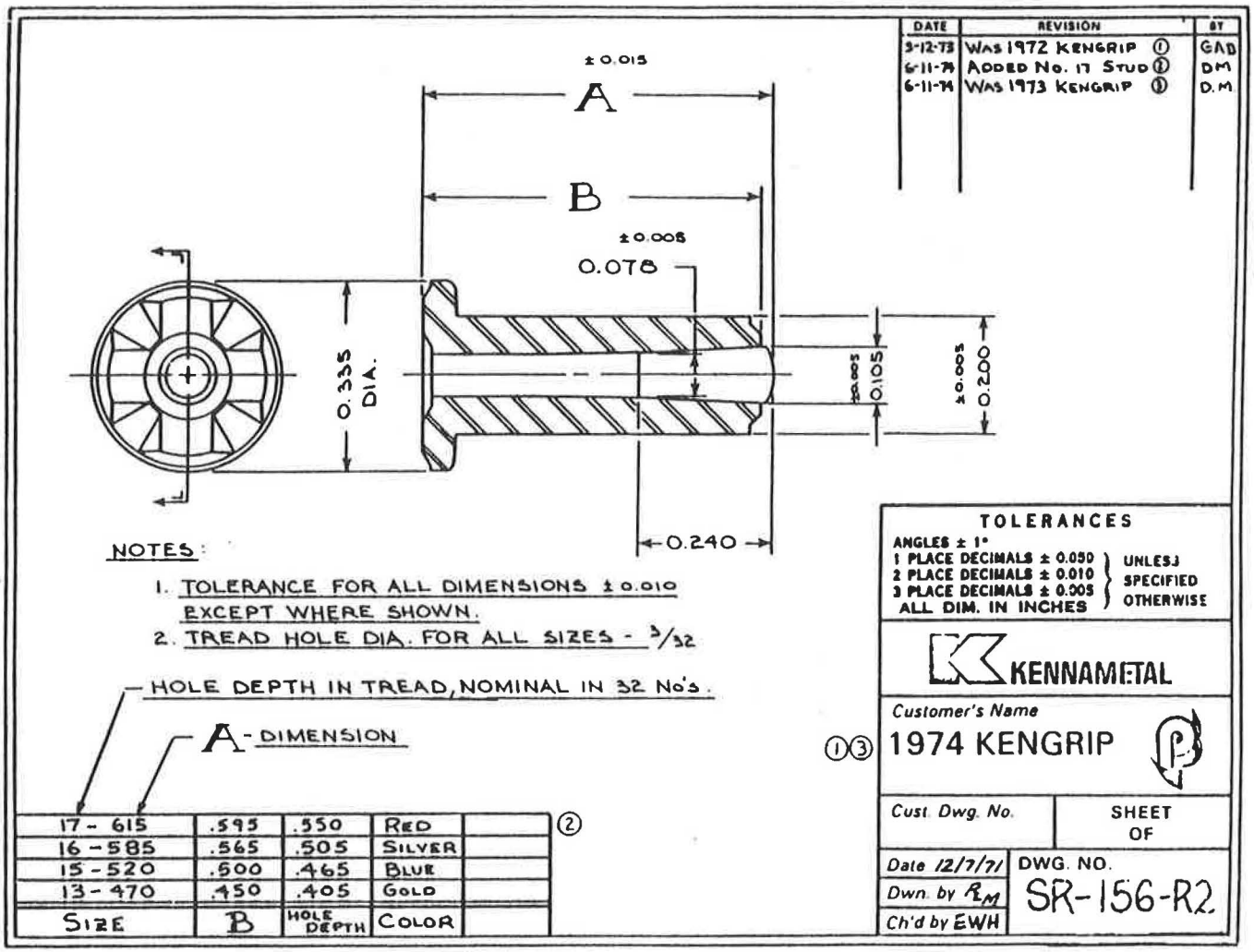

FIGURE 4 Typical dimensions for a controlled protrusion stud (*1*).

laboratory testing. The literature review and survey yielded some basic information, as shown in Table 8. In general, these results indicate

1. Reported wear rates, and the units used, vary considerably between agencies. Differences in wear rates are probably due to differences in materials and in percentages of vehicles with studded tires.
2. Pavement type has a great effect on pavement wear. Asphalt surfaces wear at a faster rate than portland cement concrete.
3. In areas of acceleration and deceleration, pavement wear increases substantially.

As part of an Alaskan investigation of wheelpath rutting, measurements of rut depths were correlated with rates of studded tire use. Data were collected at three locations in Juneau using the device shown schematically in Figure 7. The results are summarized in Table 9. The wear rate was computed by dividing the maximum rut depth by the estimated studded tire passes. The area of wear is characterized by rut-depth values taken at five locations across the 5.5-ft measure-

TABLE 6 CAUSE OF PAVEMENT WEAR UNDER STUDDED TIRES (*2*)

Cause	Description
1	The scraping action of the stud produces marks of wear on the mastic formed by the binder and the fine-grained aggregate.
2	The aggregate works loose from the pavement surface as a result of scraping by studs.
3	Scraping by the stud produces marks of wear on stones. Only in very soft aggregate does a rock fragment wear away completely by this action.
4	A stone is smashed by the impact of a stud and the pieces are loosened by the scraping action of the stud.

TABLE 7 FACTORS AFFECTING PAVEMENT WEAR (*3*)

Factor	Component	Characteristic
Vehicle, tire, and stud	Vehicle	Type and weight Axle load Number of studded tires (front, rear)
	Tire	Type (snow or regular with or without stud receiving holes) Pneumatic pressure Age Configuration of studs Number of studs
	Stud	Type (material, shape) Protrusion length Orientation of studs with respect to tire wear
	Stud wear vs. tire wear	
Pavement	Geometry	Cornering (curve, sharp turn) Straight section Intersection Slope (up and down)
	Surfacing Material	Type and characteristics (bituminous mixtures, surface treatment, precoated, chipping, portland cement, hardness) Age
	Surface Condition	Surface texture and profile Icy Compacted snow (compactness) Sanded or salted icy surface Slush
Environment	Humidity, temperature	Wet, dry, humid
Traffic	Volume	Number of passes and composition
	Speed	
	Wheel track	Width; Distribution of wheel load
	Contact mode	Start (normal, abrupt) = spin Stop (normal, abrupt) = skid Acceleration (rate) = spin Deceleration (rate) = skid
Measure	Method and precision	

ment bar in each wheelpath. This area was used to estimate the loss of material per lane mile.

The rates of wear are very consistent at each of the three sites and are much less than any rate reported by the other agencies surveyed (except Connecticut). The data collected on the bridge and before the bridge (see Table 9) produced very similar wear rates, eliminating the possibility that the measured rutting resulted from subgrade deformation. Measurements were also taken at different times of the year to isolate the pavement wear attributable to stud use during the winter and the "no studs allowed" summer seasons. Esch (*10*) reported that rut depths increased much more rapidly during the winter than the summer months. Furthermore, about 10 percent of the total rutting comes from stud use during summer.

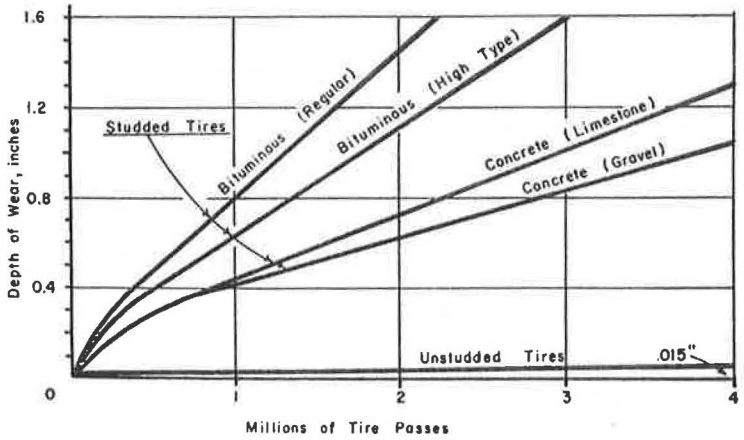

FIGURE 5 Relationship of studded-tire–induced wear versus pavement type, Minnesota research: wear rates of pavement specimens at test track (*19*).

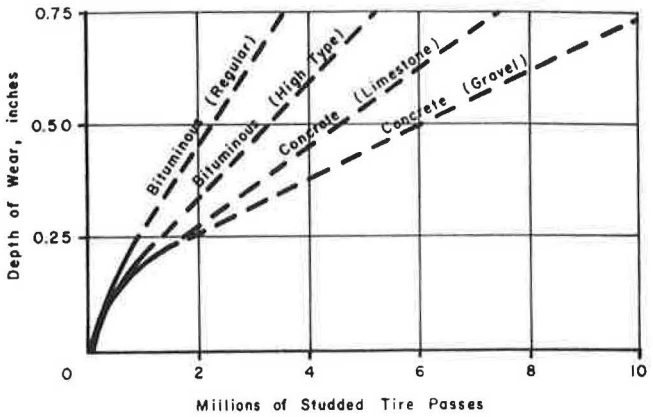

FIGURE 6 Relationship of studded-tire–induced wear versus pavement type, Minnesota research: wear rates of pavements of typical Minnesota highways (*19*).

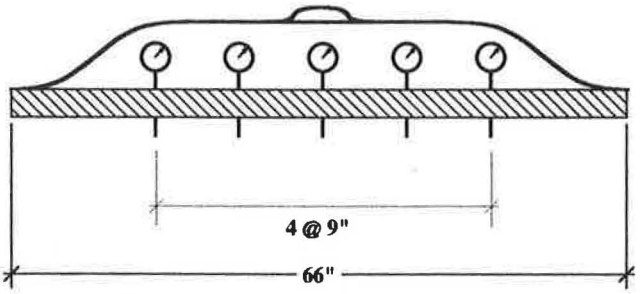

FIGURE 7 Rut-depth measurement device used for data collection in Alaska.

IMPACTS OF STUDDED TIRE USE

The impacts of studded tire use are twofold: (a) increased costs to the agencies through accelerated pavement wear and through safety problems created by the wheel track ruts, and (b) benefits derived through increased traction during icy conditions that either improve safety or allow increased speeds (Table 10). This section discusses each of these effects; it is based on the literature review, the survey of agencies, and limited cost analysis.

Benefits

The literature has some data that are useful in defining the economic benefits of studded tire use (Table 11). Finland and Sweden show significant benefits attributable to the increased safety. In contrast to the findings in Scandinavia, studies conducted in the United States in the 1970s show mixed results.

TABLE 8 SUMMARY OF ROAD WEAR STUDIES

Reference		Rate of Wear (in./passes)	Avg. Rate in inches/ 100,000 passes
a) Literature (14)			
Quebec		0.25/100,000	0.25
Quebec	Acceleration	0.36-0.44/100,000	0.40
	Deceleration	0.18-0.20/100,000	0.19
	Normal	0.11/100,000	0.11
Germany		0.11/120,000	0.09
Finland		.15-.2/10,000 AADT	
Sweden		0.5/40,000 AADT	
Maryland		0.28-1.07/100,000	0.7
Minnesota		1.5/4,000,000	0.04
Oregon	Concrete	0.026/100,000	0.03
	Asphalt	0.066/100,000	0.07
b) Survey (14)			
California		0.0005-0.0018/1000	0.12
Connecticut		0.08/1,000,000	0.01
Maryland		0.028-0.107/10,000	0.68
New Jersey		0.05 per year for 5400 AADT per lane	
New York		0.009-0.016/year PCC pavements 0.022-0.025/year ACC pavements	
Oregon		0.032/100,000 PCC pavements 0.073/100,000 ACC pavements	.03 .07
Norway		SPS[a]: AC = 25 Topeka = 15 Mastic stone = 10-15 PCC = 10	
Sweden		35 g/vehicle (4 studded tires)/km driven	

[a]SPS = g/cm (specific wear in grams worn out of the surfacing when a car with 4 studded wheels drives a 1 km distance)

TABLE 9 JUNEAU PAVEMENT WEAR PER MILLION STUDDED TIRES

Location	Total Stud Passes by 4/91 (Millions)	Wear per Million Passes		
		Wear Rate (inches)	Wear Area $(inches)^2$	Tons/Lane/Mile
Juneau-Douglas Bridge				
On Bridge	5.37	0.148	9.31	23.9
Before Bridge	5.37	0.134	9.92	25.5
Douglas Road	3.87	0.122	9.08	23.3
Mendenhall Loop	5.84	0.102	7.56	19.3

TABLE 10 IMPACT OF STUDDED TIRE USE

Factor	Consequences	Benefit
Effect on safety	• Increased rutting, ponding and hydroplaning • Increased splash and spray • Increased stopping distance on wet or dry concrete pavement	• Improved stopping distance on ice • Improved maneuverability on ice
Effect on pavement	• Increased rutting • Destruction of pavement markings • Build up of snow and ice in ruts	• Possible improvement in surface roughness
Effect on agency	• Increased frequency of maintenance/rehabilitation due to rutting	• Possible reduced winter maintenance costs

TABLE 11 ANNUAL COST EFFECTS OF STUDDED TIRES ON PAVEMENT WEAR AND SAFETY

Agency	Pavement Wear Costs	Winter Maintenance Costs	Accident Costs
Oregon DOT (*17*)	+1.1 million	NA	NA
Finland (*18*)	+175 to 250 million mks	-44 million mks	-0 to 190 million mks
Sweden (14)	+160 to 250 million SEK (national roads)	NA	-560 to 1160 million SEK (switch to snow tires)
	+95 to 150 million SEK (municipal roads)	NA	-1230 to 2590 million SEK (switch to summer tires)

Notes: 6 SEK = 1 U.S. dollar; 4 mks = 1 U.S. dollar
+ Increase in costs; - Decrease in costs
NA = Not available

Smith et al. (*11*) show a minor benefit in terms of stopping distance on asphalt pavements and mixed benefits on concrete pavements when the pavements are not icy. Other studies (*12*,*13*) attempted to determine the improvement in safety resulting from the use of studded tires. Neither study could conclusively associate a reduction in traffic accidents with the use of studded tires. Figure 8 clearly indicates the benefits of studded tires on ice.

Finland reportedly is able to reduce the level of winter maintenance as a result of the use of studded tires. This reduction is probably due to the high percentage of vehicles that use studded tires (90 to 95 percent of cars, 40 percent of trucks). It is doubtful that other agencies, with lower use rates, would be able to reduce winter maintenance and therefore realize this benefit.

Consequences

As shown in Table 10, the surveyed agencies identified several consequences of studded tire use. Almost all are precipitated by the development of ruts and the associated decrease in safety or pavement life. Little information was found in the literature regarding the decrease in road safety associated with hydroplaning, spray and splash, and rut avoidance.

The cost of increased maintenance and rehabilitation attributable to the use of studded tires can be estimated if pavement wear rates, use rates, and the approximate area of wear is known. For example, data were collected in Juneau over several years (see Table 9). Pavement wear rates ranged from 0.10 to 0.15 in./million studded tire passes. The measured cross-sectional area of wear and the wear rate resulted in

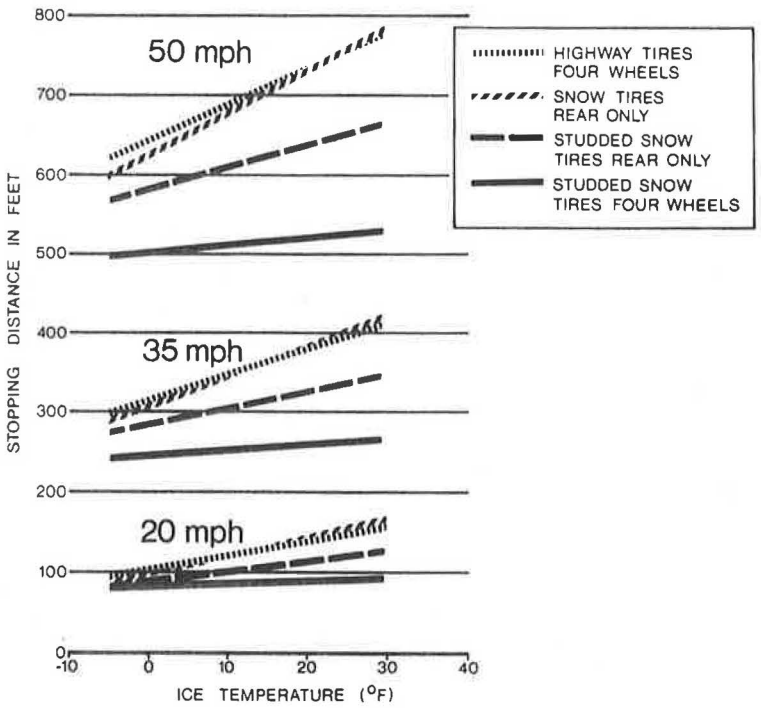

FIGURE 8 Stopping distance versus ice temperature for four cars traveling at 20, 35, and 50 mph (*11*).

asphalt pavement surfacing losses of between 19 and 25 tons/lane-mi/million studded tire passes. If a studded tire is assumed to last 30,000 mi and rehabilitation costs are equal to material costs only, then each studded tire could be equated to 0.5 and 0.75 tons of asphalt concrete mix. For this particular example, the cost of material replacement alone would range from $8 to $15/studded tire, depending on material costs.

Car owners continue to spend millions each year on studded tires for perceived or real benefits. The benefits associated with radial versus bias-ply tire designs and all-season tread versus snow-tire tread designs have not yet been assessed in this country. Furthermore, the continuing shift from rear- to front-wheel-drive vehicles will affect the effectiveness and the wear rates of studded tires. This factor has also not been investigated. The combination of these factors may alter many of the commonly held notions about the costs and benefits of studded tire use. Because several agencies still allow the use of studded tires, further studies on these issues appear to be warranted.

SUMMARY

This paper presented a summary of the results of a literature review, a survey of agencies on the use and effects of studded tires, and the results from a field study of studded tire use and pavement wear rates conducted in Alaska. Significant findings include the following:

1. Very little research has been done since 1975 in this area, except in Scandinavian countries.
2. Telephone conversations with the manufacturers and distributors revealed that only the controlled protrusion type stud is currently used in the United States.
3. Many agencies continue to prohibit or restrict the use of studded tires, but enforcement efforts appear minimal in most areas.
4. Very little new information on the percentage of vehicles using studded tires or on tire wear studies was available. Only Alaska has completed recent data collection, which shows about one studded tire for every two vehicle passes.
5. Factors affecting wear rates were defined and wear rates in Alaska were shown to be about 0.10 to 0.15 in./million studded tire passes.
6. Studded tires contribute greatly to the development of ruts in pavements, and most agencies do not have data to factor effectively this contribution into their rutting analysis.
7. The public attributes a substantial safety benefit to the use of studded tires, yet the costs of studded tire use remain largely unquantified.

On the basis of this limited study, it is clear that the use of studded tires should be reevaluated. Furthermore, the benefits derived from radial tires and front-wheel-drive vehicles need additional study.

ACKNOWLEDGMENTS

The authors wish to thank the Alaska Department of Transportation and Public Facilities for their support and cooperation in this study. This study was funded by the department as part of a larger study of the causes of wheel track rutting in urban areas.

REFERENCES

1. *NCHRP Synthesis of Highway Practice 32: Effects of Studded Tires*. TRB, National Research Council, Washington, D.C., 1975.

2. A. Niemi. Technical Raid Studies Related to Studded Tires. *Proc., Road Paving Research*, Helsinki University of Technology, Finland, 1978, pp. 25–33.
3. J. H. Keyser. Effect of Studded Tires on the Durability of Road Surfacing. In *Highway Research Record 331*, HRB, National Research Council, Washington, D.C., 1970, pp. 41–53.
4. J. H. Keyser. Mix Design Criteria for Wear-Resistant Bituminous Surfaces. In *Highway Research Record 418*, HRB, National Research Council, Washington, D.C., 1972.
5. J. H. Keyser. Resistance of Various Types of Bituminous Concrete and Cement Concrete to Wear by Studded Tires. In *Highway Research Record 352*, HRB, National Research Council, Washington, D.C., 1971, pp. 16–31.
6. M. Krukar and J. C. Cook. *The Effect of Studded Tires on Different Pavement and Surface Textures*. Report H-36. Washington State University, Pullman, 1972.
7. M. Krukar and J. C. Cook. *Studded Tire Pavement Wear Reduction and Repair, Phase I*. Report H-39. Washington State University, Pullman, 1973.
8. M. Krukar and J. C. Cook. *Studded Tire Pavement Wear Reduction and Repair, Phase II*. Report H-40. Washington State University, Pullman, 1973.
9. M. Krukar. *Studded Tire Pavement Wear Reduction and Repair, Phase III*. Report H-41. Washington State University, Pullman, 1973.
10. D. C. Esch. Memorandum. Alaska Department of Transportation and Public Facilities, Fairbanks, June 13, 1991.
11. R. W. Smith, W. E. Ewens, and D. J. Clough. Effectiveness of Studded Tires. In *Highway Research Record 352*, HRB, National Research Council, Washington, D.C. 1971, pp. 39–49.
12. J. Normand. Influences of Studded Tires on Winter Driving Safety in Quebec. In *Highway Research Record 352*, HRB, National Research Council, Washington, D.C., 1971, pp. 50–58.
13. C. K. Preus. Studded Tire Effects on Pavements and Traffic Safety in Minnesota. In *Highway Research Record 418*, HRB, National Research Council, Washington, D.C., 1972.
14. R. G. Hicks, T. V. Scholz, and D. C. Esch. *Wheel Track Rutting Due to Studded Tires*. Report AK-RD-90-14. Alaska Department of Transportation and Public Facilities, Fairbanks, Dec. 1990.
15. R. W. Smith and D. J. Clough. Effectiveness of Tires Under Winter Driving Conditions. In *Highway Research Record 418*, HRB, National Research Council, Washington, D.C., 1972, pp. 1–10.
16. M. Huhtala. Studded Tires and Their Use in Finland. *Proc., Road Paving Research*, Helsinki University of Technology, Finland, 1978, pp. 8–13.
17. *The Use and Effects of Studded Tires in Oregon*. Oregon Department of Transportation, Salem, Dec. 1974.
18. V. Pelkonen. Costs Caused by Studded Tires. *Proc., Road Paving Research*, Helsinki University of Technology, Finland, 1978, pp. 37–40.
19. C. K. Preus. Discussion. In *Highway Research Record 352*, TRB, National Research Council, Washington, D.C., 1971, pp. 31–38.

Publication of this paper sponsored by Committee on Surface Properties–Vehicle Interaction.

Analysis and Recommendations Concerning Profilograph Measurements on F0081(50)107 Kingsbury County

DAVID L. HUFT

In 1990, the South Dakota Department of Transportation (SDDOT) noted significant discrepancies between its ride-quality measurements and those taken by a contractor paving a portland cement concrete project. The contractor's measurements were consistently smoother than SDDOT's and would have generated incentive payments approximately twice as large. About half of the observed difference could be attributed to increased pavement roughness after paving, but the rest appeared to result from differences between the department's manual profilograph and the contractor's computerized unit. Analysis revealed that a numerical filtering algorithm used by the computerized profilograph strongly attenuated profile features with wavelengths shorter than 10 ft. Such attenuation was observed directly on the computerized unit's profile traces. Because of the attenuation, SDDOT considered the computerized measurements unsuitable calculating incentive payments. However, SDDOT could not use its own measurements as a basis for payment because they were not taken within the specified 48-hr period after paving. To estimate a fair incentive payment, SDDOT developed a correlation between the computerized and manually interpreted profile indexes for the project. Using the correlation, SDDOT awarded an incentive payment approximately midway between its original estimate and the contractor's. SDDOT has suspended use of computerized profilographs pending improvement of the filtering algorithm. Preliminary experiments indicate that although the computerized profilograph's first-order filter attenuates profiles too strongly and produces artificially low profile indexes, a third-order filter might generate higher profile indexes than does a manual interpreter. This suggests that a second-order filter might best approximate a human's visual interpretation of the profile. Further research is needed to confirm this hypothesis and to establish a foundation for standard filtering procedures.

During the summer of 1990, Castle Rock Construction Company placed portland cement concrete pavement on an 8.9-mi segment of US-81 south of Arlington, South Dakota (Figure 1). The project number was F0081(50)107.

In accordance with contract provisions, the contractor conducted profilograph tests (ASTM E1274-88) to determine the ride quality of the finished pavement. The contractor's measurements indicated that high ride quality had been achieved and that he was entitled to an incentive bonus of nearly $89,000.

Profilograph tests performed by the South Dakota Department of Transportation (SDDOT) Office of Materials and Surfacing also showed good ride quality, but not as good as the contractor's tests had indicated. Profile indexes measured during SDDOT's quality control tests were typically 1 to 2

Office of Research, South Dakota Department of Transportation, Pierre, S.D. 57501.

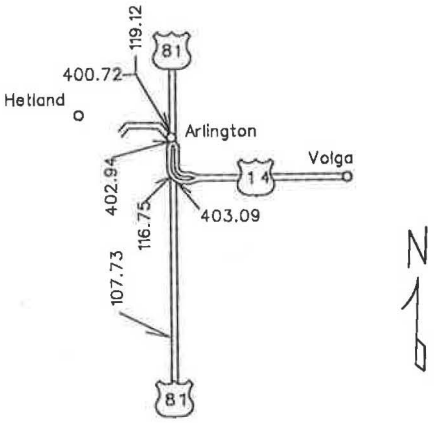

FIGURE 1 F0081(50)107 location.

in./mi higher than those measured by the contractor. Traces generated by the SDDOT unit consistently showed greater profile amplitude than did traces from the contractor's (Figure 2).

SDDOT attempted a simple check to determine whether the contractor's profilograph measured the pavement profile accurately. When the profilograph was run over a short piece of 1-×-2 lumber, it indicated approximately ½ in. rather than ¾ in., the nominal wood thickness. This unexpected result seemed to suggest a problem in the contractor's profilograph.

The contractor and SDDOT also tested sections of pavement simultaneously to determine whether their profilographs produce the same profile indexes. On August 28, 1990, northbound and southbound lanes were tested at Stations 21+71 to 48+11 and 438+83 to 470+51. Again, SDDOT's profile indexes and trace amplitudes were higher than Castle Rock's.

The contractor attempted to verify the operation of his profilograph by comparing its performance with a manual unit owned by the Iowa Department of Transportation. Castle Rock's profilograph measured profile indexes that agreed closely with Iowa's. When asked why the profilograph underestimated the thickness of the 1-×-2, Iowa personnel speculated that the unit's filtering algorithm might be responsible. They also advised SDDOT to evaluate traces carefully, to avoid misinterpreting spikes as roughness.

After the discrepancies were discovered, SDDOT retested the entire project. Again, profile indexes were consistently higher than those originally measured by the contractor. On

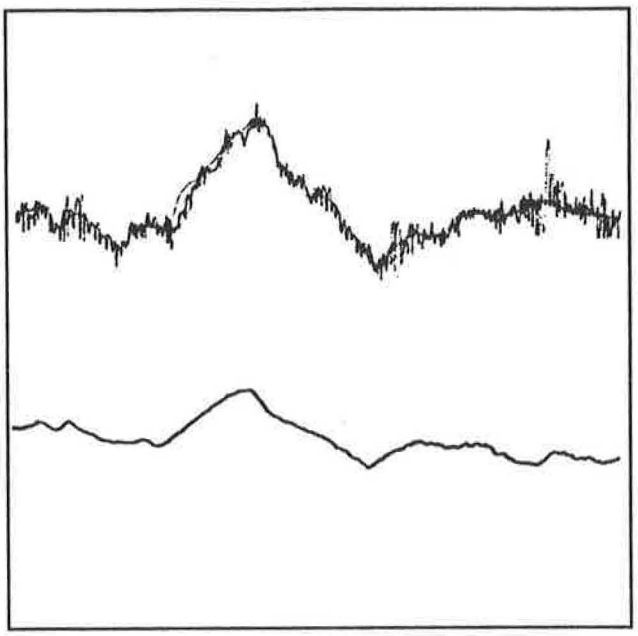

FIGURE 2 Traces from SDDOT and Castle Rock profilographs.

the basis of SDDOT's measurements, the contractor would be entitled to a bonus of less than $48,000. It seemed clear that the contractor's profilograph performed differently than SDDOT's profilograph, perhaps because of a filtering process performed by its on-board computer. But because SDDOT's tests were performed weeks after the contractor's, direct comparisons were not possible.

Because of the unresolved questions surrounding the profilograph measurements, SDDOT's Aberdeen Region asked SDDOT's Office of Research to provide technical assistance. Specifically, the objectives of this study were to

- Determine whether profilograph measurements obtained by the contractor's automated profilograph differed significantly from those obtained by SDDOT's manual profilograph;
- Determine the cause of any differences; and
- Develop a method to determine a fair ride-quality bonus if differences were attributable to the filtering used by the contractor's profilograph.

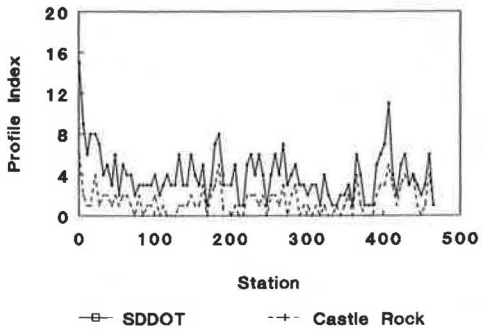

FIGURE 3 Project-wide profile indexes measured by SDDOT and Castle Rock Construction (northbound lane).

SIGNIFICANCE OF PROFILOGRAPH MEASUREMENT DIFFERENCES

It was essential to first establish that the profile indexes measured by the two profilographs were statistically different. If the observed differences represented only random variations, it would have been pointless to conclude that either instrument was in error. But if systematic differences existed, their causes might be determined. Two statistical tests were performed.

First, the projectwide profile indexes obtained by SDDOT on September 5–6 and 10–11, 1990, were compared with the profile indexes measured by the contractor within 48 hr of construction (Figures 3 and 4). The hypothesis that "projectwide profile indexes measured by SDDOT were higher than the contractor's" was tested using the one-sided t-statistic with unknown standard deviations. The test demonstrated the hypothesis to be true with greater than 99 percent confidence.

Second, the profile indexes obtained during head-to-head tests on August 28, 1990, were compared (Figures 5 and 6). The hypothesis that "SDDOT's profilograph generated higher profile indexes than did the contractor's" was tested, using the same statistical test. With more than 99 percent confidence, the hypothesis was also determined to be true. On the

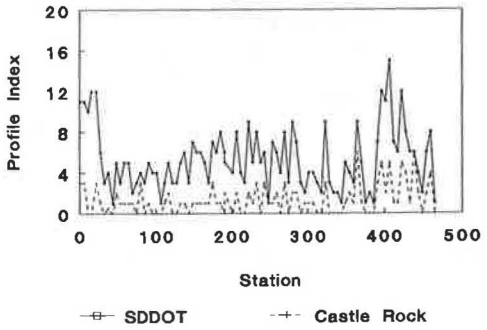

FIGURE 4 Project-wide profile indexes measured by SDDOT and Castle Rock Construction (southbound lane).

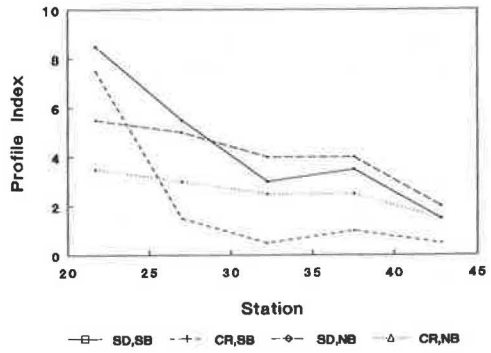

FIGURE 5 Profile indexes measured simultaneously by SDDOT and Castle Rock Construction on August 28, 1990 (Station 21+71 to 48+11).

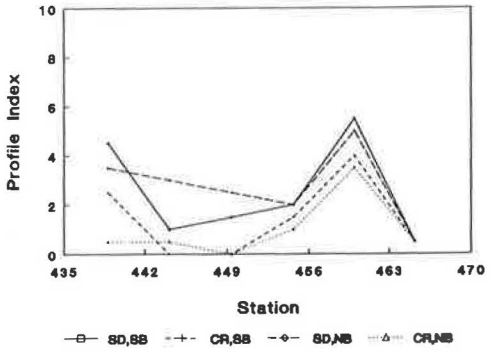

FIGURE 6 Profile indexes measured simultaneously by SDDOT and Castle Rock Construction on August 28, 1990 (Station 438+83 to 470+51).

basis of these statistical tests, SDDOT concluded that its projectwide measurements were higher than the contractor's and that its profilograph generated higher profile indexes than did the contractor's.

PROFILE INDEX DIFFERENCE CAUSES

Two causes—time between measurements and differences between manual and automated profile interpretation—were considered to be likely explanations for the differences between the profile indexes measured by SDDOT and those measured by the contractor.

Time Between Measurements

Although it appeared probable that differences between the profilographs were responsible for much of the discrepancy between the profile index measurements, it was clear that pavement roughness had changed since paving. Indexes obtained by the contractor's profilograph on August 28 were higher than those taken immediately after construction, suggesting that the pavements had become slightly rougher after construction. This was reasonable, because the curing process and temperature changes can easily affect slab shape. This observation was important, because it meant that SDDOT's measurements, which were taken too long after construction, could not be used to determine ride-quality incentive payments.

Profilograph Differences

From the comparison of profile index measurements taken with both profilographs on the same pavement sections on August 28, 1990, it was clear that the contractor's profilograph measured lower profile indexes than did SDDOT's. Because the two machines were geometrically identical, the profile filtering process incorporated in the contractor's unit was considered the most likely cause of the difference. It should be noted that SDDOT's manual procedures were also evaluated, primarily because of Iowa's concern that spikes may have been incorrectly interpreted. However, no incorrect procedures were discovered. SDDOT's engineer had correctly smoothed the profile so spikes were ignored, just as Iowa had advised.

Castle Rock's unit was a Model CS8200 profilograph from James Cox and Sons, Inc. The CS8200 includes an on-board computer that digitizes the profile signal at 1.3-in. intervals and computes profile index automatically. To make profile interpretation less difficult, the computer uses a simple recursive digital filter to remove spikes caused by extraneous mechanical vibrations from the profile signal.

Mathematically, the filter was a first-order recursive filter of the form

$$Y_n = AY_{n-1} + BX_n \tag{1}$$

where

X_n = raw (unfiltered) digitized elevation at Point n,
Y_n = filtered elevation at Point n, and
Y_{n-1} = filtered elevation at Point $n - 1$.

A and B are constants that determine the filter's effect, and are defined

$$B = N/65{,}536 \tag{2}$$

Cox recommended using a filter factor of $N = 8{,}000$ for most purposes.

$$A = 1 - B \tag{3}$$

The filter's performance was analyzed with standard signal processing techniques. One useful analysis determines the response of the filter as a function of profile wavelength λ. Specifically, the analysis defines the filter's amplitude response $H(\lambda)$, which is the ratio of the filter's output to its input. It can be shown analytically that the amplitude response of this filter is given by the formula

$$H(\lambda) = \frac{B}{\sqrt{C^2 + D^2}} \tag{4}$$

where

$$C = 1 - A\cos\left(\frac{2\pi\lambda_s}{\lambda}\right), \tag{5}$$

$$D = A\sin\left(\frac{2\pi\lambda_s}{\lambda}\right), \text{ and} \tag{6}$$

λ_s = sampling interval of 1.3 in. used by the Cox profilograph.

As shown in Figure 7, the filter attenuates short wavelengths most. Wavelengths shorter than 1 ft are attenuated by more than 80 percent to greatly reduce the effect of spikes. However, the filter significantly attenuates longer wavelengths as well. Wavelengths of 2 ft are attenuated by more than 60 percent; 5-ft wavelengths are attenuated by 30 percent. Even 10-ft wavelengths are attenuated by 10 percent.

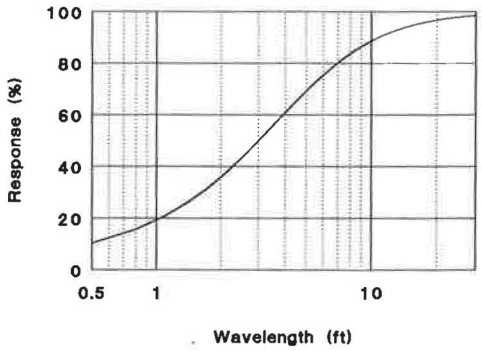

FIGURE 7 Response to Cox data filter as a function of wavelength (N = 8,000).

The filter can also be described in terms of its response to a step input. As Figure 8 shows, the filter is quite slow to recognize a step in the pavement profile. After the profilograph travels 1 ft past the step, it measures only 70 percent of the step's height. It is not until the profilograph has traveled 3 ft past the step that it measures 95 percent of the true height. This explains why the profilograph failed to measure the correct thickness of the 1-×-2, which was less than a foot long.

The significance of Figures 7 and 8 is that although the filter successfully removes spikes from the raw profile, it also removes longer features that are known to affect pavement ride quality. Because the filter underestimates the amplitude of the pavement profile, estimates of profile index are low.

Cox acknowledges that the profile index is influenced by the filter. Its manual states, "It is important to understand that the test results are heavily affected by the selected filter factor" (*1*). However, the filter's performance is fundamentally a consequence of its simple, first-order formulation. Regardless of the filter factor used in the computation, the filter's selectivity is not good. Invariably, longer wavelengths are removed along with the short. The selectivity of the filter could be improved by using a higher-order filtering algorithm, assuming the profilograph's computer has sufficient power.

The filter's ultimate effect on computed profile index cannot be simply determined. Because the amount of attenuation depends on the wavelengths in the pavement profile, the reduction of profile index also varies. If a pavement contains predominantly short wavelengths, the profile index is reduced greatly. If only longer wavelengths are present, the reduction is slight.

This explains why Castle Rock's automated profilograph correlated well with Iowa's manual profilograph. Iowa's test section consisted of large-amplitude bumps at wavelengths predominantly longer than 20 ft. At these wavelengths, the effect of filtering was too slight to be detected either by visually inspecting profilograph traces or by observing differences in profile indexes.

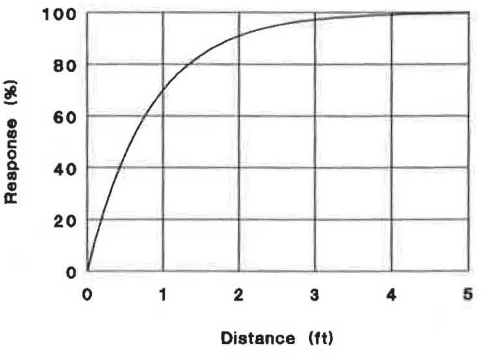

FIGURE 8 Cox filter step response (N = 8,000).

INCENTIVE/DISINCENTIVE COMPUTATION

In view of the discrepancies between profilograph measurements taken by SDDOT and Castle Rock, the question of fair incentive/disincentive payments arose. The construction contract specified ride-quality incentives and disincentives according to the following schedule (*2*):

Profile Index	*Payment (%)*
0–2	105
3	104
4	103
5	102
6	101
7–10	100
11 or more	grind or replace

Because the contractor's profilograph underestimated the height of profile features on the pavement, profile indexes were artificially low and inconsistent with the measurement method assumed in the specifications. Consequently, SDDOT considered the bonuses computed from the contractor's profile indexes to be excessive. SDDOT's profilographs did not underestimate the profile, but because measurement were not taken within 48 hr of paving, they could not be used directly as a basis for incentive payment.

In the interest of fairness to the contractor and the state, SDDOT attempted to adjust the contractor's measurements to compensate for the filtering. Direct correction would have required that all profile traces taken from the contractor's profilograph be completely redigitized, complex mathematics (Fourier transforms and inverse Fourier transforms) be used to reconstruct a profile of proper amplitude, and new profile indexes be computed. That approach was deemed difficult and prone to error.

Instead, SDDOT correlated the two profilographs, using measurements taken by both instruments on August 28, 1990. The resulting regression equation was used to adjust the contractor's profile indexes to better represent unfiltered values. Figure 9 shows the profile indexes measured by the two profilographs. From the data obtained in the simultaneous testing, the best equation relating filtered (Castle Rock) and unfiltered (SDDOT) profile indexes was

$$PI_{\text{unfiltered}} = 1.95 + 0.93PI_{\text{filtered}} \quad (7)$$

When this equation was applied to the contractor's profile indexes, the adjusted values more realistically represented the ride quality of the pavements. The bonus computed from these adjusted values totaled $68,975.36, which coincidentally fell about halfway between the contractor's original estimate and SDDOT's estimate derived from late measurements.

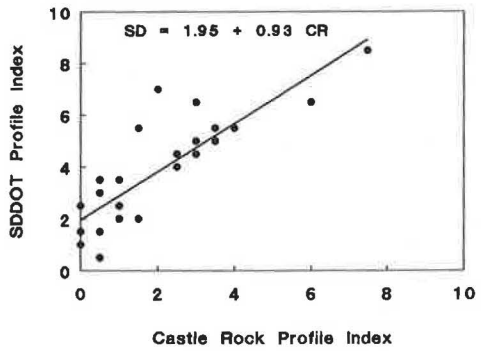

FIGURE 9 Correlation of SDDOT profile index and Castle Rock profile index.

POLICY CONSIDERATIONS

After the profile attenuation problem was discovered, SDDOT considered three alternatives for using computerized profilographs.

Prohibit Use of Computerized Profilographs

Even though computerized units remove the subjectivity associated with the manual interpretation of profile traces and greatly speed the computation of profile indexes, SDDOT believed the present filtering errors unacceptably biased measurements. In early 1991, the department disallowed the use of computerized profilographs on its paving projects. In summer 1991, SDDOT modified its policy to permit the use of computerized profilographs as long as the instruments were programmed to plot unfiltered projects that could be interpreted manually later.

Lower Ride-Quality Specifications

One alternative suggested by James Cox and Sons, Inc., (*1*) was to adjust ride-quality specifications to account for differences in computed profile indexes. Even though SDDOT had used an adjustment on F0081(50)107, it did not believe it had sufficient basis for a general adjustment. To eliminate possible controversy over computerized-versus-manual profilograph specifications, the department rejected this alternative (the department did lower the ride-quality specifications for reasons unrelated to the attenuation problem, however: to encourage improved paving quality, the entire payment schedule was shifted downward 2 in./mi).

Improve Filtering Algorithm

SDDOT shared its technical information with James Cox and Sons, Inc., which manufactures Castle Rock's profilograph, and with McCracken Concrete Pipe Machinery Company, which manufactures a similar product. Both Cox and McCracken consulted the Michigan Department of Transportation to obtain suggestions for a better filter formulation. Michigan DOT suggested that a second- or third-order Butterworth filter with a cutoff wavelength of 1 ft would filter the profile more selectively (J. W. Reinke, unpublished data).

McCracken installed the third-order filter in its profilograph during summer 1991. On June 18, 1991, McCracken and SDDOT took simultaneous measurements on in-service portland cement concrete pavements near Pierre, South Dakota. SDDOT made four passes on six ⅒-mi test sections. McCracken made two passes on each section for each of three different filter selections—the original Cox filter and two settings of the third-order Butterworth filter. Average profile indexes are shown in Table 1.

Although not conclusive, the results suggest that for the chosen cutoff wavelengths of 1 ft and 2 ft, the third-order filter produced profile indexes significantly higher than either the manual interpretation or the first-order filter. For these limited tests, the first-order filter actually approximated the manual interpretation better than did the third-order filter. At low roughness levels (Station 5+78 to 11+06 in Wheelpath 2), all three filters generated lower profile indexes than did manual interpretation. It is not clear that any of the computerized methods consistently approximates a manual interpretation.

CONCLUSIONS AND RECOMMENDATIONS

Comparisons between profile indexes measured by SDDOT and Castle Rock Construction Company show that the filtering method used by computerized profilographs can strongly

TABLE 1 AVERAGE PROFILE INDEXES OBTAINED BY MANUALLY INTERPRETED PROFILOGRAPH AND BY COMPUTERIZED PROFILOGRAPH USING FIRST- AND THIRD-ORDER FILTERS

Wheelpath	Station	Manual	1st-Order Recursive (Cox)	3rd-Order, 1' cutoff	3rd-order, 2' cutoff
1	0+50—5+78	12.0	11.8	14.4	15.0
	5+78—11+06	5.1	6.5	8.4	8.6
	11+06—16+34	15.0	14.9	19.4	18.6
2	0+50—5+78	11.9	11.6	15.2	13.6
	5+78—11+06	3.4	1.2	1.8	2.2
	11+06—16+34	10.9	10.8	13.7	14.0

affect measured profile indexes. Analysis of the filtering algorithm used on the contractor's profilograph demonstrates that the Cox unit significantly underestimated profile heights at wavelengths shorter than 10 ft. Therefore, profile indexes were also underestimated.

It was possible to derive a regression equation from profile indexes measured by the SDDOT unit and the contractor's unit on the same pavement sections on the same day. The contractor's profile indexes were adjusted using this equation, yielding new indexes that more realistically described the ride quality achieved in the paving operation. The incentive payment computed from the adjusted profile indexes was about midway between the bonus computed from the contractors unadjusted indexes and the bonus computed by SDDOT from its late measurements.

In the opinion of SDDOT, the filter algorithm incorporated in the Cox unit should not be used in conjunction with SDDOT's special provision for paving incentives. Accordingly, the department has restricted use of computerized profilographs. Preliminary experiments with other filter algorithms have been inconclusive. Until a satisfactory algorithm is demonstrated, the department will require manual interpretation of profile traces.

Transportations agencies must take care how they determine whether a contractor's profilograph operates acceptably. It is common practice to accept a contractor's profile indexes if they fall within 2 in./mi of the state's indexes. This criterion fails if a profilograph generates indexes that are within 2 in./mi but are consistently high or low. Tests to determine whether mean profile indexes are statistically different would more reliably indicate measurement validity. To ensure their relevance, any validation tests should be performed on test sections with roughness characteristics similar to those anticipated on newly constructed pavements.

Finally, a standard method of profile interpretation is needed. This would be an appropriate activity for ASTM, but it could only take place after additional research is accomplished.

REFERENCES

1. *CS8200 Users Manual.* James Cox and Sons, Inc., pp. 18–19.
2. *Special Provision for Profilograph Test for PCC Pavement.* South Dakota Department of Transportation, Pierre, April 1987.

Publication of this paper sponsored by Committee on Surface Properties–Vehicle Interaction.

Use of Smooth-Treaded Test Tire in Evaluating Skid Resistance

JOHN JEWETT HENRY AND JAMES C. WAMBOLD

Since its first use in the 1960s, the locked-wheel skid testers have used the ribbed (ASTM E501) rather than the smooth (ASTM E524) tire. The early history of the ASTM E274 locked-wheel testers is discussed, and reasons the ribbed tire was originally the standard tire are explained. The use of smooth versus ribbed tires is also examined. First the effect of film thickness on the two tires is reviewed; then the use of each or both tires is discussed in the evaluation of accident data. Finally, the relationship of skid measurement using one or both tires with texture is reviewed. It is concluded that both current research and current use would recommend that the use of both tires produces the best data; however, if a single tire is to be used, then the smooth tire would be recommended because it gives more-useful data than the ribbed tire.

Since the early 1960s, the locked-wheel skid tester has been the predominant instrument in the United States for evaluating pavements for their skid resistance under wet conditions. The publication of the ASTM Standard Test Method for Skid Resistance of Paved Surfaces Using a Full-Scale Tire in 1965 further encouraged the adoption of the locked-wheel method in the United States as well as other countries (ASTM E274-70, ASTM E274-90).

The original ASTM standard specified the use of a bias-ply test tire with five circumferential ribs (ASTM E249-66). The standard for the tire preceded the standard for the test method, because the standard tire had been developed for and used on a two-wheel trailer on which both wheels were locked and the hitch force was measured (*1*). The lateral stability problem resulting from locking both wheels on the trailer was alleviated to some degree when a ribbed test tire was used. In 1961, the development of torque-measuring locked-wheel trailers in California and Tennessee allowed locking only one of the wheels and was a forerunner of the system described in the E274 standard.

In developing the standard for the test tire, the sensitivity to water flow rate was also a concern. It was noted that the ribbed tire was less sensitive to water flow rate than a smooth tire, hence the data would be more reproducible with unsophisticated water delivery systems. The NCHRP report on the correlation and calibration of skid testers concluded: "The ribbed tire, because of its lesser sensitivity to water-film thickness, is therefore the preferred choice for skid-resistance measurement, which ideally is insensitive to all operational factors" (*2*).

The tolerance on water flow rate was large: 3.6 ± 10 percent gal/min/in. of wetted width at 40 mph. The corresponding equivalent water film thickness is 0.023 in. Because the water flow rate is specified to be directly proportional to speed, the effective water film thickness should be independent of speed. However, the effective water film thickness is somewhat artificial because the water is not deposited in a uniform sheet, as anyone who has observed a skid test would know.

In 1973 the E249 tire was superseded by a seven-ribbed bias-belted tire (ASTM E501-88). The nominal water flow rate was increased slightly, but the tolerance remained 4.0 ± 10 percent gal/min/in. of wetted width. This corresponds to an effective water film thickness of 0.025 in.

In 1975 the standard for a smooth-tread companion to the E501 tire was developed and issued as the Standard Specification for Standard Smooth-Tread Tire for Special-Purpose Pavement Skid-Resistance Tests (ASTM E524). In 1988 its name was amended to Standard Specification for Standard Smooth Tire for Pavement Skid-Resistance Tests. In 1990 the E274 standard was amended and the E501 and E524 were given equal status, whereas previous versions of the standard had referred to the smooth tire as used in "alternative testing for special purposes." The current version, E274-90, also specifies that the data be reported as SN40R for a 40-mph test with the ribbed E501 tire and as SN40S for a 40-mph test with the smooth E524 tire.

This background demonstrates the increased awareness that the smooth tire has significant advantages for skid testing. As stated earlier, the ribbed tire is less sensitive to water film thickness and therefore is insensitive to macrotexture while being mostly sensitive to microtexture. In the past, some agencies were reluctant to use the smooth tire, stating that their skid numbers would be lower. Another reason for resistance was that the historical data are important, and changing to a smooth tire would produce data that could not be compared with the histories of pavement performance. At present, as a result of voluntary consensus through the ASTM procedures, the two tires have equal standing. Both tires have their merits in the evaluation of skid resistance, but the information they provide must be interpreted correctly. The use of both tires provides the most information; however, if only one tire is to be used, experience has shown that the smooth tire should be used because of its equal sensitivity to micro- and macrotexture.

SKID RESISTANCE AND ACCIDENT DATA

It has long been argued that the smooth tire produces more-significant results for evaluating wet pavement safety. Early attempts to relate accident data to skid resistance measured

Pennsylvania Transportation Institute, Pennsylvania State University, 201 Research Office Building, University Park, Pa. 16802.

with a ribbed tire were frustrating. Rizenbergs et al., using accident data from Kentucky, plotted the ratio of wet- to dry-accident frequency against skid number (Figure 1;*3*). It is evident from this plot that there is no direct correlation between this measure of wet pavement safety and skid number measured with the ribbed tire.

During the late 1970s after the smooth-tread tire standard was issued, there was increased interest in its use for skid resistance surveys, particularly with respect to its relationship to accidents. In Connecticut one study included an inventory survey along Route 15 (*4*). This study reported that "a good correspondence between low smooth-tire skid numbers and accident experience can be seen" and that "ribbed-tire correspondence was quite poor." It was concluded that areas that had smooth-tire skid numbers (SN40S) greater than 25 were areas where no wet skidding accidents occurred, but that there was no corresponding cutoff in terms of the ribbed-tire skid numbers (SN40R).

In 1984 the Florida Department of Transportation began collecting smooth- and ribbed-tread tire data at wet-accident sites (L. Hewlett and G. C. Page, unpublished report). It reported the data for two categories: pavements having more than 50 percent of accidents in wet weather and pavements having less than 25 percent. Pavements having between 25 and 50 percent were not reported. These data are tabulated in Table 1 and plotted in Figure 2. Referring to Table 1, note that the normalized separation of the means for the smooth tire is nearly twice that of the ribbed tire, where the normalized separation of the means is defined here as

$$\Delta m = (X_{high} - X_{low})/{}^1/_2(X_{high} + X_{low}) \quad (1)$$

where X_{high} is the mean value of the high-accident skid numbers and X_{low} is the mean value of the low-accident skid numbers. This is a measure of the difference of the ability of the two data sets to distinguish between the high-accident population and the low-accident population. The values are .63 for the smooth tire data and .33 for the ribbed tire data. Therefore, the smooth tire sees a much greater difference between the high- and low-accident sites.

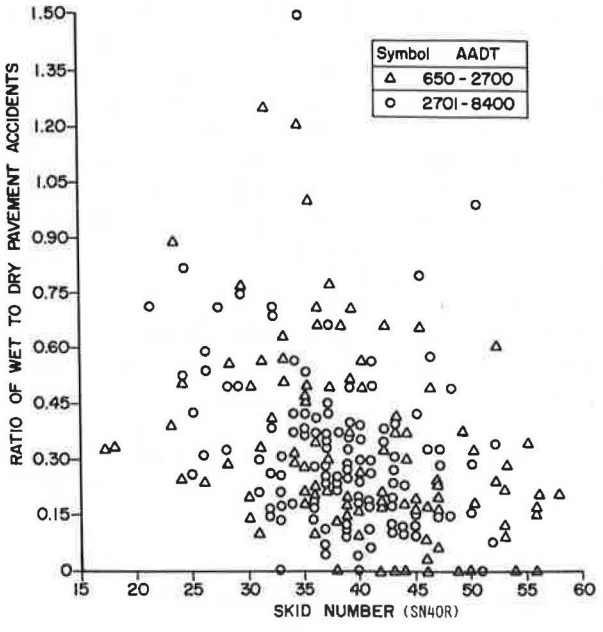

FIGURE 1 Ratio of wet- to dry-pavement accidents versus skid number for a 3-year period in Kentucky (AADT = annual average daily traffic).

A useful way to examine the two-tire data is to plot them as shown in Figure 2, with the SN40S on the vertical axis and the SN40R on the horizontal axis. The data for most of the sites will fall below the line of equality, because the smooth-tire skid numbers are usually lower than the ribbed-tire numbers. However, this is not always true, particularly when the macrotexture is very high and the microtexture is low, which happens when the texture depth is good but the aggregate is polished. The data close to the line of equality generally have good macrotexture. The significance of the data with respect to texture is discussed further.

It is noteworthy that the level on the vertical axis that separates most of the high wet-accident rate sites from the low wet-accident rate sites is 25. In other words, sites with an SN40S greater than 25 are low wet-accident sites, and sites with an SN40S less than 25 are high wet-accident sites. No value on the horizontal axis separates the high- and low-accident sites, which means that one cannot select a level of SN40R that separates the high- and low-accident sites.

A project was conducted in Pennsylvania from 1981 through 1983 to collect data at wet-accident sites using the two tires (*5*). The project team was notified of all wet-weather accidents by local police agencies in selected communities in central Pennsylvania. The sites were tested with both tires within 2 days after the accidents. The data set included 79 sites, 21 of which had multiple accidents. At the time the accident sites were tested, control sites no more than 1.6 km (1 mi) from the accident site were also tested. The data for the accident sites were compared with the data from the control sites. The results were not enlightening, because the skid resistances of the control sites were not significantly different from the accident sites with either tire. The control sites had, on average, a skid resistance of only about 2 skid numbers (SN) higher than the accident sites for both the smooth and ribbed tires. This experiment demonstrates the difficulty of working with accident data, because many factors other than skid resistance should be considered in an analysis of wet accidents. Although the data were not statistically significant, the trends were consistent with other experiences indicating a slightly higher sensitivity of the blank tire to distinguish high-accident sites.

Wet-pavement accidents are caused by complex interactions among many roadway, vehicle, human, and environmental factors. Accidents also occur because of unpredictable factors such as inattentiveness, misjudgment, recklessness, and random variables such as unforeseeable events or obstacles. In a research project for Pennsylvania (*6*), various models were developed to determine a relationship between wet-weather accidents involving injuries or fatalities and

- Total number of accidents,
- Skid number (SNR only),
- Rutting,
- Roughness,
- Surface type and age,
- Posted speed limit,

TABLE 1 SKID NUMBERS MEASURED AT ACCIDENT SITES IN FLORIDA (*10*)

PVT. TYPE ACC. RATE	DENSE GRADED GREATER THAN 50%		FLORIDA DATA DENSE GRADED LESS THAN 25%		OPEN GRADED LESS THAN 25%	
SKID NO.	SN40S	SN40R	SN40S	SN40R	SN40S	SN40R
	33.5	43.5	48.5	49.0	36.5	39.0
	30.5	41.5	47.0	57.0	36.5	37.0
	27.5	22.0	42.5	51.0	35.5	39.0
	27.5	20.5	41.5	51.5	35.5	35.5
	26.5	32.0	40.0	46.0	35.5	34.5
	23.5	28.5	38.5	51.0	34.5	35.5
	21.5	38.0	37.5	50.0	34.5	33.5
	20.5	40.5	37.5	46.0	33.5	37.0
	19.5	38.5	35.5	43.5	33.5	34.5
	19.5	30.5	35.5	46.0	30.0	33.0
	19.5	28.0	34.5	41.5	30.0	31.0
	14.5	33.5	34.5	51.5	28.0	31.0
	14.5	29.0	32.5	46.0	28.0	29.5
	14.5	27.0	32.5	40.5		
	13.5	34.0	31.5	42.0		
	13.5	33.0	30.5	43.5		
	13.5	24.0	30.5	39.5		
	13.5	20.5	30.0	46.5		
	12.5	35.0	29.0	45.5		
	12.5	33.0	27.0	45.5		
	12.5	27.0	26.0	45.5		
	12.5	22.0	25.0	40.5		
	12.5	20.0	25.0	41.5		
	11.5	31.0	25.0	42.5		
	10.5	26.0	23.0	45.0		
	10.5	29.5				
	9.0	27.0				
MEAN	17.4	30.2	33.6	45.9	33.2	34.6
STD. DEV.	6.8	6.6	6.9	4.3	3.1	3.0

COMBINED DATA FOR LESS THAN 25%	SN40S	SN40R
MEAN	33.5	42.1
STD. DEV.	5.8	6.7

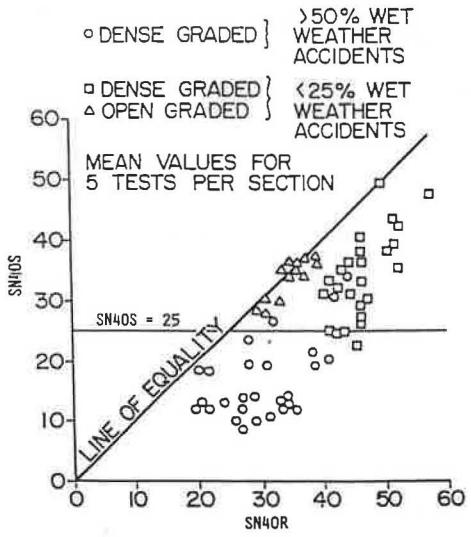

FIGURE 2 Skid numbers SN40R and SN40S measured at accident sites in Florida; mean values for five tests per section.

- Percentage wet time,
- Horizontal curvature,
- Vertical alignment, and
- Driving difficulty (number of signals, turn lanes, crossroads, land use, etc.).

Stepwise regression reduced the independent variables to two: driving difficulty index (DDI) and SNR, where

$$DDI = 1/3 * (\text{curvature} + \text{grade} + \text{driving difficulty}) \quad (2)$$

However, the regression coefficients found in the Pennsylvania Department of Transportation study for 308 sites were found to be 14.4 for the DDI, compared with 0.62 for the SNR. This relative insignificance of the treaded-tire skid resistance data in accident prediction is not surprising. Unfortunately, smooth-tire data were not available for this study; it would be interesting to conduct a similar study for which both ribbed- and smooth-tire data were available.

EFFECT OF WATER FILM THICKNESS ON SKID NUMBERS

As noted, the concern that variations in water flow rates through the nozzle of a skid tester may cause excessive var-

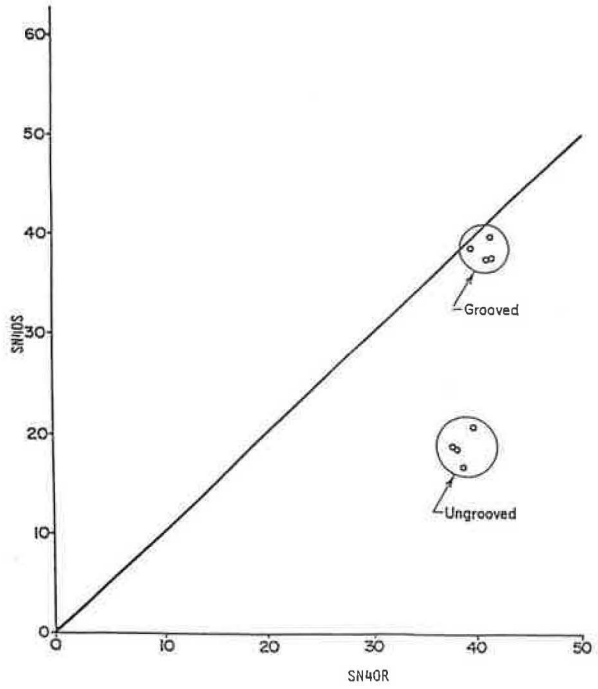

FIGURE 3 Skid numbers of grooved and ungrooved PCC pavements [test speed = 65 km/hr (40 mph)].

iations in skid number was one consideration that led to the selection of the ribbed test tire. Another consideration in the selection of the test tire was that the tire have little sensitivity to temperature. This consideration was well founded, and a compound that produces little variation over a wide temperature range was specified. The ribs of the test tire provide a significant path for water to escape from the interface between the pavement and the tire sliding over it. The additional drainage path provided by the pavement macrotexture is fairly small, even for pavements with high levels of macrotexture.

An example of the ability of the ribbed tire to mask the benefits of macrotexture is its recognized inability to distinguish between longitudinally grooved and ungrooved portland cement concrete (PCC) pavements. If ribbed-tire skid numbers were the meaningful measure of safety, no longitudinal grooving would be performed. A study of four sites on Interstate 80 in Pennsylvania shows this effect well (*7*). Longitudinal grooving was done over sections several miles long, leaving ungrooved sections that otherwise had similar characteristics. Measurements were made with both tires at the grooved and ungrooved sections. The results are shown in Figure 3, in which the data are plotted on the SN40S/SN40R coordinates. Note that there is no significant difference in the ribbed-tire data, whereas the smooth-tire skid numbers of the grooved sections are more than twice as high as those for the ungrooved sections. An idealized cross section of the tire-pavement interface is shown in Figure 4, using the grooving geometry and the tire design geometry. Note that even when the test tire is fully worn, it provides as much drainage capacity as the grooves.

In the NCHRP study on the correlation and calibration of skid testers, tests were performed on one coarse-textured surface with varying amounts of water flow corresponding to effective film thicknesses ranging from 0.005 to 0.030 in. (*2*). Neither the new nor the worn ribbed test tire showed the effect of water film thickness between 0.020 and 0.030 in., so the choice of the effective water film thickness of 0.025 in. was reinforced. This corresponds to a flow rate of 4.0 gal/min/in. of wetted width, which is the nominal value for the E274 standard. It was also noted that the smooth tire decreased significantly over the range of water film thickness of the test, as shown in Figure 5.

To further address the concern that the smooth tire might be too sensitive to water film thickness to provide reliable data, a study with conducted at the Pennsylvania Transportation Institute in 1981 (*8*). The water flow rate delivered through the skid tester nozzle was varied from 7.5 to 22.5 m^3/hr (30 to 100 gal/min). This corresponds to 3.7 to 12.5 gal/min/in. of wetted width, while E274-90 requires 4 ± 10 percent gal/min/in. of wetted width. Four sites were measured with both tires at three water flow rates. The results shown in Figure 6 indicate that the smooth tire is definitely more sensitive to water flow than the ribbed tire is. However, the insensitivity of the ribbed tire to the water flow further shows that the tire can handle excessive amounts of water with relatively little effect on the skid number regardless of the level of macrotexture.

Another difficulty in the use of a treaded test tire is that variations due to tread depth over the useful life of the tire must be insignificant. One could argue that the test tire should have a tread depth so large that as it reaches its wear limit it still has a tread depth large enough so that it does not affect the measurement. In fact, in a study comparing the test tires with a new commercial tire of the same size and construction, the ribbed tire produced higher friction than the new commercial passenger-car tire (*9*). For the commercial tire worn to the legal limit, it was hypothesized that its performance would degrade toward the smooth-tire performance.

If reasonable care is exerted to control the water flow rates of a skid tester, the effect on SN40S data is not a problem. The largest effect in the data in Figure 6 is 1 SN/10 gal/min. Therefore, using the tolerance required in the ASTM E274 test method, the resulting variation is only ± 0.3 SN.

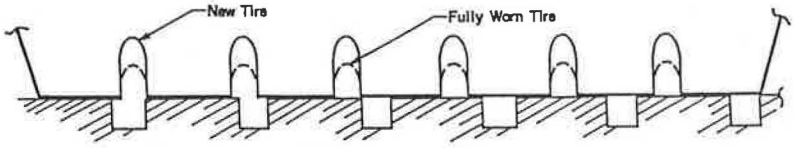

FIGURE 4 Idealized geometry of interface between ribbed tire and grooved PCC pavement (0.65- × -0.65-mm grooves on 25-mm spacing).

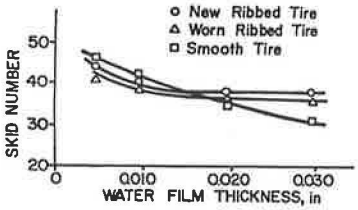

FIGURE 5 Skid resistance with ribbed and smooth tires on coarse-textured bituminous concrete pavement.

RELATIONSHIPS BETWEEN SKID RESISTANCE MEASUREMENTS AND TEXTURE

It is easier to generate meaningful quantitative data for texture and skid resistance studies than for accident and skid resistance studies. Several recent studies have attempted to develop statistical models relating skid resistance to texture parameters.

An early attempt to relate skid resistance to observations of texture was made in Virginia (*10*). Unfortunately, only qualitative descriptions of the texture of the sites were given, but when the data are plotted on SN40R/SN40S coordinates, the groupings fall into cluster according to the qualitative descriptions (see Figure 7). Note that, with the exception of one data point, the clusters can be separated by levels of

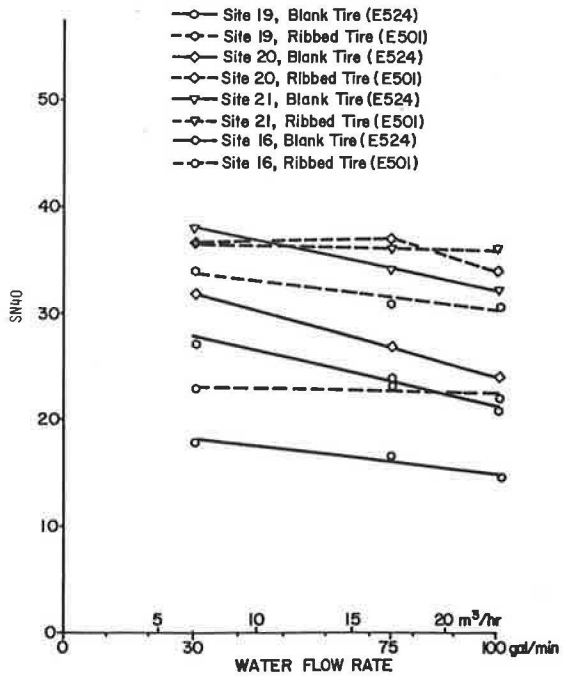

FIGURE 6 Effects of water flow rate on skid resistance measurements.

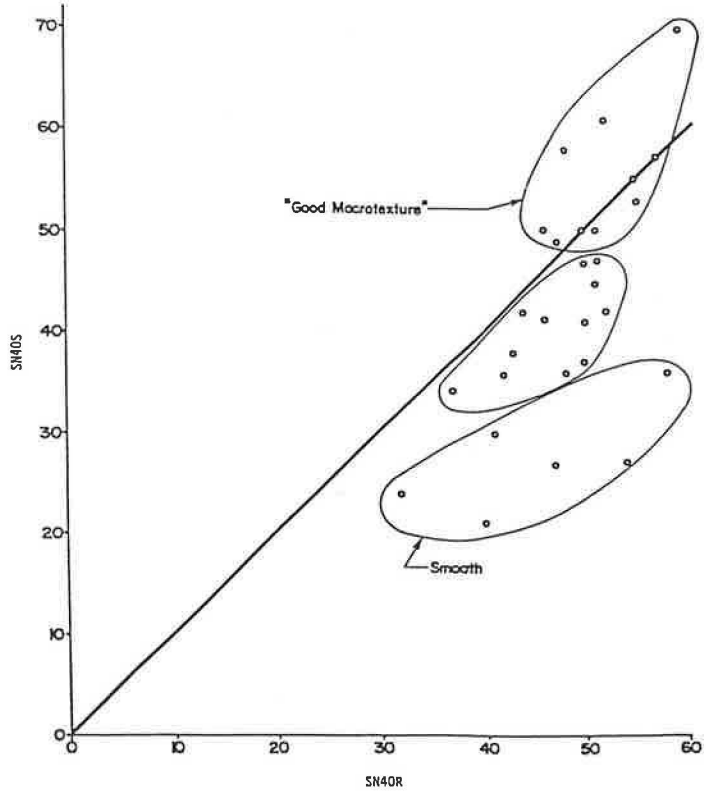

FIGURE 7 Skid numbers for sites in Virginia [test speed = 65 km/hr (40 mph)].

SN40S. The "good macrotexture" sites are above 47, and the "smooth" sites are below 30.

Data from a Pennsylvania study conducted from 1978 through 1979 included both skid resistance with the two tires as well as pavement texture measurements (7). The texture data were sandpatch mean texture depth (MTD) and British pendulum numbers (BPN), which serves as a surrogate for microtexture. The data are presented in Table 2. Initially, 23 sites were included in the study, which began in the fall of 1978. Two of the sites (20 and 23) were dropped from the study early in the program because they were too inhomogeneous. Sites 5 and 6 were severely damaged by winter maintenance and were replaced by Sites 24 and 25 in spring 1979. With these exceptions, the same sites were used in the fall of 1978 and the spring of 1980. Figures 8 and 9 are plots of the data showing the site number, MTD, and BPN data for each point.

Linear multiple regressions were run with the skid numbers as dependent variables and MTD and BPN as the independent variables. For the spring and the fall data sets, the improvement resulting from including the MTD in the regression for SN40R was negligible. For the SN40S data, however, the MTD and BPN were equally significant. The fall data produced the following results:

$$SN40R = -6.1 + 0.72\ BPN \qquad R^2 = .74 \tag{3}$$

$$SN40S = -20.5 + 0.65\ BPN + 16.4\ MTD \qquad R^2 = .82 \tag{4}$$

where MTD is expressed in millimeters. The spring data produced higher correlation coefficients:

$$SN40R = -10.5 + 0.83\ BPN \qquad R^2 = .90 \tag{5}$$

$$SN40S = -16.9 + 0.54\ BPN + 19.6\ MTD \qquad R^2 = .91 \tag{6}$$

Although the intercepts and the coefficients of BPN and MTD are different for the two data sets, they are similar in magnitude. The excellent correlation coefficients, especially of the spring 1979 data, confirm the insensitivity of the ribbed tire to macrotexture and the approximately equal sensitivity of the smooth tire to the macro- and microtexture.

The skid resistance data may also be used to predict macro- and microtexture from skid resistance measurements by performing regressions for BPN and MTD as the independent variables and SN40S and SN40R as the independent variables.

$$MTD = 0.59 - 0.036\ SN40R + 0.053\ SN40S \qquad R^2 = .86 \tag{7}$$

$$BPN = 10.33 + 1.62\ SN40R - 0.49\ SN40S \qquad R^2 = .93 \tag{8}$$

TABLE 2 SKID NUMBERS MEASURED AT ACCIDENT SITES IN PENNSYLVANIA

FALL 1978					SPRING 1979						
SITE	SNR	SNB	MTD (mm)	BPN	SNR	SNB	MTD (mm)	BPN	CONSTRUCTED	TYPE	ADT
1	32.4	22.8	0.41	50.7	31.7	22.7	0.36	46.3	1970	DG	6630
2	28.2	19.0	0.36	59.0	27.4	14.7	0.41	51.7	1950	PCC	7700
3	49.4	28.4	0.33	69.9	38.0	19.7	0.38	68.1	1973	PCC	3640
4	39.4	25.6	0.30	58.7	35.0	23.3	0.33	50.1	1972	DG	3640
5	53.0	56.0	1.30	86.0					1976	OG	7700
6	52.5	42.5	0.56	81.1					1976	DG	7700
7	48.5	27.2	0.41	70.4	40.4	23.4	0.38	64.0	1973	PCC	1820
8	46.2	44.2	0.74	59.3	32.2	26.7	0.71	52.0	1972	DG	1820
9	52.2	46.8	0.69	66.0	43.2	34.6	0.79	56.9	1972	DG	1710
10	48.4	26.2	0.36	73.0	43.2	22.7	0.33	70.1	1973	PCC	1710
11	30.2	21.6	0.36	59.9	27.3	18.8	0.48	47.8	1963	DG	4490
12	39.8	34.8	1.02	67.7	40.6	31.0	0.79	57.6	1970	DG	4490
13	60.0	61.4	1.04	94.2	64.5	60.7	1.32	88.7	1969	OG	7920
14	37.0	24.8	0.41	63.8	37.9	21.4	0.46	61.1	1967	PCC	8770
15	62.6	61.6	1.30	96.9	68.6	62.2	1.37	86.6	1969	OG	7920
16	25.4	17.8	0.66	55.5	24.1	14.7	0.58	44.1	1966	DG	6500
17	35.8	33.0	1.02	58.0	35.4	29.4	1.12	50.0	1961	DG	800
18	50.6	37.8	0.51	69.5	47.6	34.0	0.53	67.0	1973	PCC	1200
19	37.4	26.6	0.43	63.0	30.3	19.5	0.51	49.1	1968	DG	7000
21	36.2	36.6	1.24	70.0	36.2	32.3	1.22	53.2	1969	OG	2500
22	57.6	61.4	1.40	87.5	60.2	56.2	1.63	87.7	1969	OG	2500
24					26.1	14.4	0.41	46.2	1963	DG	4490
25					53.8	40.8	0.69	76.7	1969	OG	7920

NOTE: OG = open graded, DG = dense graded, ADT = Average daily traffic, and SNB = skid number for smooth (blank) tire

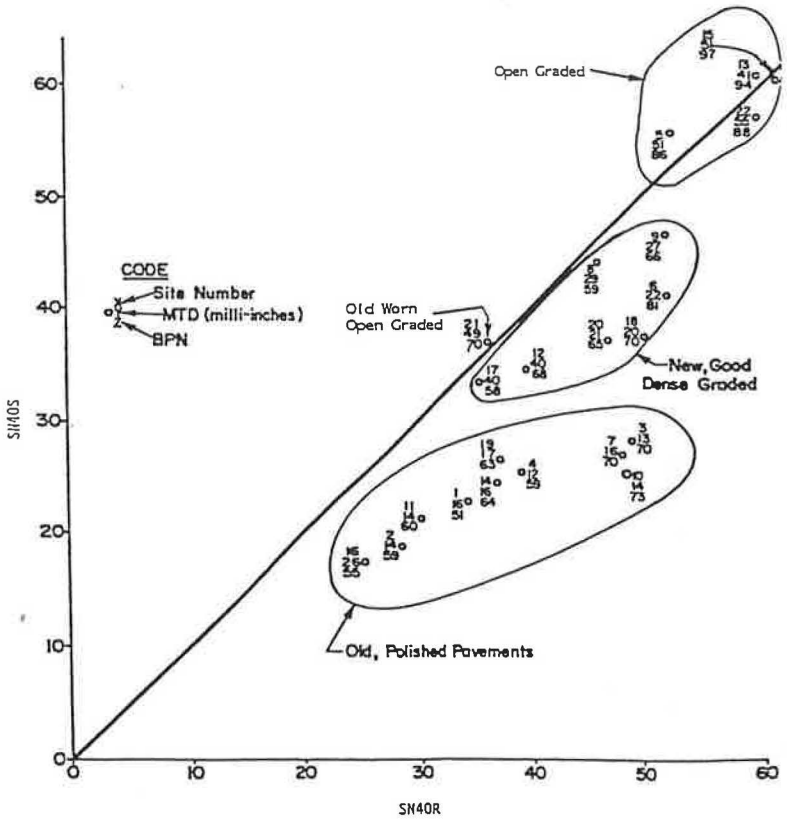

FIGURE 8 Skid numbers and texture for sites in Pennsylvania, fall 1978 [test speed = 65 km/hr (40 mph); 1 milli-inch = .0254 mm].

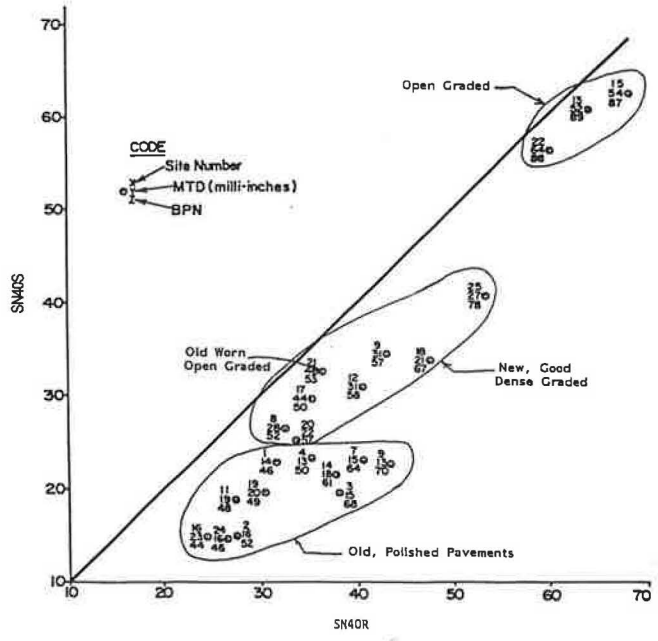

FIGURE 9 Skid numbers and texture for sites in Pennsylvania, spring 1979 [test speed = 65 km/hr (40 mph); 1 milli-inch = .0254 mm].

These results demonstrate that knowledge of skid resistance with both tires enables the investigator of a pavement having low skid resistance to evaluate whether there is a deficiency in macro- or microtexture and can suggest suitable corrective measures.

Using these same data, lines of constant MTD and BPN were mapped onto the SN40R-versus-SN40S plots by Wambold (*11*). From these, he developed acceptance criteria for pavements on the basis of the two skid numbers. Also using these data, Saito and Henry regressed the ratio of the two skid numbers with MTD (*8*). The results produced a high coefficient of correlation:

$$\text{SN40S/SN40R} = 0.887(\text{MTD})^{0.36} \qquad R_2 = 0.94 \tag{9}$$

or

$$\text{MTD} = 1.13(\text{SN40S/SN40R})^{2.78} \tag{10}$$

A similar study in Illinois, based on a new set of data, showed a relationship between MTD and a "macrotexture index" defined as

$$\text{MTI} = (\text{SN40R} - \text{SN40S})/(\text{SN40R} + \text{SN40S}) + 1 \tag{11}$$

This relationship, when converted to MTD in millimeters, is

$$\text{MTD} = 1.02(\text{MTI})^{-3.78}$$
$$= 0.074(1 + \text{SN40S/SN40R})^{3.78} \quad (12)$$

These data agree reasonably well with the Pennsylvania data. Equations 10 and 12 produce the same results at an MTD of about 0.84 mm.

That all of these studies have produced significant correlations between texture and skid resistance data with the two tires suggests that the data produced by both tires are useful in assessing pavement condition. However, the consistent lack of response of the ribbed tire to macrotexture suggests that if only one tire can be used in surveys it should be the smooth tire. This suggests that surveys be conducted with the smooth tire and that sections that produce SN40S values less than a selected level be revisited with the two tires. This would allow for a rational strategy for correcting sites with low skid resistance.

CONCLUSIONS AND RECOMMENDATIONS

The original ASTM E274 standard specified that the E249 five-rib tire be used. In 1973 the E249 tire was replaced with the E501 tire, a seven-rib tire. Since then the E274 standard has changed several times, first stating that the ribbed tire is standard, then stating that the ribbed tire is standard and the smooth tire is allowed, and, in the current version, stating that either tire can be used without indicating a preference.

In research studies over the past decade, it has been shown that the use of both tires provides many more data than does the use of either tire by itself. Relationships of macro- and microtexture are given that would be useful to maintenance personnel in determining the cause of loss of skid resistance and thus what maintenance procedures should be used. Thus measurement with both tires is recommended for project-level surveys.

However, if only one tire is used (as would be the case in a network-level survey), the smooth tire is recommended because it is sensitive to macro- and microtexture whereas the ribbed tire responds primarily to the microtexture. As a result, several states now use the smooth tire for routine measurement.

REFERENCES

1. R. A. Moyer. Skid Resistance Measurements with a New Torque Device. *Bulletin 348*, HRB, National Research Council, Washington, D.C., 1962, pp. 44–77.
2. W. E. Meyer, R. R. Hegmon, and T. D. Gillespie. *NCHRP Report 151: Locked-Wheel Pavement Skid Tester Correlation and Calibration Techniques*. TRB, National Research Council, Washington, D.C., 1974.
3. R. L. Rizenbergs, J. L. Burchett, and L. A. Warren. Relation of Accidents and Pavement Friction on Rural Two Lane Roads. In *Transportation Research Record 633*, TRB, National Research Council, Washington, D.C., 1977, pp. 21–27.
4. G. A. Ganung and F. J. Kos. *Wet Weather, High-Hazard Accident Locations: Identification and Evaluation*. Report FHWA-CT-RD-403-F-79-4. Connecticut Department of Transportation, Whethersfield, 1979.
5. J. C. Wambold, J. J. Henry, and R. R. Hegmon. Skid Resistance of Wet-Weather Accident Sites. *ASTM Special Technical Publication 929*, Philadelphia, Pa., 1986, pp. 47–60.
6. B. T. Kulakowski, J. C. Wambold, C. E. Antle, C. Lin, and J. M. Mason. *Development of a Methodology to Identify and Correct Slippery Pavements*. Research Report 88-06. Pennsylvania Department of Transportation, Harrisburg, 1990.
7. J. J. Henry. The Use of Blank and Ribbed Test Tires for Evaluating Wet Pavement Friction. In *Transportation Research Record 788*, TRB, National Research Council, Washington, D.C., 1981, pp. 23–28.
8. K. Saito and J. J. Henry. Skid-Resistance Measurements with Ribbed and Blank Test Tires and Their Relationship to Pavement Texture. In *Transportation Research Record 946*, TRB, National Research Council, Washington, D.C., 1983, pp. 38–43.
9. J. J. Henry. Comparison of the Friction Performance of a Passenger Car Tire and the ASTM Standard Test Tires. *ASTM Special Technical Publication 793*, Philadelphia, Pa., 1983, pp. 219–231.
10. D. C. Mahone. *An Evaluation of the Effects of Tread Depth, Pavement Texture, and Water Film Thickness on Skid Number–Speed Gradients*. Virginia Highway and Transportation Research Council, Charlottesville; FHWA, U.S. Department of Transportation, 1979.
11. J. C. Wambold. Road Characteristics and Skid Testing. In *Transportation Research Record 1196*, TRB, National Research Council, Washington, D.C., 1988, pp. 294–305.

This work was sponsored by the Pennsylvania Department of Transportation and the U.S. Department of Transportation, FHWA. The contents of this paper reflect the view of the authors, who are responsible for the facts and the accuracy of the data presented herein.

Publication of this paper sponsored by Committee on Surface Properties–Vehicle Interaction.

Overview of Smooth- and Treaded-Tire Friction Testing by Illinois Department of Transportation

JAMES P. HALL, DAVID B. BERNARDIN, AND J. G. GEHLER

The Illinois Department of Transportation (IDOT) has been involved in pavement friction testing with locked-wheel equipment since 1968. In 1980 IDOT started testing with a smooth (blank) tire in addition to the treaded (ribbed) tire. Since 1985 IDOT has routinely tested with both smooth and treaded tires and has accumulated a multitude of test data. In 1987, IDOT developed tentative guidelines for evaluating both smooth- and treaded-tire data in analyzing high wet accident sites. The history of friction testing equipment development in Illinois and the upgrading process used for constructing IDOT's current friction testers are described. A summary of various distributions of smooth- and treaded-tire friction test data collected since 1985 on IDOT's highway network is presented.

The Illinois Department of Transportation (IDOT) has been involved in pavement friction testing with locked-wheel equipment since 1968. In 1980 IDOT started testing with a smooth (blank) tire in addition to the treaded (ribbed) tire.

Since 1985 IDOT has routinely friction-tested with both the smooth and treaded tires and has accumulated a multitude of test data. In 1987 IDOT developed tentative guidelines for evaluating smooth- and treaded-tire data in analyzing high wet accident sites.

This paper describes the history of friction testing equipment development in Illinois and describes the upgrading process used for constructing IDOT's current friction testers. It also presents a summary of various distributions of smooth- and treaded-tire friction test data since 1985 on the highway network.

STATUS OF FRICTION TESTERS IN 1983

IDOT bought its first friction tester in 1968 and its second system in 1978. System maintenance was difficult because parts from the systems were not interchangeable, complicating repairs and lengthening downtime. IDOT investigated upgrading or replacing its two friction testing systems in the fall of 1983. At that time, IDOT had two complete friction testing systems and an extra trailer designed and built in-house.

The condition of IDOT's friction testers in 1983 necessitated immediate action to improve friction testing operations. The average downtime for IDOT's two friction testers was averaging 2 days a week. Minor repairs often stretched into days or weeks because parts were unavailable. The two friction testers were completely incompatible, further complicating repairs. Neither friction tow vehicle could tow the other's trailer or interface to the control equipment.

Hand processing of data often resulted in substantial delays in evaluating and reporting test results. The results of previous tests were difficult or impossible to reference because of manual recordkeeping.

A major problem with both of IDOT's existing systems was that they relied on too many different parts from nonstandard sources. Many of the subassemblies were custom-designed, and when one component failed the parts to reconstruct it were no longer available. These conditions hurt the effectiveness and efficiency of IDOT's friction testing programs.

CRITERIA FOR FRICTION TESTER UPGRADE

Although several friction testing systems were available commercially, retrofitting IDOT's existing equipment was determined most advantageous, economically and operationally. IDOT already owned the basic components for two complete friction testers plus the extra trailer frame. IDOT decided to retrofit the existing systems in stages over 3 years. This was done to replace obsolete mechanical components, improve the mounting design of electrical and mechanical subsystems, and replace the control system with a state-of-the-art microcomputer that would record test data on magnetic storage media.

There were several advantages to doing the work in-house. First, the implementation time frame met budget constraints. Second, redesigning the systems in-house allowed complete control over the selection of components. Third, IDOT personnel would develop the background necessary to repair or modify the systems as necessary. Be redesigning the systems in-house, IDOT could make timely repairs and incorporate future upgrades as necessary.

The goal of the upgrade was to design and build a system composed of standard components with off-the-shelf availability. This was not an easy task because a friction tester is a custom device. Top priorities were locating and purchasing interchangeable components and building a system that allowed in-house modification of equipment and software. The system was to meet or exceed the following requirements:

1. All electronics are interchangeable between systems.
2. Parts are readily available.
3. Calibration techniques are compatible and efficient.

Bureau of Materials and Research, Illinois Department of Transportation, 126 East Ash Street, Springfield, Ill. 62704.

4. Test cycle can be controlled and modified using software developed in-house.
5. Calibration is accurate within 1 percent.
6. Data are recorded on magnetic media.
7. Operation is menu-driven.
8. Either test wheel can be tested.
9. Water flow is monitored during tests.
10. Design and installation are modular.
11. Equipment is reliable.

The planning and researching manufacturers took about 3 months. IDOT wanted equipment and mounting techniques that made it relatively simple to remove and reinstall equipment in either tow vehicle when necessary. Commercial products were selected for as many components as possible to eliminate the necessity for in-house construction of circuit boards or manufacturing of special parts. It was necessary to have some circuit boards modified to provide the necessary functions and also to do some custom machining of parts. This was kept to an absolute minimum. IDOT also eliminated as much interfacing as possible between the computer system and the electrical subassemblies.

The friction tester upgrade project was a cooperative effort between the University of Illinois Civil Engineering Department and IDOT's Bureau of Materials and Physical Research. By spring 1984, upon evaluation of different upgrade methodologies, the major components were selected and detailed design criteria were approved.

It was determined feasible to design, build, and operate a friction tester with a commercially available microcomputer. Several microcomputer systems were available that could control the friction test cycle, write test data to a magnetic media, provide a hard-copy printout, and visually display current tests for the operator. A system that had all or most of these capabilities built into a single unit was desired, because complexity was reduced by minimizing external cabling and interfaces. A single unit also provided the capability to modularize design components to allow easier access of mounting and removal. Under this arrangement, a backup unit is required for each module of the system in case of malfunction.

In addition to data collection, various methods of managing and reporting the collected data were also evaluated. A microcomputer data base was designed to interact with the data collection activities and provide automated data management of various testing programs. The Pavement Technology Information Base (PTIB) was designed to document the location of test sites, provide historical test information regarding specific sites, and provide traffic and test information for use by field crews. Reporting procedures developed on the PTIB issue a field sheet for the field crews. The field sheet provides the field crews with information to determine the location of test sites, the type of pavement, how much traffic to expect and the results of previous tests. To do this, information from several sources is combined into one data base.

The upgrade of all of the systems took several years and was completed in 1986.

FRICTION TESTER SYSTEM OVERVIEW

A Hewlett-Packard Integral Personal Computer (HP-IPC) running AT&T System V UNIX and an HP-3497A Data Acquisition Controller were chosen to be the heart of the system. The HP-IPC came with a IEEE 488 equipment bus that interfaces directly with the HP-3497A data acquisition controller. The HP-IPC has a built-in flat-screen VDT, a built-in ThinkJet printer, and a built-in 3.5-in. microfloppy disk drive. The HP-3497A data acquisition controller provides the necessary digital counters and relay-operated control of peripheral devices for friction tests. Because the amperages of some devices were near the maximum load for the 3497A's device actuator circuitry, an additional bank of heavy-duty relays was added between the 3497A and the water pump, brake relays, and water valves.

The HP-IPC was designed for scientific system development and as the replacement for the HP-85 data collection microcomputer. The HP-85 microcomputer had become a standard in field data collection. The HP-IPC microcomputer came configured as follows:

- HP-IB (IEEE 488) equipment interface bus,
- Electroluminescent display screen,
- 3.5-in. microfloppy disk drive,
- Detachable 101-key keyboard,
- Built-in ThinkJet printer,
- 512 KB of memory, and
- UNIX operating system in ROM.

The following were purchased as options:

- HP Technical Basic (HP-TB) in ROM,
- 256-KB plug-in memory card,
- Modem card, and
- RS-232c interface card.

All of the peripherals IDOT specified were built into the HP-IPC. It also interfaced directly to the HP-3497A device control unit with a single cable The 3497A may be optionally configured with up to five cards available from the company. IDOT configured the 3497A with a 16-channel digital actuator and four digital accumulator cards. Using HP-TB, the HP-IPC can control all the functions necessary to do a friction test. These two pieces of equipment and the heavy-duty relay chassis control the entire system. The options to the HP-IPC were added to simplify system operation and enhance the system's capabilities.

The 3497A controls the devices associated with the friction tester through an auxiliary box for high-current relays. One card slot in the 3497A contains the 16-line controller device that activates system components through high-current relays. The other four slots contain digital counter devices that accumulate digital counts for torque, speed, and water flow and those from the wheel pulse transducer on the test wheel. Twelve power relay control devices are controlled by the control device in the 3497A.

HP-TB was purchased in ROM to eliminate the need for two disks in the field. Without this feature, one disk would be necessary for HP-TB and one for the friction control software. RAM was added to ensure that no shortage of memory would affect the testing cycle. The modem and a single RS-232 interface were added to ensure compatibility with the office systems. An HP-IPC is used in the office to preprocess

data and serves as a backup unit should a field unit fail during the test season.

The test-cycle control software was developed using HP-TB by the University of Illinois Civil Engineering Department to specifications provided by IDOT. The software was debugged and later modified by IDOT to provide header information to identify test sites.

The friction test program loads automatically if the program disk is in the HP-IPC's internal drive when power is applied to the computer. The operator is given a sequence of prompts to name a file and then identify the test location by answering a series of prompts and entering information from a field sheet generated by the PTIB.

Field crews fill in header information about the test location, direction of test, number of lanes, ID number, construction contract number, their initials, and the system number. Once the header information is entered, a test can be initiated by pressing a single function key on the computer keyboard. There are 16 function keys that can be programmed from HP-TB. Function keys are assigned to allow the test crew to select alternating wheel tests or single wheel tests with either wheel. Other function keys are assigned to denote direction changes, lane changes, and section changes during a test. Friction tests are printed out on the built-in printer and displayed on the HP-IPC's screen. The test data are recorded to the floppy disk as the tests are taken. Header information entered by the field crews is also recorded to disk and allows automatic processing and printing of reports when used in conjunction with the PTIB.

In the office, test data are sorted, verified, and merged into the PTIB electronically for processing. The results are matched to existing records on the PTIB using the header information entered by the field crews. Printed reports, generated by the PTIB, consist of a detail report, listing each test by log mile, a test section summary that shows the average of all the treaded-tire tests (FNt), and the average of all the smooth-tire tests (FNs). The PTIB also contains information about mix and aggregate types, ADT data, and a history of friction test results at various sites. All of this information is synthesized into a single-page summary report. IDOT categorizes various testing projects as High Wet Accident, New Construction, Retest of New Construction, or Special Studies. A cover memo is generated automatically by the PTIB to the appropriate agency or individual.

ANCILLARY EQUIPMENT

In addition to the purchased equipment, a central power control panel was added to control 110 VAC and DC power. This panel also provides the operator with a switch to apply a calibration resistor across the system electronics to check their operation. AC power for the HP-IPC and the 3497A is provided by a generator powered by the two vehicles' two batteries. Friction tests are also recorded on a Gould strip chart recorder using a separate signal line. The strip chart recorder is used to record operator comments and visually check system functions such as locked brake and event timing. The strip chart can also be used to process data should the other electronic system fail.

Mechanical modifications to the existing system were handled jointly by the University of Illinois staff and the Materials and Physical Research staff. These included new torque transducers, signal amplifiers, and modifications to the trailers' axles and brake systems. IDOT's in-house electronics staff reviewed and developed boards for the heavy-duty relays and designed and built cables and connectors. A specially fitted water pump driven off of the drive shaft of the tow vehicle was fabricated by IDOT personnel.

The signals from the torque transducers are amplified using a high-gain bridge amplifier. The output from the amplifier is split; one signal goes to the strip chart and the other to a voltage-controlled oscillator (VCO). The VCO converts the input signal to torque. It is stored in one of the 3497's digital accumulators. The split system makes it possible to continue testing even if there is a problem with one of the recording devices.

The braking mechanism uses an air over hydraulic system. It took considerable research to obtain an off-the-shelf brake assembly that is self-retracting and rated to hold a locked wheel. IDOT finally settled on a brake designed for use on mining cars. Tow vehicles were ordered with on-board air compressors driven off of the engine. Air supply lines are run to the rear bumper to a quick disconnect air fitting. A flexible hose on the trailer connects to air lines run along the trailer frame to electric solenoids that control the brake for each test wheel.

When the test wheel is selected by the operator and the test sequence activated, air is applied to the brake modulator and the test wheel is locked. The original testers' electric brakes had problems with slippage during calibration and during the actual friction test. The current brake system has performed for several years with few failures except when testing high-friction mixes. Another modification to the brake system that uses brake calipers for each wheel is being considered. Each trailer's braking system components are examined during the off-test-season and repaired as necessary.

Water is delivered to the pavement from a 1.5-in. diameter water line connected to a pump driven off of the drive shaft of the test vehicle. The water output is then proportional to the tow vehicle speed. The water pump itself is mounted to the rear axle of the tow vehicle by a bracket welded to the rear axle. Belt tension may be adjusted by setting the bolt tension adjuster on the water pump mounting bracket. The water pump and water solenoid are the first devices activated when a test is initiated. A magnetic clutch on the water pump is engaged and the water solenoid for the selected test wheel is activated, and water is delivered to the pavement through the outlet of a 250-gal agricultural tank mounted in the bed of the tow vehicle. Water is pumped through the ASTM-specified nozzle (Ohio State nozzle). The test vehicle is equipped with 100 ft of fire hose and adjustable fire hydrant wrenches and thread adaptors. The water tank is filled through the water tank fill tub assembly. A shut-off handle is included to stop the water flow from the fire hydrant.

During the correlation tests, results from the three trailers were virtually identical over the entire process. Test sites for the correlation were chosen to represent several ranges of friction numbers. Tests were conducted with one test vehicle leading and the other following and locking up the test wheel at the same locations. After the pavement dried, the vehicles switched positions and crews and reran the courses.

SMOOTH- AND TREADED-TIRE TEST RESULTS

Since 1985 IDOT has routinely performed friction testing using both a smooth and a treaded tire on the same axle at every test location. The test is performed alternating between the smooth and the treaded tires at 0.1-mi increments. This is routinely done for testing for high wet-pavement accident locations, new construction, follow-up retests of new construction, and special studies.

Figure 1 shows the number of sites tested from 1984 through 1990. The equipment upgrades during 1985 and 1986 provided a dramatic increase in the number of sites tested. The breakdown of sites tested in 1990 included approximately 23 percent high wet accident sites, 20 percent new construction sites, 35 percent reruns of new construction, and 22 percent special study projects.

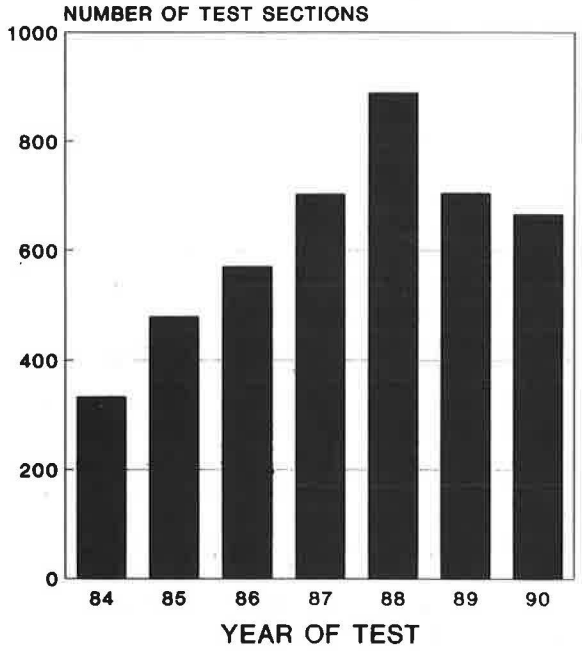

FIGURE 1 Histogram of friction test sections by year of test.

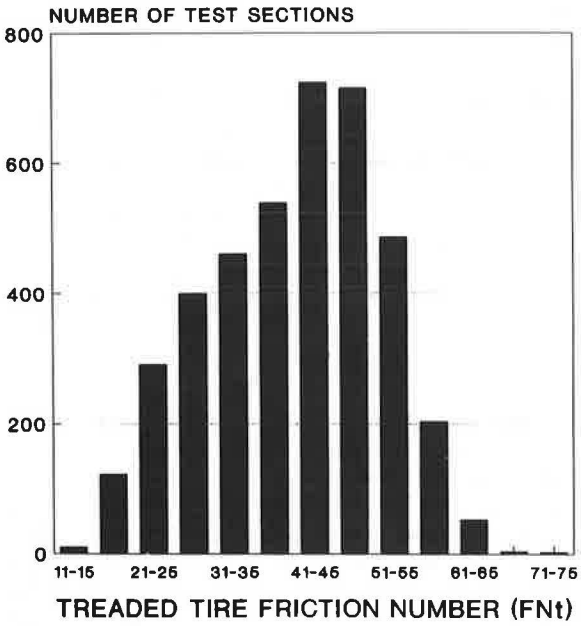

FIGURE 2 Histogram of average treaded-tire friction test values for all sections.

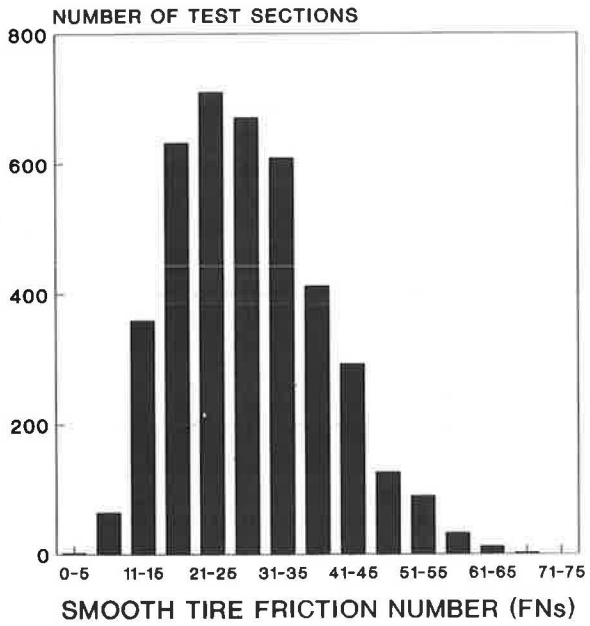

FIGURE 3 Histogram of average smooth-tire friction test values for all sections.

The treaded-tire friction number (FNt) and the smooth-tire friction number (FNs) test results summarized in the following figures are averaged over the length of the test section. For ease of data analysis, only one direction of travel was selected.

Figures 2 and 3 show the histogram of the range of average friction numbers for the test sites for treaded tire (FNt) and smooth tire (FNs) test data respectively from 1985 through 1990.

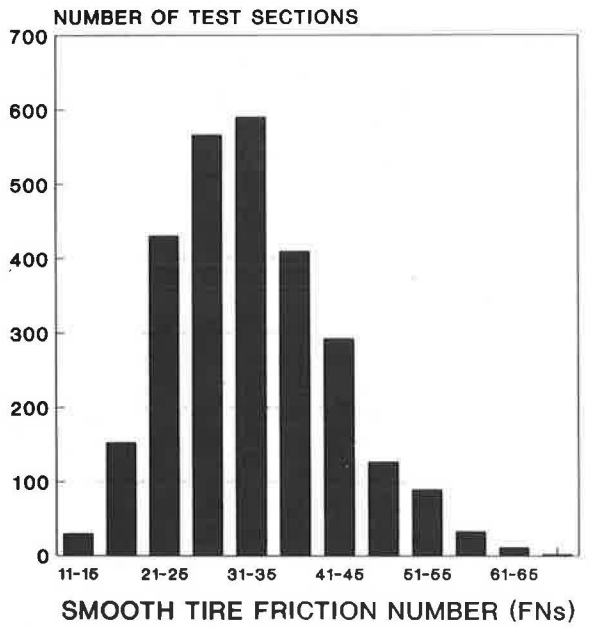

FIGURE 4 Histogram of average smooth-tire test values for sections with FNt greater than 35.

TABLE 1 TENTATIVE GUIDELINES FOR EVALUATING FRICTION AT HIGH WET ACCIDENT SITES BEFORE 1987

Friction Number Range	Tentative Guidelines
1. FNt 30 or less	Friction is probably a factor contributing to wet-pavement accidents.
2. FNt between 31 and 35	Uncertainty exists as to whether pavement friction is the primary factor.
3. FNt is 36 or more	Probably some condition other than pavement friction may be the primary factor causing wet pavement accidents.

TABLE 2 TENTATIVE GUIDELINES FOR EVALUATING FRICTION AT HIGH WET ACCIDENT SITES AFTER 1987

Friction Number Range	Tentative Guidelines
1. FNt 30 or less or FNs less than 15	Friction is probably a factor contributing to wet-pavement accidents.
2. FNt greater than 30 and FNs between 15 and 25 or FNt between 31 and 35 and FNs greater than 25	Uncertainty exists as to whether pavement friction is the primary factor.
3. FNt is 36 or more and FNs is greater than 25	Probably some condition other than pavement friction may be the primary factor causing wet pavement accidents.

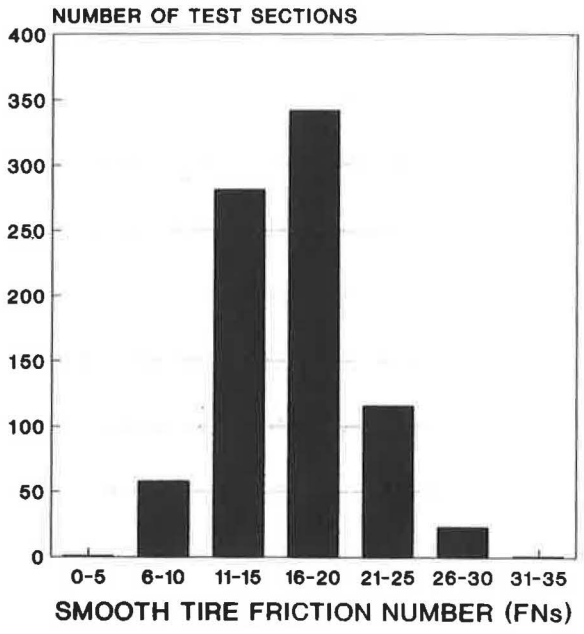

FIGURE 5 Histogram of average smooth-tire test values for sections with FNt less than 31.

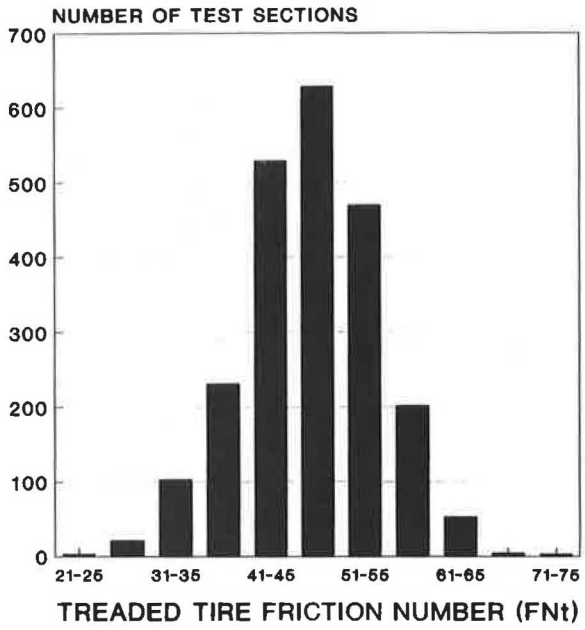

FIGURE 6 Histogram of average treaded-tire friction test values for sections with FNs greater than 25.

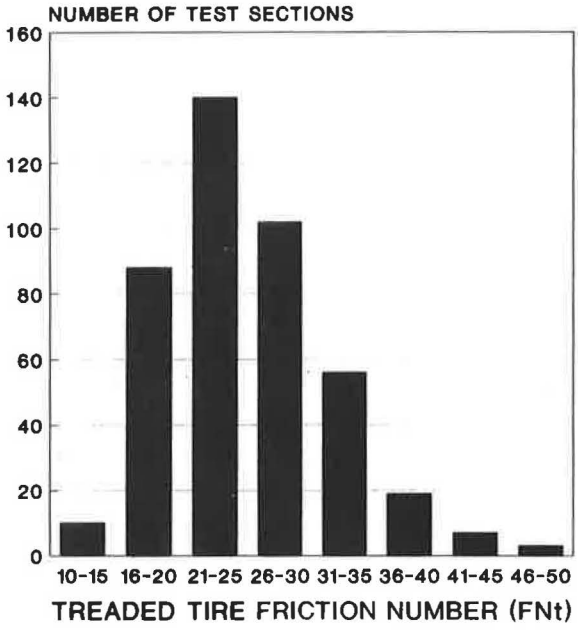

FIGURE 7 Histogram of average treaded tire friction test values for sections with FNs less than 15.

In the 1970s, tentative guidelines were developed for evaluating treaded friction numbers for high wet-pavement accident sites. These are given in Table 1.

In 1986, somewhat on the basis of IDOT's limited experience with smooth-tire data, the tentative guidelines shown in Table 2 were established, incorporating smooth-tire friction data in evaluating high wet-pavement accident sites. This was done to address the concern that whereas the treaded tire is a measure of surface microroughness (microtexture), the smooth tire pro-

vides a measure of surface drainage (macrotexture) in addition to microtexture. Thus, test results from each tire should be evaluated.

Figure 4 shows the histogram of FNs data for FNt greater than 35. Figure 5 portrays FNs data for FNt less than 31. Figure 6 shows the histogram of FNt data for FNs greater than 25. Figure 7 portrays FNt data for FNs less than 15. It appears that pavements can show adequate friction characteristics with either tire, yet exhibit inadequate friction characteristics with the other.

FUTURE EFFORTS

IDOT plans to continue actively testing pavement friction characteristics in the categories outlined. It appears that both the treaded tire and smooth tire tests provide needed information on the frictional characteristics of the pavement. The use of both tests appears appropriate.

REFERENCES

1. J. E. LaCroix. *A Summary of the Illinois Skid-Accident Reduction Program—August 1985 to December 1986*. Illinois Department of Transportation, Springfield, Dec. 1986.
2. J. E. LaCroix. *A Summary of the Illinois Skid-Accident Reduction Program—December 1986 to December 1987*. Illinois Department of Transportation, Springfield, Dec. 1987.

Publication of this paper sponsored by Committee on Surface Properties–Vehicle Interaction.

Summary of NASA Friction Performance Data Collected with ASTM E501 and E524 Test Tires

THOMAS J. YAGER

A summary of friction performance data collected during NASA Langley Aircraft Landing Dynamics Facility track, diagonal-braked vehicle, and instrumented tire test vehicle evaluations using the ASTM E501 (rib tread) and E524 (blank tread) test tires is given. A variety of pavement types, both grooved and ungrooved, and conditions are included. The principal factors influencing tire-pavement friction performance are discussed, and the advantages of using the blank-tread tire for wet pavement evaluations are identified. An indication of some future tire-pavement friction investigations is also given.

Personnel at the National Aeronautics and Space Administration (NASA) Langley Research Center's Landing and Impact Dynamics Branch have been involved in instrumented aircraft, ground vehicle, and controlled track tests since in the mid-1950s. Extensive aircraft tire tests at the Aircraft Landing Dynamics Facility (ALDF) track at Langley have provided a basic understanding of the phenomenon of tire hydroplaning and identified the major factors influencing tire-pavement friction performance (*1–7*). Concurrent with these ALDF track tests, several joint NASA/FAA/Air Force/aviation industry programs were conducted with different instrumented aircraft and a variety of ground friction measuring vehicles (*8–13*). During these tests, a diagonal-braked vehicle (DBV) was developed by NASA Langley engineers for measuring runway friction performance under locked-wheel friction conditions (*14,15*). Because of tire tread wear under locked-wheel conditions, impetus was generated to develop a blank- or smooth-tread test tire, but one with full-tread rubber skid depth. The ASTM E17 Committee on Pavement Management Technologies had a standard for a rib-tread test tire designated E501. In the early 1970s, ASTM Standard E524 was approved for a blank- or smooth-tread test tire of the same bias-ply construction and tread rubber composition as the E501 tire tread. Since then, thousands of test runs have been conducted with the NASA DBV equipped with the E524 blank-tread test tires. In tire friction studies using the NASA Langley instrumented tire test vehicle (ITTV), both the rib-tread and blank-tread ASTM tires have been evaluated under a variety of pavement surface types and conditions. The NASA DBV has conducted tests on more than 150 runways in 42 states in the United States and also in Canada, England, Germany, Italy, and Spain. Other DBVs equipped with the ASTM E524 tires have been used successfully in Sweden, France, Switzerland, Japan, and other countries to evaluate runway friction performance and identify problem runways under less-than-ideal surface conditions. The purpose of this paper is to summarize the test results from NASA ALDF track, DBV, and ITTV studies using the ASTM E501 and E524 test tires for pavement friction evaluations. Justification is given to prefer use of the blank-tread E524 tire for meaningful wet pavement friction assessments. Future test plans and requirements aimed at improved techniques for adequately measuring wet pavement friction capability are also described.

NASA Langley Research Center, Mail Stop 497, Hampton, Va. 23665.

ALDF TRACK RESULTS

The influence of automobile tire tread design, pavement surface texture, and speed on the locked-wheel friction coefficient developed on wet surface conditions is shown in Figure 1. These results were obtained during ALDF track tests (*7*) on highly textured and very smooth (trowel-finished) concrete surfaces with a water depth of 1 mm (0.04 in). The tire size was 6.50-13 with a vertical load of 3.7 kN (835 lb) and a tire inflation pressure of 186 kPa (27 psi), comparable specifications for the current ASTM test tires. The upper plot of Figure 1 shows the results obtained with the four-groove rib-tread tire, and the lower plot shows the blank- or smooth-tread tire results. The friction values obtained with the smooth-tread tire are significantly lower than the rib-tread tire, as expected. Increased speed and reduced surface texture under wet conditions also decrease the friction performance of both tires. The additional effects of surface contaminants reducing surface texture and tire friction performance are described from NASA DBV test results.

NASA DBV RESULTS

The effects of surface water and rubber contaminants on vehicles stopping capability and tire friction performance is shown in Figure 2. This evaluation was performed with the DBV shown in Figure 2. The brake system diagram illustrates the modification made to implement stable and controlled vehicle performance during the friction measurements at high speed with two diagonal wheels locked (equipped with ASTM E524 blank-tread tires) and the remaining pair free rolling (unbraked). The DBV wet/dry stopping distance ratios depicted in the bar graphs for different rainfall rates and surface types were obtained from test runs conducted at the same distance off runway centerline with brakes applied at 98 km/hr (60

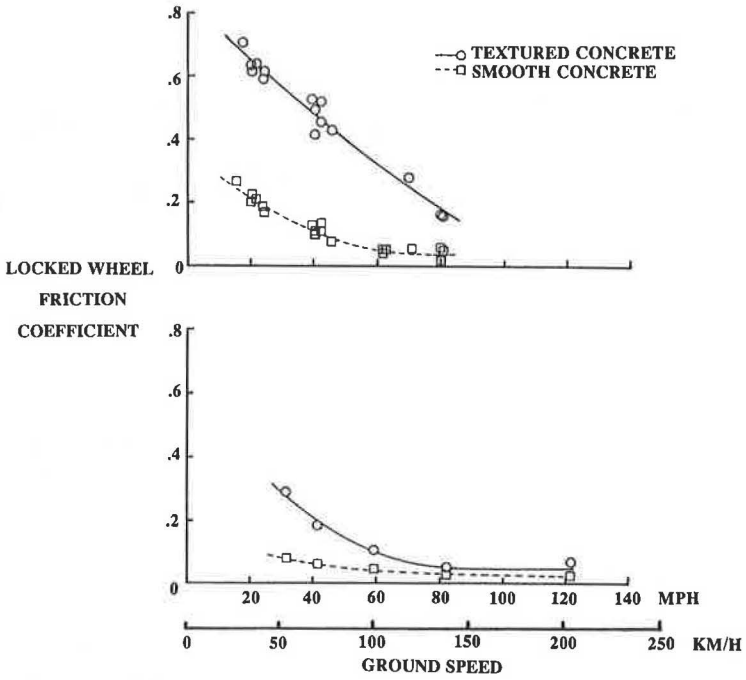

FIGURE 1 Effect of tire tread design, pavement texture, and speed on locked-wheel friction developed on a wet surface: *top*, four-groove rib-tread tire; *bottom*, smooth-tread tire (ALDF track data).

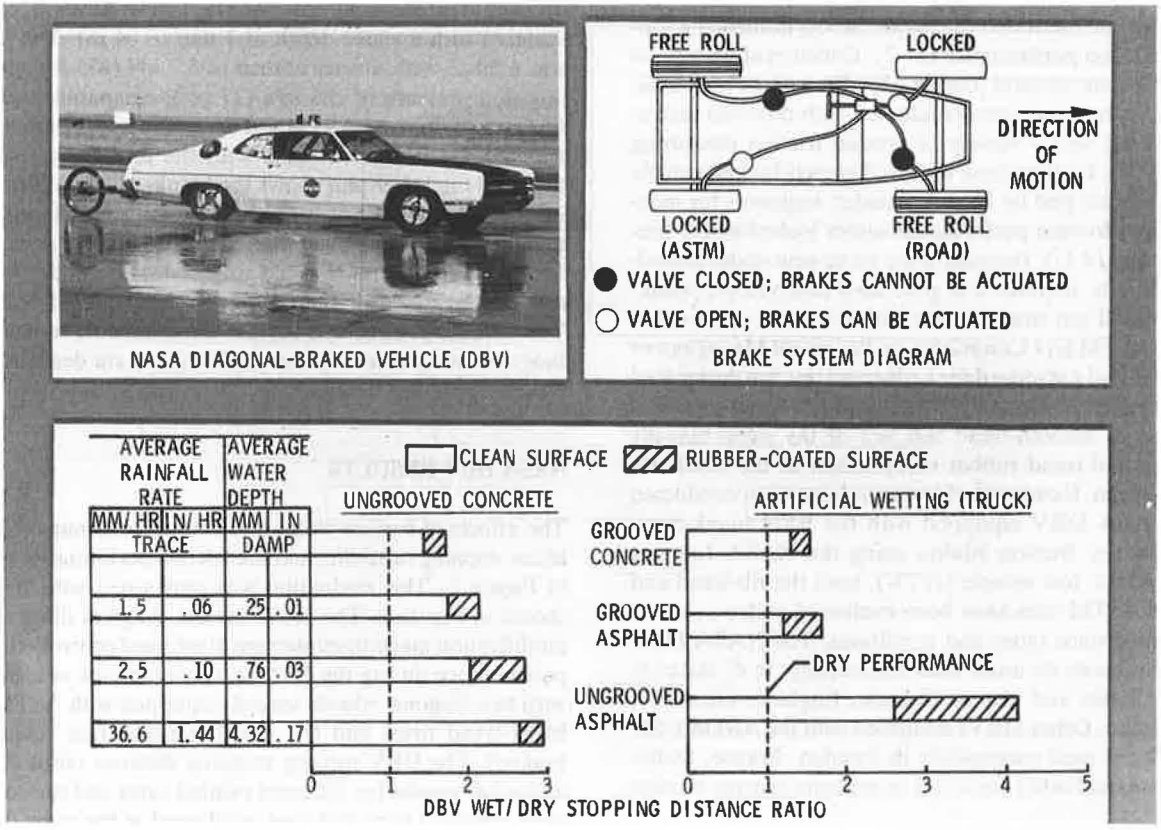

FIGURE 2 Effect of surface contaminants on DBV stopping performance.

mph) to a complete stop. Measurements of surface water depth and DBV stopping distance during different periods of rainstorm activity on an ungrooved concrete runway with a 1 percent crown reveal a direct relationship between average water depth and stopping distance. As rainfall rates increase, greater water buildup on the runway surface occurs, which decreases tire friction performance as reflected in the increased stopping distance ratios. The runway was even more slippery near the end of it, where it was contaminated by rubber deposited during aircraft tire spin-up following touchdown. The buildup of the rubber coating on runway surfaces tends to reduce pavement texture and hence degrade tire friction, particularly under wet conditions. The cross-hatched DBV stopping distance increment shown in Figure 2 illustrates the effects of rubber contamination on the ungrooved concrete runway slipperiness measurements for different rainfall rates. Also shown in the figure are comparable DBV measurements made on other grooved and ungrooved runways under artificially wetted (truck) conditions where the average water depth was 0.5 mm (0.02 in.). The longer DBV wet/dry stopping distance ratios measured on the ungrooved asphalt runways compared with the concrete surfaces are the result of lower surface macrotexture.

In the late 1960s, Runway 4/22 at the NASA Wallops Flight Facility on the eastern shore of Virginia was modified to provide a level test section 16 m (50 ft) wide and 1128 m (3,700 ft) long in the middle portions of the runway. Both grooved and ungrooved, concrete and asphalt test surfaces were installed as shown in the runway schematic in Figure 3. NASA DBV tests were conducted on these surfaces after truck wetting that left wet and puddled surface conditions. Results from these DBV tests are shown in Figure 4 for the ungrooved and grooved surfaces on Runway 4/22 at NASA Wallops. Tests with ASTM bald- and rib-tread tires were conducted with the DBV. On the grooved surfaces, the variation in locked-wheel friction coefficient with speed shows similar results for these two test tires, but on the ungrooved surfaces, the rib-tread tire developed higher friction—particularly at the higher test speeds. The ASTM bald-tread E524 tire data suggest a greater sensitivity to surface texture variation than the rib-tread E501 tire for the ungrooved surfaces shown in Figure 4.

ITTV RESULTS

A photograph of the NASA ITTV during a wet surface run at NASA Wallops Flight Facility is shown in Figure 5, and the general specifications for this test vehicle are indicated. The test fixture can be rotated horizontally to accommodate testing at fixed yaw angles. The test-wheel axle can be coupled to a chain-drive gearbox off the left rear truck wheel to obtain data at fixed braking slip conditions. Figure 6 shows five test

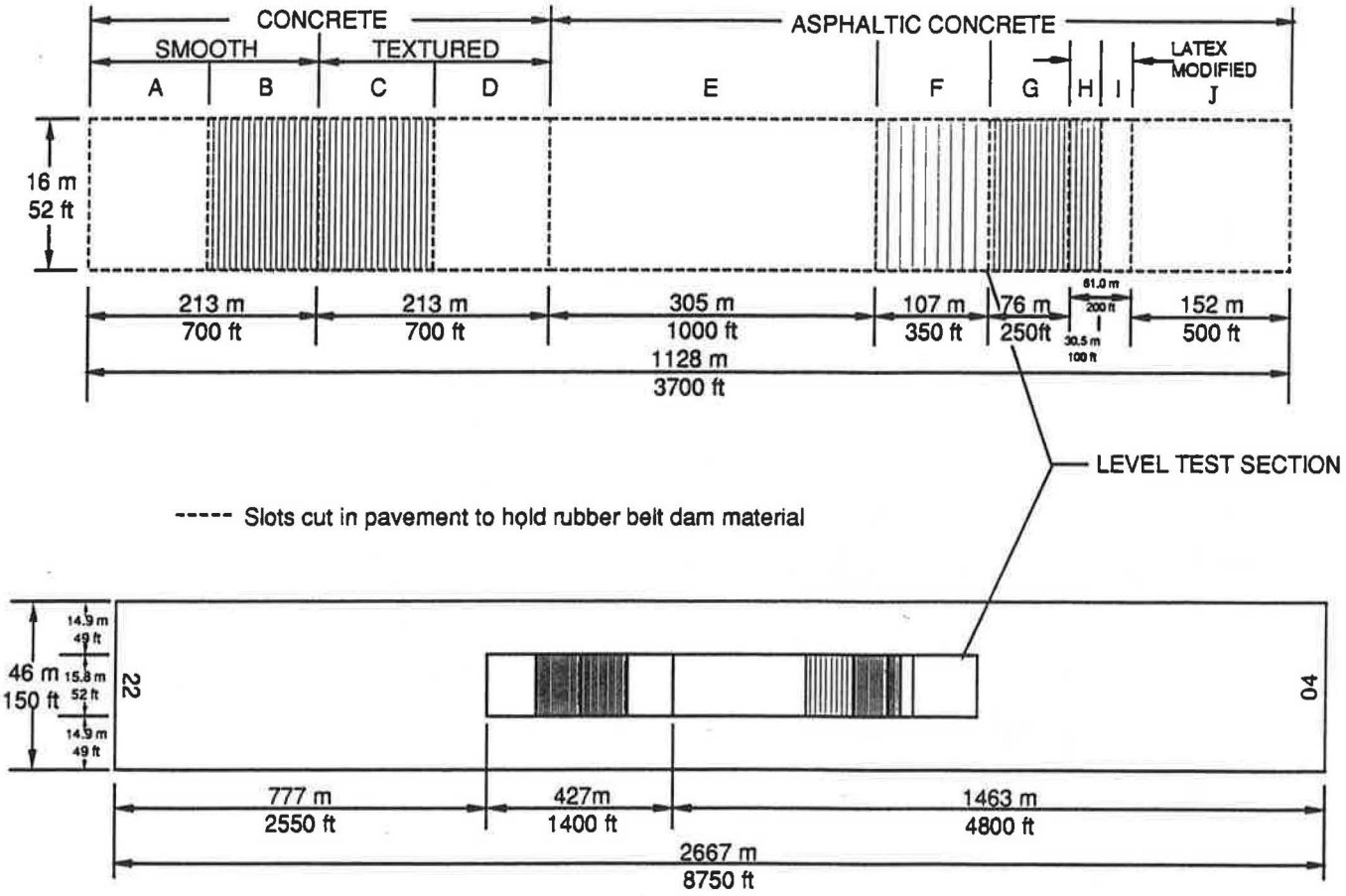

FIGURE 3 Schematic of NASA Wallops Flight Facility Runway 4/22 test surfaces (Surfaces B, C, G, and H transversely grooved 0.25 × 0.25 × 1.0 in.; Surface F transversely grooved 0.25 × 0.25 × 2.0 in.).

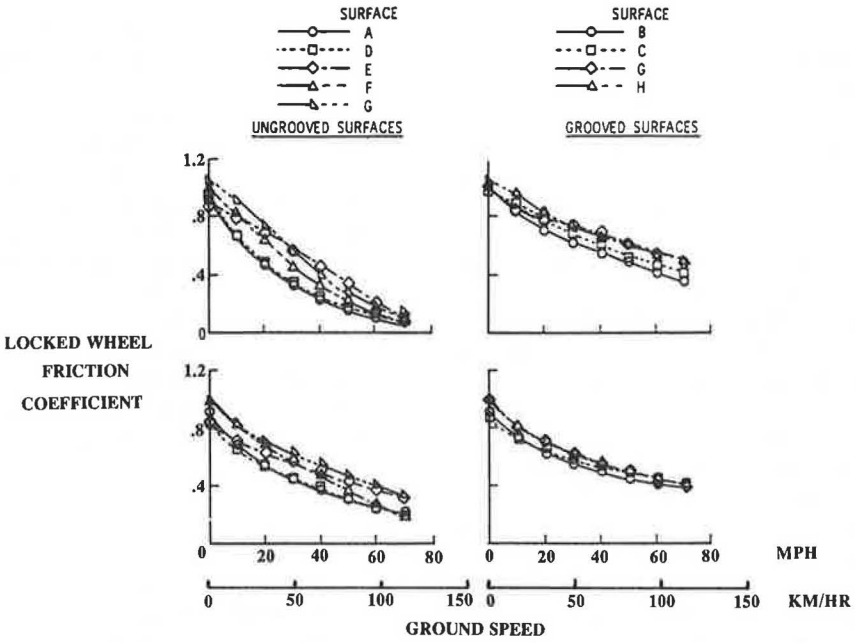

FIGURE 4 Variation of DBV locked-wheel friction coefficient with ground speed: *top*, ASTM smooth-tread tire; *bottom*, ASTM rib-tread tire.

FIGURE 5 Instrumented tire test vehicle.

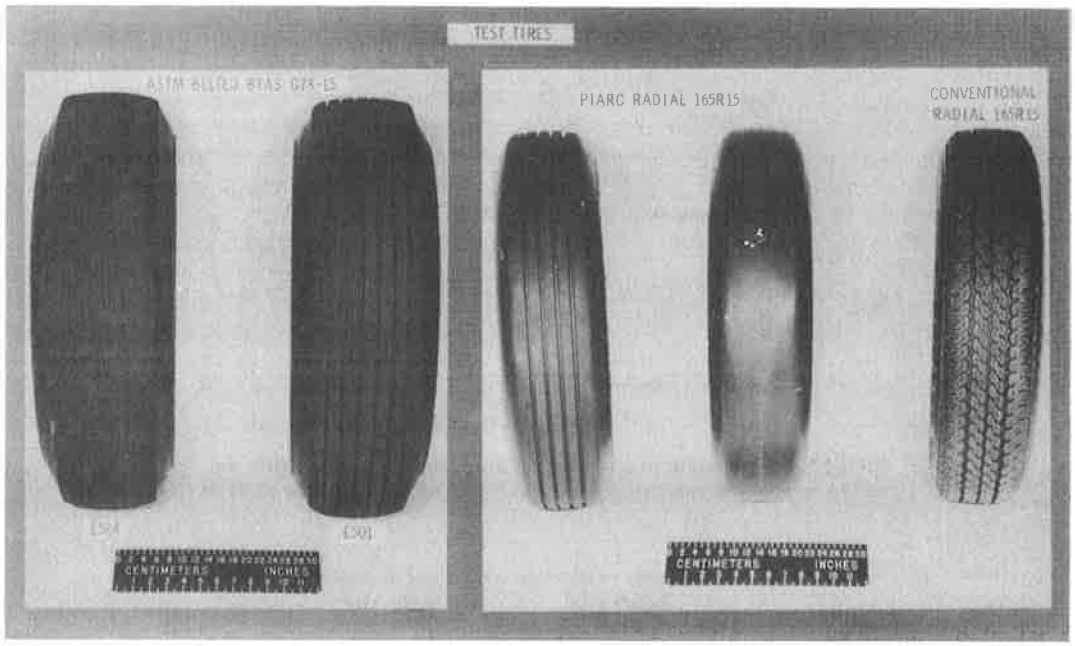

FIGURE 6 Test tires used in ITTV evaluation at NASA Wallops Flight Facility.

tires, including the ASTM E501 and E524 tires, that were used in a study of tire friction performance. Close-up photographs of the two concrete test surfaces used in this study are shown in Figure 7 with their average macrotexture depth values. The variation of braking drag force friction coefficient with slip ratio for the five test tires under wet conditions is given in Figure 8 for the ungrooved concrete surface and Figure 9 for the grooved concrete surface. The smooth-tread test tires showed the greatest influence of speed on braking friction, as expected, and the grooved concrete gave higher friction values, particularly at the higher slip ratio. In general, the peak braking friction coefficient was developed between

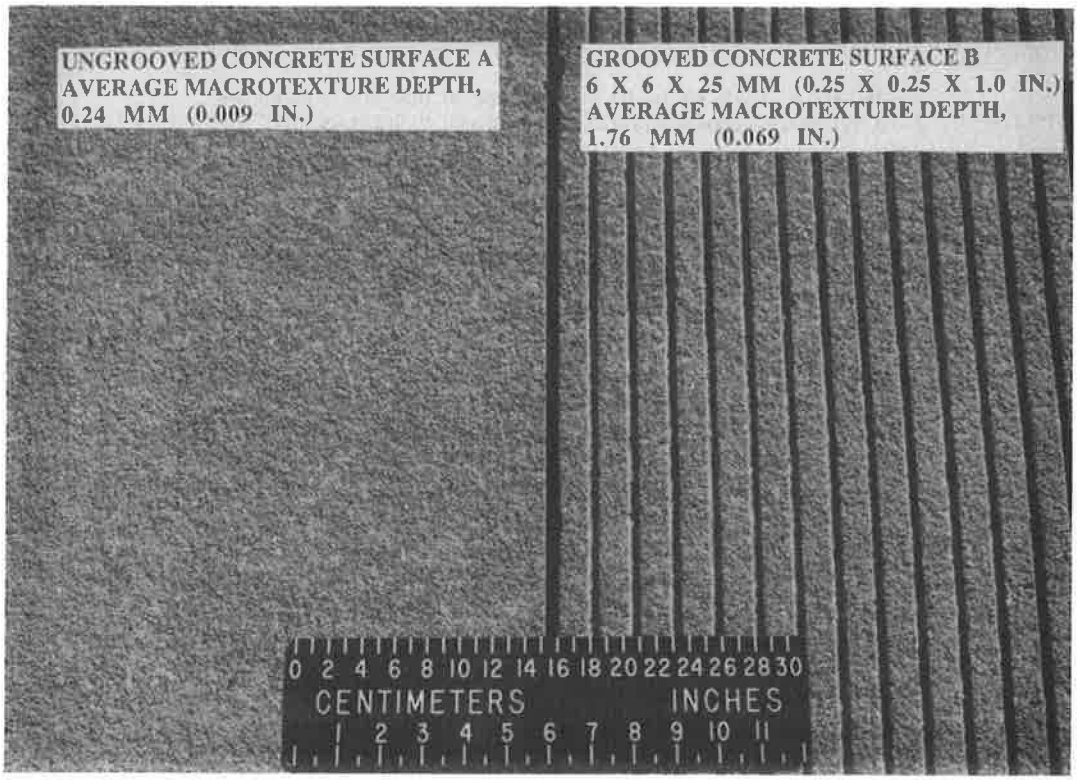

FIGURE 7 Concrete test surfaces at NASA Wallops Flight Facility.

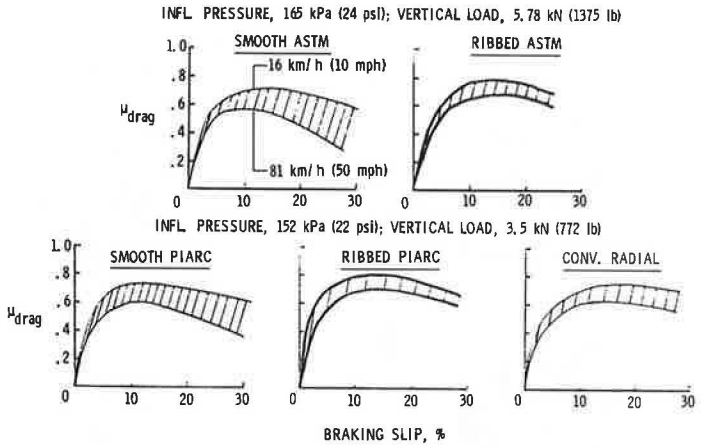

FIGURE 8 Variation in tire braking drag friction with braking slip on wet ungrooved concrete [average water depth = 0.25 mm (0.01 in.)].

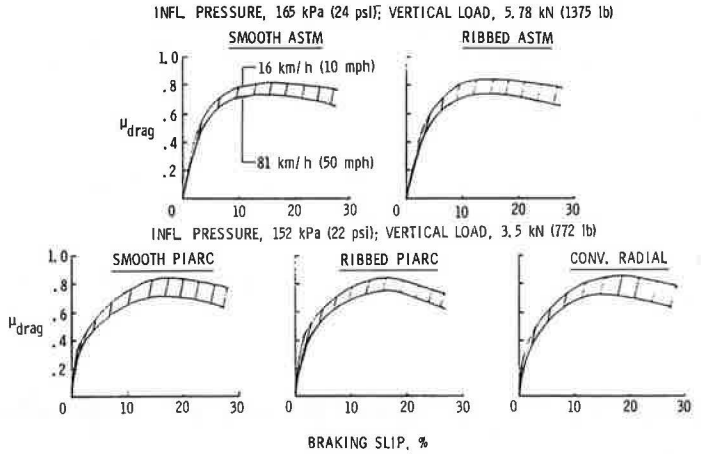

FIGURE 9 Variation in tire braking drag friction with braking slip on wet grooved concrete [average water depth = 0.25 mm (0.01 in.)].

10 and 20 percent braking slip for these five tires. Results from another study using the ITTV to evaluate the effects of tire footprint aspect ratio (footprint width divided by length) on hydroplaning speed are shown in Figure 10. These data were obtained using the ASTM E524 tire inflated at three different pressures (open symbols) with a larger truck size (solid symbols). As expected, the hydroplaning speed increased with inflation pressure, but with greater tire footprint aspect ratio values, the tire hydroplaning speed value decreased significantly. Additional tests are planned using the ITTV to study a variety of ground vehicle tires to better identify how the footprint aspect ratio influences tire hydroplaning speeds. Other future test programs include a joint program with the Air Force and aviation industry to define the factors effecting tire tread wear and consequently optimize tire tread design.

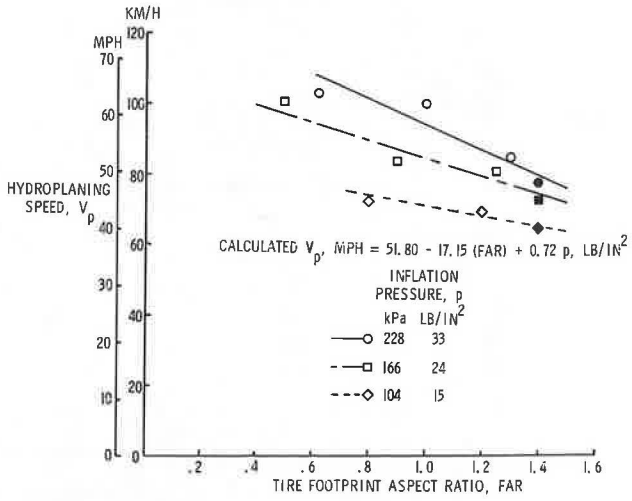

FIGURE 10 Variation of dynamic hydroplaning speed with tire footprint aspect ratio (open symbols = automobile tire data, closed symbols = truck tire data).

CONCLUDING REMARKS

A summary of friction performance data collected during NASA Langley ALDF track, DBV, ITTV evaluations using the ASTM E501 and E524 test tires is given. A variety of pavement types and contaminants were included, and the principal factors influencing tire-pavement friction performance were discussed. These results indicated that under wet pavement conditions, the ASTM E524 smooth-tread tire is more sensitive to variations in speed, surface texture, and contaminants than the ASTM E501 rib-tread tire. Another advantage is that the influence of tire wear on the friction data is eliminated using the blank-tread tire. Some future test plans aimed at improving tire-pavement friction performance have also been described.

REFERENCES

1. W. B. Horne and T. J. W. Leland. *Influence of Tire Tread Pattern and Runway Surface Condition on Braking Friction and Rolling Resistance of a Modern Aircraft Tire*. NASA TN D-1376. NASA, 1962.
2. W. B. Horne and R. C. Dreher. *Phenomena of Pneumatic Tire Hydroplaning*. NASA TN D-2056. NASA, 1963.
3. T. J. W. Leland and G. R. Taylor. *An Investigation of the Influence of Aircraft Tire-Tread Wear on Wet-Runway Braking*. NASA TN D-2770. NASA, April 1965.
4. W. B. Horne, T. J. Yager, and G. R. Taylor. *Review of Causes and Alleviation of Low Tire Traction on Wet Runways*. NASA TN D-4406. NASA, 1968.
5. T. J. W. Leland, T. J. Yager, and U. T. Joyner. *Effects of Pavement Texture on Wet-Runway Braking Performance*. NASA TN D-4323. NASA, Jan. 1968.
6. R. F. Smiley and W. B. Horne. *Mechanical Properties of Pneumatic Tires With Special Reference to Modern Aircraft Tires*. NASA TR R-64. NASA, 1960.
7. W. B. Horne and U. T. Joyner. *Pneumatic Tire Hydroplaning and Some Effects on Vehicle Performance. Proc., SAE International Automotive Engineering Congress*, Detroit, Mich., Jan. 1965.
8. U. T. Joyner, W. B. Horne, and T. J. W. Leland. Investigations on the Ground Performance of Aircraft Relating to Wet Runway Braking and Slush Drag. *Advisory Group for Aerospace Research and Development*. Report 429. Jan. 1963.
9. *Pavement Grooving and Traction Studies*. NASA SP-5073. NASA, 1969.
10. T. J. Yager, W. P. Phillips, W. B. Horne, and H. C. Sparks. *A Comparison of Aircraft and Ground Vehicle Stopping Performance on Dry, Wet, Flooded, Slush, and Ice-Covered Runways*. NASA TN D-6098. NASA, Nov. 1970.
11. W. B. Horne, T. J. Yager, R. K. Sleeper, and L. R. Merritt. *Preliminary Test Results of the Joint FAA/USAF-NASA Runway Under Wet and Dry Conditions with a Boeing 727, a Diagonal-Braked Vehicle, and a Mu-Meter*. NASA TM X-73909. FAA; NASA, 1977.
12. W. B. Horne, T. J. Yager, R. K. Sleeper, E. G. Smith, and L. R. Merritt. *Preliminary Test Results of the Joint FAA-USAF-NASA Runway Research Program, Part II—Traction Measurements of Several Runways Under Wet, Snow-Covered, and Dry Conditions with a Douglas DC-9, a Diagonal-Braked Vehicle, and a Mu-Meter*. NASA TM X-73910. FAA; NASA, 1977.
13. T. J. Yager, W. A. Vogler, and P. Baldasare. *Evaluation of Two Transport Aircraft and Several Ground Test Vehicle Friction Measurements Obtained for Various Runway Surface Types and Conditions*. NASA TP 2917. NASA, Feb. 1990.
14. T. J. Yager. Progress in Airport Pavement Slipperiness Control. Presented at the Air Line Pilots Association 18th Air Safety Forum, Dallas, Tex., July 1971.
15. W. B. Horne. *Status of Runway Slipperiness Research*. NASA SP-416. NASA, Oct. 1976, pp. 191–245.

Publication of this paper sponsored by Committee on Surface Properties–Vehicle Interaction.

FAA Guidance on Use of Friction Measuring Equipment for Maintaining Highly Skid Resistant Runway Pavement Surfaces at Civil Airports

THOMAS H. MORROW

A revision is presented to the procedures and guidelines recommended by FAA for frictional standards involving maintenance of highly skid resistant runway pavement surfaces at civil airports that have commercial turbojet aircraft operations. Revision of AC 150/5320-12B presents guidance relative to the visual inspection of runway pavement surface condition, when continuous friction measuring equipment is not available at civil airports, and the use of continuous friction measuring equipment, when available at civil airports, to monitor the deterioration of runway pavement surfaces. Periodic friction surveys will help identify those areas on the runway that are potentially hazardous conditions for aircraft braking and directional control. Once the deficient areas have been located and the cause of the deterioration identified, corrective action can be determined and expedited by the airport management. Guidance is also given on types of surface treatments that successfully mitigate aircraft hydroplaning potential and maintenance methods used to remove rubber deposits in the touchdown zones of runway pavement surfaces.

FAA conducted a tire performance evaluation and friction equipment correlation study in August 1989 at NASA Wallops Flight Facility at Wallops Island, Virginia. The study was performed in response to a request from ASTM to evaluate the performance of tires manufactured according to its specifications ASTM E524 and ASTM E670. Some 1,650 tests were conducted on five types of surfaces using three brands of tires and four types of friction measuring device. Friction tests were conducted at 40 and 60 mph (65 and 95 km/hr), using each device's self-water system on dry test surfaces. The water was applied at a depth of 0.04 in. (1 mm). The analyses conducted involved 156 reliability and performance studies and 31 correlation comparisons.

Limits of acceptability were established for the data evaluation. The McCreary tire performed best on the runway friction tester (RFT), Saab friction tester (SFT), and the skiddometer (SKD). The Dico tire performed best on the mumeter (MUM).

The tire formulation given in ASTM E524 specification for locked-wheel trailers will be put into a new ASTM standard to describe the characteristics of the McCreary tire. The current ASTM E670 specification will contain the specifications for the Dunlop and Dico tires.

FAA, U.S. Department of Transportation, 800 Independence Avenue S.W., Washington, D.C. 20590.

REQUEST FOR RESEARCH

On June 17, 1988, the chairman of ASTM Subcommittee E17.21 asked FAA to conduct tests to evaluate tire performance on friction measuring devices. The chairman requested that these tests be performed by the FAA Technical Center at the National Aeronautics and Space Administration (NASA) Wallops Flight Facility.

PURPOSE OF TIRE PERFORMANCE STUDY

The purpose of the tire performance study was twofold:

1. To establish the reliability, performance, and consistency of tires on all types of dry runway pavement surfaces, using continuous friction measuring devices equipped with self-water systems (T. H. Morrow, unpublished studies, Dec. 1980 and Aug. 1991).
2. To select the best-performing tires that will achieve consistent correlation between the various friction measuring devices and to develop guidelines that will be dependable and useful to airport operators in maintaining runway pavement surfaces for safe aircraft operations during wet weather conditions.

Further details can be found in works by Morrow concerning the tire performance study (*1,2*).

FACTORS THAT AFFECT SKID-RESISTANT PAVEMENTS

Over time, several factors cause the skid resistance of the runway pavement to deteriorate:

- *Mechanical wear and polishing action*: aircraft tires' rolling or braking on the pavement surface causes texture loss.
- *Accumulation of contaminants*: contaminants such as rubber, jet fuel, oil spillage, chemicals, and dust particles cause the runway to be slippery when wet.
- *Influence of seasonal variances*: ambient temperature, wind, sun, rainfall intensity, and such cause deterioration to the pavement surface.

- *Airport maintenance practices and subsequent surface treatment*: poor maintenance and repair practices cause textural loss.
- *Structural and other surface deficiencies*: rutting, raveling, cracking, joint failure, slab faulting, and depressions caused by settling, or other indicators of distressed pavement, cause frictional loss.

CONDUCTING FRICTION EVALUATIONS WITHOUT CFME

If the airport does not own or have access to continuous friction measuring equipment (CFME), the following procedures are given to evaluate the potential loss of frictional properties caused by one or more of the factors identified in the previous paragraph.

Touchdown Zone

The evaluator should investigate each 500-ft segment of the touchdown zones. In addition, the evaluator should observe the condition of the midpoint zone of the runway.

Minimum Survey Frequency

Table 1 shows the frequency for conducting friction surveys according to annual aircraft traffic activity at runway end.

Recording Pavement Condition Survey

The evaluator should complete the following information in Figure 1 on the pavement condition survey form:

- Date of Visual Survey.
- Runway Designation.
- Contaminants in Touchdown Zone on Runway—The evaluator classifies the rubber accumulation according to the levels given in Table 2, for example, very light, medium, very dense. The evaluator also includes a recommendation for scheduling rubber removal, where applicable.
- Other Contaminants Found on Runway—The evaluator lists any other contaminants found on the runway and provides recommendations for removal.
- Surface Treatment Condition—Table 3 shows two types of grooves and a rating of their conditions.
- Other Contaminants Found on Runway—The evaluator lists any other contaminants found on the runway and provides recommendations for removal.
- Surface Treatment Condition—Table 3 shows two types of grooves and a rating of their conditions.
- Pavement Surface Type Condition—Table 4 shows two pavement types and a rating system for each.
- Additional Relevant Observations—The evaluator can record any other relevant observations of conditions that may result in significant friction loss.

TABLE 1 SCHEDULE FOR CONDUCT OF FRICTION SURVEYS

NUMBER OF DAILY TURBOJET AIRCRAFT LANDINGS PER RUNWAY END	MINIMUM FRICTION SURVEY FREQUENCY
LESS THAN 15	ANNUALLY
16 TO 30	6 MO
31 TO 90	3 MO
91 TO 150	MONTHLY
151 TO 210	2 WKS
GREATER THAN 210	WEEKLY

Note: Each runway should be evaluated separately.

Pavement Textural Measurement

Pavement texture measurements should be taken in conjunction with visual inspections and the results recorded on the form provided in Figure 1. The method for measuring texture was developed by NASA and is called the NASA grease-smear test (GST). The measurements represent the average distance between the peaks and valleys of the surface texture. Over time, the measurements will indicate any textural deterioration that has taken place on the pavement surface. A minimum of three measurements should be taken in each of the touchdown, midpoint, and rollout zones of the runway. A good skid resistant pavement surface should have an average texture depth of 0.025 in. or more.

For grooved portland cement concrete pavements, measurements can be taken in traffic areas either near transverse joints or at light-fixture locations, wherever the surface has not been grooved. Likewise, on grooved asphalt concrete pavements, the measurements may be taken in nongrooved areas near light-fixture locations.

CONDUCTING FRICTION EVALUATIONS WITH CFME

Background Information on CFME

Performance Standards

Performance standards for CFME and friction measuring tires are given in ASTM ES17 for the fixed-brake slip devices and ASTM E670 for the side force device. These standards were developed through research conducted at the NASA Wallops Flight Facility.

Federal Funding

The Airport and Airway Improvement Act of 1982 includes friction measuring equipment as an eligible item for airport development; before programming or procuring equipment,

DATE OF VISUAL SURVEY	RUNWAY	CONTAMINANTS IN TOUCHDOWN ZONE ON RUNWAY			OTHER CONTAMINANTS OBSERVED ON RUNWAY			AVERAGE TEXTURE DEPTH MEASUREMENT	
		LOCATION OF RUBBER DEPOSIT ACCUMULATION AND CLASSIFICATION LEVEL		RECOMMENDED ACTION	LOCATION OF OTHER CONTAMINATES AND THEIR IDENTIFICATION		RECOMMENDED ACTION	STATION	DEPTH
		STATION	CLASSIFICATION		STATION	IDENTIFICATION			

SURFACE TREATMENT CONDITION			PAVEMENT SURFACE TYPE CONDITION		ADDITIONAL REMARKS AND OBSERVATIONS
SAW-CUT GROOVE CONDITION	PLASTIC GROOVE CONDITION	POROUS FRICTION COURSE CONDITION	ASPHALTIC CONCRETE CONDITION	PORTLAND CEMENT CONCRETE CONDITION	

FIGURE 1 Forms for visual inspection of runway pavement surface conditions.

airport operators should contact their FAA airport's field office for guidance.

Qualification

Figure 2 gives the manufacturers and CFME that meet the requirements given in the referenced ASTM standard specifications.

Training

Success in obtaining reliable data from friction measuring equipment depends heavily on the efficiency of the personnel in correctly operating and maintaining the equipment. Therefore, FAA requires the manufacturer of the equipment to provide professional training to airport personnel in operation, maintenance, and procedures for conducting friction surveys on runways. To ensure that high proficiency is maintained for those responsible for operating the equipment, FAA also recommends that the manufacturer provide a continued periodic training program.

Calibration

Before conducting friction surveys, all CFME shall be furnished with self-water systems and be calibrated according to the tolerances required by the manufacturer.

Communications Equipment

The airport operator shall ensure that all appropriate communications equipment and frequencies are provided on all vehicles used in conducting friction surveys and that all personnel that operate the equipment are properly trained and fully cognizant of current airport safety procedures.

CFME Vehicles

All vehicles used in conducting friction surveys shall be checked for adequate braking ability.

Presurvey Preparation

Before conducting friction surveys, the airport operator should conduct a thorough visual inspection of the runway pavement surface to locate, identify, and record any deficiencies encountered on the runway.

Conduct of Friction Surveys

Vehicle Speed for Friction Survey

All approved CFME can operate safely at either 40 or 60 mph. The lower speed of 40 mph is used most often and

TABLE 2 INSPECTION METHOD FOR VISUAL ESTIMATION OF RUBBER DEPOSIT ACCUMULATED ON RUNWAY

DESCRIPTION OF RUBBER COVERING PAVEMENT TEXTURE IN TOUCHDOWN ZONE OF RUNWAY AS OBSERVED BY EVALUATOR	CLASSIFICATION OF RUBBER DEPOSIT ACCUMULATION LEVELS	ESTIMATED RANGE OF MU VALUES AVERAGED 500 FOOT SEGMENTS IN TOUCHDOWN ZONE	SUGGESTED LEVEL OF ACTION TO BE TAKEN BY AIRPORT AUTHORITY
Intermittent individual tire tracks. 95 % of surface texture exposed	VERY LIGHT	0.65 or greater	None
Individual tire tracks begin to overlap. 80 % to 94 % surface texture exposed	LIGHT	0.55 to 0.64	None
Central 20 foot traffic area covered. 60 % to 79 % surface texture exposed	LIGHT TO MEDIUM	0.50 to 0.54	Monitor deterioration closely.
Central 40 foot traffic area covered. 40 % to 59 % surface texture exposed	MEDIUM	0.40 to 0.49	Schedule rubber removal within 120 days.
Central 50 foot traffic area covered. 30 % to 69 % of rubber vulcanized and bonded to pavement surface. 20 % to 39 % surface texture exposed	MEDIUM TO DENSE	0.30 to 0.39	Schedule rubber removal within 90 days.
70 % to 95 % of rubber vulcanized and bonded to pavement surface. Will be difficult to remove. Rubber has glossy or sheen look. 5 % to 19 % surface texture exposed	DENSE	0.20 to 0.29	Schedule rubber removal within 60 days.
Rubber completely vulcanized and bonded to surface. Will be very difficult to remove. Rubber has striations and glossy or sheen look. 0 % to 4 % surface texture exposed	VERY DENSE	Less than 0.19	Schedule rubber removal within 30 days or as soon as possible.

Note: The schedules given in the above table are for a runway end that has medium turbojet aircraft activity, about 31 daily operations. As aircraft activity on a runway increases above 31, especially an increase in the wide-body aircraft activity, the airport operator may have to compress the schedule. The percent of coverage should be estimated only on the central portion of the runway most heavily used at touchdown, about 20 to 30 feet on each side of the runway centerline, not edge to edge of the pavement. The MU ranges given above are from fixed-brake CFME and are representative for each classification level. Though the airport does not have a CFME, these values will indicate the projected level of deterioration in friction over time.

determines the overall macrotextural-contaminant/drainage properties of the runway pavement surface.

If the airport operator suspects that the runway is deficient in microtextural properties (pavement does not feel "sand-papery" to the touch or aircraft have reported skidding on the wet surface at the higher speeds), then friction measurements should be made at the higher speed of 60 mph to obtain a proper evaluation.

TABLE 3 ALPHANUMERIC CODING FOR GROOVE CONDITION

Pavement surface treatment	Alpha code	Numerical coding with description
Groove type	H	0-none 1-sawed grooves 2-plastic grooves (C-8 in Table 1-4)
Groove condition	G	0- ... uniform depth across pavement 1-10% ... % of grooves not effective 2-20% " 3-30% " 4-40% " 5-50% ... When this level is exceeded, 6-60% the airport operator should 7-70% take corrective action to 8-80% improve groove efficiency. 9-90% ... grooves not effective.

Location of Friction Survey on Runway

When conducting friction surveys at 40 mph, the airport operator should begin recording data at 500 ft from the threshold end of the runway to allow adequate acceleration distance for the friction vehicle. At the opposite end of the runway, the airport operator should terminate the friction survey at least 500 ft from the end of the runway to allow for adequate distance for the friction vehicle to stop safely.

When conducting friction surveys at 60 mph, the airport operator should begin recording data at 1,000 ft from the threshold end of the runway to allow adequate acceleration distance for the friction vehicle. At the opposite end of the runway, the airport operator should terminate the friction survey at least 1,000 ft from the end of the runway to allow adequate distance for the vehicle to stop safely.

Unless surface conditions are noticeably different on either side of the runway centerline, a survey on the one side in the same direction the aircraft lands should be sufficient. However, when both ends are to be evaluated, the vehicle should be programmed to record data on the return trip (both ways).

The lateral location on the runway for performing friction surveys is based on the type and mix of aircraft operating on the runway.

TABLE 4 ALPHANUMERIC CODING FOR PAVEMENT SURFACE TYPE

Pavement surface type	Alpha code	Numerical coding with description
Asphalt concrete pavement	A	0-slurry seal coat 1-new, asphalt-covered aggregate, black color 2-microtexture, 75% fine aggregate, color of aggregate 3-mixed-texture, 50-50 fine, coarse aggregate color of aggregate 4-macrotexture, 75-100% coarse aggregate 5-worn surface, coarse aggregate protrudes and/or abraided out 6-open-graded surface course, PFC 7-chip seal 8-rubberized chip seal 9-other
Portland cement concrete pavement	C	0-belt finished 1-microtextured, predominately fine aggregate 2-macrotextured, predominately coarse aggregate 3-worn surface, coarse aggregate protrudes and/or abraided out 4-burlap dragged 5-broomed or brushed 6-wire comb 7-wire tined 8-float grooved 9-other

Runways Serving Only Narrow-Body Aircraft Friction surveys should be conducted 10 ft to the right of the runway centerline.

Runways Serving Narrow- and Wide-Body Aircraft Friction surveys should be conducted 10 and 20 ft to the right of the runway centerline to determine the worst-case condition.

K. J. LAW ENGINEERS, INC.
President
Transportation Testing Equipment Division
42300 West Nine Mile Road
Novi, Michigan 48375-4103
FAX (313) 347-3343 **(M 6800)**
(313) 347-3300 **RUNWAY FRICTION TESTER**

BISON INSTRUMENTS, INC.
President
5708 West 36th Street
Minneapolis, Minnesota 55416
FAX (612) 926-0745
(612) 926-1846 **MU METER (Mark 4)**

AIRPORT EQUIPMENT COMPANY AB
President
Post Office Box 20079
BROMMA, SWEDEN S 161 20
(H) 46 (758) 51589
(O) 8 46 29 5070 **SKIDDOMETER (BV-11)**

AIRPORT TECHNOLOGY U.S.A.
President
6 Landmark Square
Suite 400
Stamford, Connecticut 06901
FAX (203) 378-0501 **(Mark 2)**
(203) 359-5730 **SURFACE FRICTION TESTER**

FIGURE 2 Qualified product list for CFME.

Wet and Dry Friction Surveys

Because wet pavement always yields the lowest friction measurements, CFME should routinely by used on wet pavement to simulate the worst-case condition.

Wet Pavement Simulation CFME is equipped with a self-water system to simulate rain-wet pavement surface conditions and provide a continuous record of friction values for each foot traveled along the runway.

Dry Pavement Simulation CFME is used on dry runway to establish the maximum available friction for aircraft braking performance. In addition, it sets a baseline for comparing existing and newly constructed pavements to determine the deterioration level over time.

Rainfall Survey The self-water systems used by CFME cannot simulate actual rainfall conditions on runway pavements that have depressed areas that pond during moderate to heavy rainfall. When these conditions exist on the runway, CFME cannot accurately predict the aircraft hydroplaning potential. Therefore, FAA recommends that the airport owner conduct periodic visual inspections of the runway surface during rainfall, noting the location and extent of any ponded areas. If the water depth exceeds 0.125 in. over a longitudinal distance of 500 ft, the depressed area should be corrected to the standard transverse slope.

CFME Correlation Chart

Research tests concluded at NASA Wallops Flight Center in 1989 confirmed the qualification and correlation of the CFME.

TABLE 5 CORRELATION OF MU-VALUES FOR CFME USING SELF-WATER SYSTEM

TYPE OF FRICTION EQUIPMENT	MOUNTED WITH DICO TIRE		MOUNTED WITH McCREARY TIRE			
	MARK 4 MU METER TRAILER		M 6800 RUNWAY FRICTION TESTER		BV-11 SKIDDOMETER TRAILER	MARK 2 SAAB FRICTION TESTER
RUNWAY SURFACE	FRICTION SURVEY SPEED		FRICTION SURVEY SPEED		FRICTION SURVEY SPEED	
FRICTION LEVEL	40 MPH	60 MPH	40 MPH	60 MPH	40 MPH	60 MPH
CLASSIFICATION	FRICTION VALUES		FRICTION VALUES		FRICTION VALUES	
MINIMUM	42	26	50	41	50	34
MAINTENANCE PLANNING	52	38	60	54	60	47
NEW DESIGN/ CONSTRUCTION	72	66	82	72	82	74

Table 5 shows the correlation relationship for the four approved CFMEs.

Corrective Action Guidelines

Mu numbers measured by CFME should be used as maintenance guidelines for identifying the appropriate corrective action required to improve and maintain runway pavement surfaces for safe aircraft operations. Poor friction conditions for short distances on the runway do not pose any serious threat, but long stretches of slippery pavement are of concern to the airport operator and require appropriate corrective methods.

Friction Deterioration Below Maintenance Planning Friction Level for 500 ft (152 m) When the averaged mu value on the wet runway pavement surface is below the maintenance planning friction level but above the minimum friction level for 500 ft, and the adjacent 500-ft segments are at or above the maintenance planning friction level, no corrective action may be required. These readings indicate that the pavement friction is deteriorating but the overall condition is acceptable. The airport operator should monitor the situation closely by conducting periodic friction surveys to establish the rate and extent of the deterioration.

Friction Deterioration Below Maintenance Planning Friction Level for 1,000 ft (305 m) When the average mu value on the wet runway pavement surface is less than the maintenance planning friction level for 1,000 ft (305 m) or more, the airport operator should conduct extensive evaluation of the cause and extent of friction deterioration and take appropriate corrective action.

Friction Deterioration Below Minimum Friction Level When the average mu value on the wet pavement surface is below the minimum friction level for 500 ft (152 m), and the adjacent 500-ft (152 m) segments are below the maintenance planning friction level, corrective action should be taken immediately after determining the cause of the friction deterioration. The overall condition of the entire runway pavement surface should be evaluated with respect to the deficient area before undertaking corrective measures.

New Design and Construction Friction Level for Runways For newly constructed runway pavement surfaces that are sawcut, grooved, or have a porous friction course overlay, the average mu value on the wet runway pavement surface for each 500-ft (152 m) segment should be no less than the new design and construction friction level.

Evaluation of Paint Areas on Runway Paint on wet runway pavement surfaces causes very slippery conditions. Friction surveys should be conducted over painted surfaces at 40 mph, under dry and wet conditions, to check the magnitude of the change in friction values between the unpainted and painted surfaces. When the averaged mu value is at the minimum friction level for 100 ft (30 m) or more or the difference between the wet and dry averaged mu readings is greater than 40, corrective action should be taken. Usually this means adding a small amount of sand to the paint mix to increase the friction properties of the paint to an acceptable level.

SURFACE TREATMENTS TO PREVENT HYDROPLANING

Three surface treatments have been used successfully to alleviate hydroplaning on wet runway pavement surfaces. Portland cement concrete pavements can be constructed with sawcut or plastic grooves. Asphalt concrete pavements can have either sawcut grooves or a porous friction course overlay.

MAINTENANCE METHODS FOR RUBBER REMOVAL

Two methods are used successfully to remove rubber on runways: high-pressure water and chemical/detergent. A combination of both may also be used.

High-Pressure Water

Most equipment used today operates at pressures between 5,000 to 8,000 psi and can exceed 15,000 psi. Some contractors can operate at pressures in excess of 35,000 psi.

Chemical/Detergent Application

Chemical/detergents have been successfully used to remove rubber deposits on runways. Chemical/detergents must meet Environmental Protection Agency requirements; those that are volatile and toxic in nature are not used on runways.

High-Pressure Water and Chemical/Detergents

Some asphalt concrete pavements are more susceptible to damage by the high-pressure water technique; therefore, applying chemical/detergents before using the high-pressure water method has been demonstrated successfully. Usually, the use of the chemical/detergents lowers the overall pressure required to remove rubber.

SUMMARY

This paper shows the application of the results obtained from an FAA research program that has led to the development of national and international standards for friction measuring equipment, pavement textural and drainage design, and friction measuring tire performance. The research effort has resulted in the publication of the following standards:

1. *Measurement, Construction, and Maintenance of Skid-Resistant Airport Pavement Surfaces*—Revisions included a new correlation table for friction measuring devices and closer tolerances for sawcut grooves.
2. *Emergency Standard Specification for Special Purpose, Smooth-Tread Tire*, ASTM ES17-90, 1990—A new specification that includes new performance standards for friction measuring tires developed during the research program.
3. *Standard Test Method for Side Force Friction on Paved Surfaces Using the Mu-Meter*, ASTM E670-87 (under revision)—Includes new performance standards for friction measuring tires developed in the research program.
4. *International Civil Aviation Organization: Revisions to Aerodromes, Annex 14* and *Airport Services Manual, Part 2* are in final preparation for publication.

Standards for the various friction measuring devices were provided to the International Civil Aviation Organization by FAA and are included in the revisions.

CONCLUSIONS

The importance of setting well-defined goals and developing a test plan before conducting the field test program resulted in the successful completion of the study. The program was designed to establish and improve standards for friction equipment and friction measuring tire performance. The resulting standards are published in FAA standards and are accepted worldwide by the aviation community.

REFERENCES

1. T. H. Morrow. *Reliability and Performance of Friction Measuring Tires and Friction Equipment Correlation*. REPORT DOT/FAA/AS-90-1. Federal Aviation Administration, Office of Airport Safety and Standards, Washington, D.C.; National Technical Information Service, Springfield, Va., March 1990.
2. T. H. Morrow. *Reliability and Performance of Friction Measuring Equipment and Friction Equipment Correlation*. In *Transportation Research Record 1307*, TRB, National Research Council, Washington, D.C., 1991.

Publication of this paper sponsored by Committee on Surface Properties–Vehicle Interaction.

Low-Cost Video Image Processing System for Evaluating Pavement Surface Distress

J. ADOLFO ACOSTA, J. LUDWIG FIGUEROA, AND ROBERT L. MULLEN

Most pavement condition surveys use rating systems in which pavement distress is measured by type, extent, and severity. Rating either bituminous or portland cement concrete pavements by the pavement condition rating (PCR) or similar systems is tedious and time-consuming. In most instances, distress measurement is subjective, which affects the actual rating. Improved data collection and data processing methods are thus needed to expedite pavement evaluation that can be used as input in pavement management systems. Recent advances in computer technology now permit the identification and quantification of distress types that can be measured by width, length, or area by automatic analyses of images captured by a microcomputer from video or film recordings. The development of a low-cost system for video image pavement distress analysis is described; the system allows the identification, classification, and quantification of commonly occurring pavement distress types in terms of severity and extent. Once pavement distress is identified, quantified, and classified, the system can be combined with rating procedures (such as PCR) to obtain a quantitative measure of pavement condition. Hardware and software characteristics of the system are described in detail. Diagrams showing the connection of system components and procedural steps leading to the calculation of a pavement rating are also included. Distress identification and classification is currently limited to distress types that can be quantified by width, length, geometry, or area covered by the distress.

Pavement management systems (PMSs) have been essential means of identifying road sections in need of maintenance or repair to allocate funds so that a maximum benefit/cost ratio can be achieved. Rating systems constitute fundamental inputs to a PMS. State transportation officials use these systems to quantify roadway performance with time. Rating systems are based on visual inspections in which pavement distress is measured by type, extent, and severity. The time-consuming procedure is normally subjective and nonrepetitive, thus affecting the actual rating.

The automation of pavement condition data collection and processing methods has become an important study topic. Some research and transportation agencies have made considerable progress in image analysis to obtain a pavement rating based on surface distress, but the system is still in the process of development.

Work by Baker et al. (*1*), Acosta (*2*), and Acosta et al. (*3*) indicates not only that automated video image pavement distress analysis is possible but that it is within the reach of implementation with currently available equipment and within a short time.

Department of Civil Engineering, Case Western Reserve University, Cleveland, Ohio 44106.

This paper describes the development of a low-cost system for video image pavement distress analysis that allows several commonly occurring pavement distress types to be identified, classified, and quantified in terms of severity and extent. Once this has been done, the system can be combined with rating procedures—such as the pavement condition rating (*4*)—to obtain a quantitative measure of pavement condition.

Hardware and software characteristics of the system are described in detail. Diagrams showing the connection of system components and procedural steps leading to the calculation of a pavement rating are included. Distress identification and classification are limited to types that can be quantified by width, length, geometry, or area covered by the distress. The system is capable of identifying, quantifying, and classifying distress within each of the most common types of pavements, namely, flexible, jointed concrete, and composite pavements.

Software development included provisions to allow the future consideration of additional distress types as specified in the PCR manual (*4*).

BACKGROUND

Computer-based image analysis was originally developed as a powerful tool in the medical sciences (*5,6*). Since then its use has been extended to a variety of disciplines, as shown by several texts on digital image processing (*7–10*).

General-purpose software currently available can perform image enhancements (*11*); however, identifying features or objects in an image is a much more difficult task. Quantifying images requires the use of specialized software that identifies features of interest and extracts geometric measurements from the digital image. Specific problem-dependent software must be developed to extract features for particular applications (*12,13*). Combinations of algorithm-based programs (for image enhancement) and rule-based programs (for object extraction) have been shown to be effective in feature extraction problems (*14,15*).

Recently, Fukuhara et al. (*16*) developed an automatic pavement distress survey system using a combination of a laser scanner, a photomultiplier tube, and a video camera connected to a signal processor. Rutting and longitudinal profile data are processed in real time and stored in a magnetic tape data bank. Cracking data is analyzed from the playback of recorded images. However, using specialized equipment may limit the system's broad application for pavement distress analysis.

GENERAL CONCEPT

The development of a video image pavement distress analysis system follows from the authors' work on crack and inclusion detection on metal and ceramic substrates. The analysis of an image proceeds in five steps: image digitizing and deblurring, image segmentation, clustering, feature extraction, and cluster classification. Image digitization is effected with a low-cost commercially available image capturing board residing in a microcomputer. Initial image segmentation is done by adaptive techniques using convolution, histogram, and primal sketch methods, among others (*17–20*). Damaged areas and other features within the pavement highlighted by segmentation are clustered to form objects (*21*). Calculation of geometric properties of these areas and features such as area, radius of gyration, aspect ratio, and others is required, along with the application of characteristic rules, to classify them as pavement distress, pavement feature, or unknown object (litter, debris, etc.). Pavement rating follows applying the dimensional guidelines specified in the rating manual.

HARDWARE CONFIGURATION

Most components of the video image analysis system for pavement distress are commercially available. This allows the assembly of a relatively low cost and reliable system, which may encourage transportation agencies and local governments to automate their pavement evaluations.

Video image recording and analysis are conducted separately, because computer storage space is limited and because data processing takes longer than data recording. This approach contributes to the versatility of the system and eliminates the need of a computer in the data collection vehicle.

A complete data acquisition and analysis system is estimated to cost about $30,000. The recording equipment includes a super VHS format video camera with mounting frame and adequate lens, depth measurement instruments, and their interfaces with video recording equipment. The video image analysis system includes a super VHS tape player, an image capturing board, a microcomputer CPU (or workstation), and monitors. The cost of a vehicle (preferably a van) to house the equipment should be added to the estimate.

Video Recording Equipment

Separating the video recording and analysis tasks simplifies image collection and reduces the possibility of equipment damage, because most of the equipment is operated in an office setting.

The video recording vehicle assembled at Case Western Reserve University consists of a pickup truck and a carry-on air-conditioned camper containing a 110-VDC power plant. A steel frame projects 7 ft from the rear of the camper to let the video recording camera be mounted perpendicular to the pavement without visual obstruction by the vehicle. The height of the steel frame is adjustable, allowing image recording at 5 to 8 ft from the pavement surface. The camera height is varied to provide the required pavement section width coverage and image resolution. Suitable video images have been obtained at vehicle speeds of up to 55 mph. Lighting fixtures are mounted on the frame to allow image recording at night. Shadows from other vehicles, the recording vehicle, roadside furniture, trees, and overpasses are avoided during nighttime recording. This simplifies and expedites further image analyses.

A super VHS format video camera with variable shutter speed of up to $1/1{,}000$ sec provides images of adequate resolution (up to 240 lines/frame) for pavement distress analysis. Individual frames are recorded every $1/60$ sec to provide continuous coverage of the selected pavement section.

A 58-mm perispheric video lens was adapted to the super VHS camera to provide a distortion-free area approximately three times the size of the area obtained by a conventional lens. The perispheric lens provides focused full-lane coverage within the height ranges of the mounting frame.

Images are recorded directly on a super VHS cassette tape, although at times the camera video and sound outputs are connected to an optional on-board super VHS videocassette recorder for backup. A microphone in the vehicle cabin allows the driver to record comments directly on the videotape. These comments about visual observations are used for future reference; they include starting log mile or continuing stationing, changes in pavement features, road and lighting conditions, and other items of interest.

Video Image Analysis Equipment

The development of a video image analysis system for pavement distress includes special requirements to obtain a system capable of

- Differentiating between cracks and joints in rigid pavements;
- Covering pavement sections a full lane wide and between 250 and 1,000 ft long;
- Processing images obtained at more than 45 mph;
- Identifying type, severity, and extent of distress; and
- Evaluating either rigid, flexible, or composite pavements.

Functional video image analysis equipment has been assembled following the configuration shown in Figure 1. The

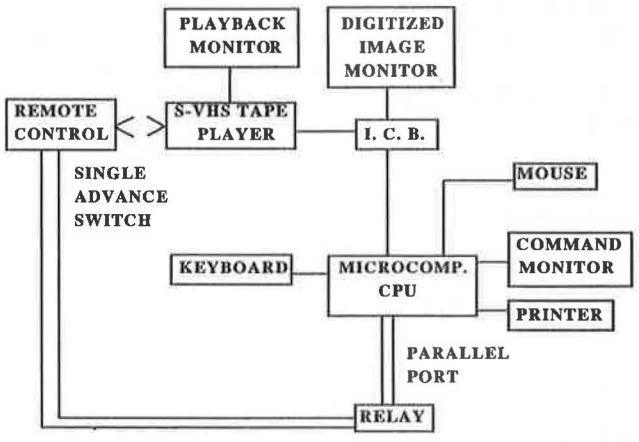

FIGURE 1 Video image analysis system components (*3*).

characteristics of the principal system components are presented next.

Super VHS Tape Player

After trying several professional models, a consumer super VHS format tape player/recorder was found to be the most suitable for attaching to other system components. Besides having the super VHS format, the player is capable of accurate single-frame advance. This is important in image analysis, because real-time processing is impossible within cost constraints. A playback monitor connected to the tape player allows the review of images and comments recorded along the roadway to initialize image analysis at the desired pavement section.

Image Capturing Board

Communication between the tape player and the CPU is effected through an image capturing board. Image processing is initiated with the playback of tapes at the beginning of the desired pavement section. But before an image can be captured, the image capturing board must be synchronized with the video signal from the tape player. Synchronization is achieved through commands issued to the image capturing board in the developed software. The image capturing board used in the system along with software library commands (*11*) enables the control of up to four boards (512 × 512, 8-bit deep frame buffer) within one system. The image capturing board is connected to a video monitor to permit viewing of digitized and processed images.

Microcomputer CPU

Currently, an MS-DOS 386-compatible microcomputer with a 16-MHz clock speed is used for image analysis control and processing. The tower-model microcomputer contains hard disk and floppy drives, a math coprocessor, 1MB RAM, and serial and parallel ports; it is attached to peripherals such as a command/graphics monitor, printer, mouse, and keyboard. The image capturing board requires two full-length 16-bit expansion slots on the microcomputer motherboard.

Relay

A 5-VDC relay is used to control single-frame advance by the videotape player remote control through timely software commands issued to the microcomputer parallel port. The parallel port generates a DC voltage signal after its activation with the software commands to close the circuit on the single-frame advance button of the remote control. Up to eight functions can be used through the parallel port without an additional interface board.

Image Resolution

Advanced high-resolution display monitors have a maximum resolution of 1024 × 1024 pixels (512 × 480 is the current standard), which mandates the width of visual images to obtain the minimum desired crack width identification of ⅛ in. If one pixel represents a minimum crack width, then a maximum width of 128 in. (10.67 ft) of roadway can be displayed on the advanced monitor to obtain the desired crack width resolution.

SOFTWARE DEVELOPMENT

This section describes general image analysis software and its five principal steps: image digitizing and deblurring, image segmentation, clustering, feature extraction, and cluster classification. Important topics concerning the developed computer program, PAVEDIST (PAVEment DISTress), are addressed in order to clarify some of its procedural steps; for more details, refer to the work by Acosta (*2*).

Background and General Description of Image Processing System

The development of a video image pavement distress analysis system follows from the work performed by Braun et al. in the nondestructive testing of ball bearings through imaging techniques conducted for the National Aeronautics and Space Administration (*22*). This research dealt in particular with the inspection of a rolling bearing component to measure the distribution, size, and shape of carbide particles (which act as crack initiation) on or near the surface of the bearing component. From this information, the predicted service life can be determined.

The effectiveness of the algorithms developed for extracting cracks and other damage from metals and composites in the identification of concrete pavement distress and further rating of a pavement section has been shown through the analysis of many video images. However, the algorithms relating to image segmentation revealed poor results in the analysis of asphalt concrete pavements, because this type of pavement yields textured and nonhomogeneous background images. The reasons for the unsatisfactory results will be addressed in further sections. Consequently, other techniques in image segmentation were studied and a new technique was developed.

A generalized flowchart of the image analysis software system is presented in Figure 2. Image analysis is initiated after the synchronization of the videotape player with the image capturing board. Scale definition before initiating the roadway survey is necessary if the distance between the camera and the road surface has changed. In practice the longitudinal and transverse length scales are recorded at the start of each tape.

PAVEDIST issues the command to advance a single frame through the parallel port, as explained. The image is captured by the board and stored in a two-dimensional array that coincides with the pixel position on the monitor. Values in the array represent the gray level on a scale between 0 (black) and 255 (white).

Before any clustering of pixels to define damaged zones, the original image is preprocessed to eliminate blurring that results from obtaining images at the high speeds of the recording vehicle. The deblurring process developed at Case Western Reserve University has been effective on images taken at speeds of up to 55 mph.

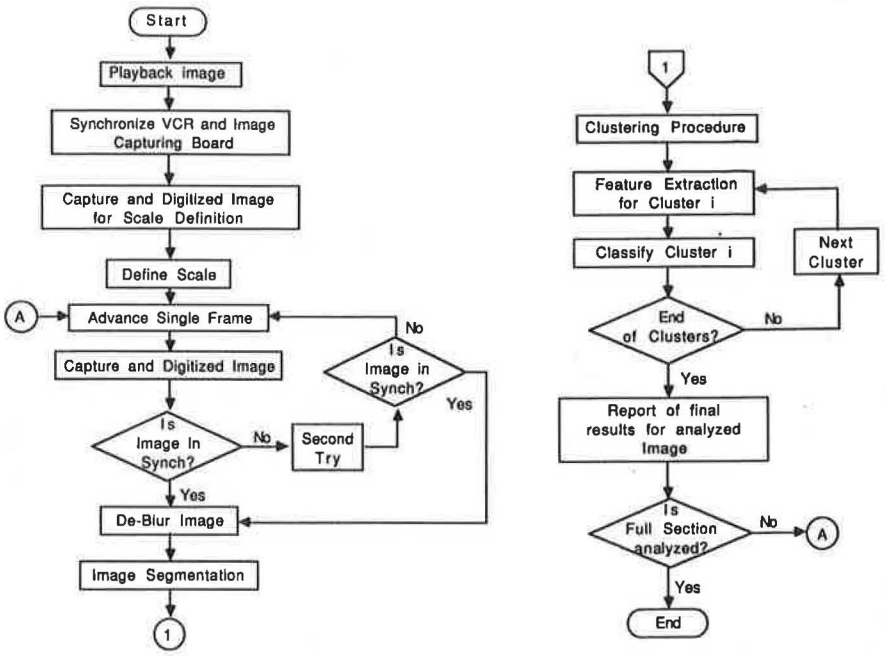

FIGURE 2 Image processing of pavement distress flowchart (*3*).

Statistical procedures are used to distinguish damaged zones from the background, for asphalt concrete pavements in particular. Once the image is segmented as background and foreground, adjacent pixels are clustered to outline damaged zones. Dimensional properties of each cluster are calculated, which will be useful in the further quantification of the type, severity, and extent of the pavement distress, according to the definitions in the PCR manual (*4*).

Image Digitizing and Deblurring

The image from the VCR player is digitized by means of the MVP-AT video digitizer and the IMAGER-AT MS-DOS software library (*10*). This software consists of routines that provide hardware controls for the MVP-AT digitizer such as frame buffer input and output, graphics, and imaging functions. The computer language directly supported by IMAGER-AT is Microsoft C.

The analog image from the VCR is digitized in a 512-×-480 array of pixels, each one stored in 1 byte of memory. Therefore, positions in the array can have values ranging from 0 (black) to 255 (white). The software digitizes the image following two steps: first the odd rows are captured (1, 3, 5, . . . , 479), then the even rows (0, 2, 4, . . . , 480). Because the film velocity in the VCR player is 60 frames/sec and because the two steps in the digitizing process take more than 1/60 sec, the final captured image is composed by odd lines corresponding to the actual frame and by even lines belonging to the next one. Thus, the deblurring can easily be accomplished either by merging the odd rows of the next frame with the even rows of the actual image or just by taking the odd rows of the actual image and compressing them, as selected in the described system. Obviously, the odd-line extraction deblurring method changes the longitudinal scale; this must be taken into account for further analysis.

Image Segmentation

Different techniques in image segmentation were attempted (*3*), including

- Histogram thresholding (*23*),
- One- and two-dimensional entropy-based approaches (*24*),
- Edge detectors (*25*), and
- Vertical region segmentation (*2,3*).

The vertical region segmentation (VRS) method was developed to overcome the drawbacks encountered when using the first four techniques to segment asphalt concrete pavement images.

Bituminous pavement images present a gradual change of brightness in the transverse direction. Darker zones are easily identifiable on the wheel-track regions as the result of stains, wear, or rubber marks from tires. In addition, the mineral aggregate displays randomly distributed tones, therefore the image must be treated as a nonhomogeneous textured image.

As explained by Acosta (*2*) and Acosta et al. (*3*), the VRS method divides the image into narrow longitudinal sections so that each section can be analyzed separately. The gray-level histogram is obtained, and the gray-level average and the standard deviation are calculated taking into account only the gray levels with significant occurrences in the frequency distribution. Three zones are delimited: background (undamaged pavement), connective (transition between background and foreground), and foreground (pavement distress). The zones are delimited on the basis of the average, the standard deviation, and two constant parameters that depend on the texture pattern of the image itself. Figure 3 illustrates the boundary positions for each zone. The pixels are assigned to one of the three zones on the basis of their gray-level values.

A distressed asphalt concrete image is shown after the VRS method is applied in Figure 4. The resulting image identifies

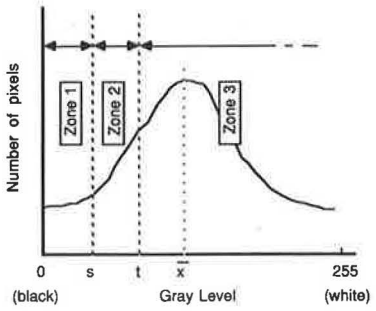

ZONE 1: Foreground
ZONE 2: Connective
ZONE 3: Background

$s = \bar{x} - \alpha\,\partial$

$t = \bar{x} - \beta\,\partial$

where:
α and β: constants
$\beta < \alpha$
∂: standard deviation
$\bar{x}$: average

FIGURE 3 VRS zones (*3*).

clearly the distress from the background, the noise produced by strains and tire marks is no longer visible, and the effect of the gradual change in darkness is eliminated. These favorable aspects are the result of the introduction of the connective zone, the analysis of separate narrow vertical regions, and the use of the gray-level histogram in conjunction with statistical operandi [for more details refer to Acosta et al. (*3*)].

Clustering

The clustering procedure is done by linking all the adjacent foreground and connective pixels so that the cluster is surrounded only by background pixels. A subroutine has been implemented to make this linking possible according to the following steps:

1. The image is scanned in a top-bottom and left-right pattern, seeking foreground or connective adjacent pixels whose coordinates are stored in a list corresponding to a particular cluster.
2. When adjacent pixels from different clusters are located, the clusters are merged.
3. All clusters with a number of pixels (foreground + connective) smaller than a minimum cluster size and clusters with foreground pixels less than a minimum value are deleted to eliminate clusters with sizes not relevant to the analysis.

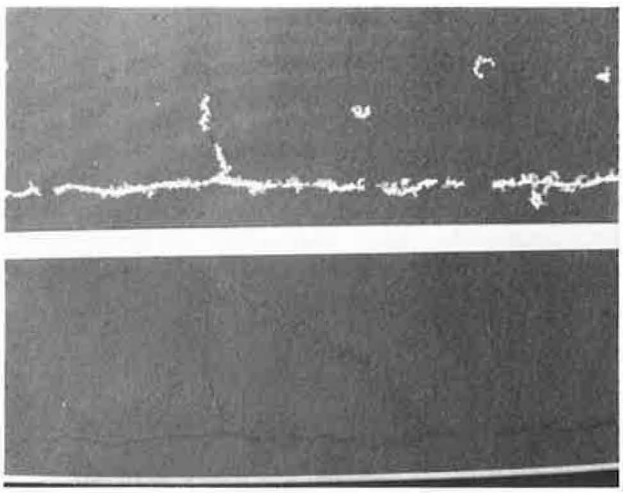

FIGURE 4 Asphalt concrete pavement image after VRS distresses are drawn in white (*top*); for comparison, digitized image is shown (*bottom*) (*3*).

Feature Extraction

A set of geometrical and statistical properties of a cluster is calculated by PAVEDIST for feature extraction. These features are used to identify a particular type of distress following a set of rules (rule-based system), as will be explained.

The total number of pixels is the sum of pixels from Zone 1 (foreground) and Zone 2 (connective); it is represented by n. The number of foreground pixels is represented by m. Transverse and longitudinal length are b and l.

The cluster is located in a bounding box with coordinates (x_{min}, y_{min}) and (x_{max}, y_{max}). Thus

$$b = x_{max} - x_{min} \tag{1}$$

$$l = y_{max} - y_{min} \tag{2}$$

The x-coordinate variation, x_{var}, is defined as

$$x_{var} = \sum \frac{x^2}{n} - (x_{cg})^2 \tag{3}$$

The y-coordinate variance, y_{var}, is defined as

$$y_{var} = \sum \frac{y^2}{n} - (y_{cg})^2 \tag{4}$$

where (x_{cg}, y_{cg}) are coordinates of center of gravity calculated as follows:

$$x_{cg} = \frac{\sum x}{n} \tag{5}$$

$$y_{cg} = \frac{\sum y}{n} \tag{6}$$

and

(x,y) = coordinates of each pixel.

The gray-level mean, $\bar{Z}$, is defined as

$$\bar{Z} = \frac{\sum z}{n} \tag{7}$$

where Z is $f(x, y)$ or gray-level of the pixel with coordinates (x, y).

The gray-level variation, Z_{var}, is defined as

$$Z_{var} = \frac{\sum Z^2}{n} - (\overline{Z})^2 \quad (8)$$

Inertia in the x- and the y-direction, I_x and I_y, are the inertias about axes parallel to the original axes with origin at the center of gravity of the cluster. They are defined as

$$I_x = \sum x^2 - x_{cg}(\sum x) \quad (9)$$

$$I_y = \sum y^2 - y_{cg}(\sum y) \quad (10)$$

The product moment of inertia, I_{xy}, is defined as

$$I_{xy} = \sum xy - x_{cg}(\sum y) \quad (11)$$

Principle moments of inertia, I_{max} and I_{min}, are defined as

$$I_{max} = \frac{I_x + I_y}{2} + {}^1/_2 [(I_x - I_y)^2 + 4(I_{xy})^2]^{1/2} \quad (12)$$

$$I_{min} = \frac{I_x + I_y}{2} - {}^1/_2 [(I_x - I_y)^2 + 4(I_{xy})^2]^{1/2} \quad (13)$$

The angle of principal axes of inertia, β, is the angle with respect to the horizontal. It is calculated from

$$\tan 2\beta = \frac{2I_{xy}}{I_y - I_x} \quad (14)$$

The inertia ratio, τ, is defined as

$$\tau = \frac{I_{min}}{I_{max}} \quad (15)$$

Each distress is isolated by a boundary box that encloses it. The ratio between the transverse and longitudinal dimensions of the box is the shape factor. Cluster length is the length of a straight line passing through the center of gravity of the cluster following the direction of the angle of principal axes of inertia and limited by the bounding box that encloses the cluster. Cluster width is the average width of the cluster calculated with the ratio between the area and the cluster length.

These features are calculated twice by means of a subroutine. First, the features are extracted from the unjointed clusters; after they are brought together, new features are measured from the joined objects. The cluster classification is performed on the basis of the new features.

PAVEDIST compares all the clusters by pairs and joins two clusters if they satisfy the following conditions:

- The clusters are close enough. The physical meaning of "close enough" depends on the scale of the image, that is, the length represented by a pixel.
- The angles of the principal axes of inertia of the clusters are similar (a tolerance is given); furthermore, these angles must be similar to the angle formed by a straight line connecting the centers of gravity of the clusters.

If the objects satisfy the conditions, they are brought together and the new object is compared with all the others. The procedure is repeated until no more cluster connections are possible.

Cluster Classification

A rule-based classification approach was developed, taking into account two distress types: transverse and longitudinal cracking. Typical ranges of values for the features extracted for transverse and longitudinal cracking were heuristically determined. A subroutine was implemented with decision rules that compare the features extracted from the object; the subroutine classifies it as transverse cracking, longitudinal cracking, or unidentified distress type. The accuracy of this subroutine is close to 90 percent, and most misclassifications arise from objects with feature similar to the groups analyzed—objects that need more features to be correctly classified.

Finally, PAVEDIST draws the clusters belonging to each particular group in the digitized image monitor and total properties are obtained to be used as input for the future PCR calculation.

PCR Routine

The PCR routine was implemented following the guidelines in the PCR manual (*4*) to calculate the PCR using data stored in an output file from PAVEDIST.

The data file must an identification of the highway analyzed and the pavement width (in feet). Each analyzed section must have data for its beginning and ending (in miles) and a set of data for which each datum must be conformed by:

- Distress Code: code assigned to the distress type. A list of distress codes is included in Table 1.
- Severity-Property-1 (sevp1) and Severity-Property-2 (sevp2): numerical values representing the severity level (low, medium, or high) of the distress type.
- Extent-Property (extp): numerical value representing the extent level (occasional, frequent, or extensive) of the distress type.

Severity-Property-1 (qualitative), Severity-Property-2 (quantitative), and Extent-Property are based on the definitions for severity and extent given in the PCR manual (*4*) for each distress type; they are also summarized in Table 2.

The PCR values calculated for the analyzed sections are stored in an output file that, like the input file, contains an identification of the highway analyzed and the pavement width (in feet). Each analyzed section must have the beginning and ending of the section (in miles) and a PCR value.

The weights for the distress types taken from the PCR manual are read from a data file.

SUMMARY AND CONCLUSIONS

An initial system for video image pavement distress analysis that allows the identification and classification of common types of structural pavement distress was developed. Signif-

TABLE 1 DISTRESS CODES

Distress Type	Type of Pavement		
	Asphalt Concrete	Composite	Port.Cem Concrete
Block and Transverse Cracking	1101	2101	3101
Longitudinal Joint Cracking	1102	2102	3102
Wheel Track Cracking	1103		
Raveling	1104	2104	
Random Cracking	1105		
Edge Cracking	1106		
Potholes	1107		
Patching	1108	2108	3108
Surface Deterioration		2109	3109
Popouts			3110
Pumping		2111	3111
Bleeding	1112	2112	
Faulting			3113
Settlements	1114	2114	3114
Joint Spalling			3115
Joint Sealant Damage	1116	2116	3116
Pressure Damage		2117	3117
Corner Breaks			3118
Rutting	1119	2119	
Corrugations	1120	2120	
Shattered Slab		2121	
Unidentified	1000	2000	3000
Debris	1001	2001	3001
Manhole Covers	1002	1003	1004
Shadows	1003	2003	3003
Noise	1004	2004	3004

TABLE 2 PCR DISTRESS DEFINITIONS FOR SEVERITY AND EXTENT WEIGHTS

Dist.	Severity Weights			Extent Weights		
Code	Low	Medium	High	Occas.	Freq.	Extens.
1101	CW<1/8"	1/8"-1"	>1"	PSL<20%	20%-50%	>50%
1102	Single CW<1/8"	Mult. 1/8"-1"	Mult. >1"	PSL<20%	20%-50%	>50%
1103	Single CW<1/8"	Mult. 1/8"-1/4"	Exten. >1/4"	PSL<20%	20%-50%	>50%
1104	Little	Moderate	Severe	PA<20%	20%-50%	>50%
1105	CW<1/8"	1/8"-1"	>1"	PSL<20%	20%-50%	>50%
1106	no break CW<1/4"	some spall. 1/8"-1"	mult. crack. >1"	PSL<20%	20%-50%	>50%
1107	Di<6"or (Di>6"& De<1")	Di>6"& De:1-2"	Di>6"& De>2"	PSL<20%	20%-50%	>50%
1108	Fair ride	Poor ride	Bad ride	PSL<10%	10%-30%	>30%
1112	Noti-ceable	Noti-ceable	Very notic.	PA<10%	10%-30%	>30%
1114	Fair ride	Poor ride	Bad ride	<1/mile	2-4/mi.	>4/mi.
1116				PSL<20%	20%-50%	>50%
1119	De<1/4"	1/4"-1"	>1"	PSL<20%	20%-50%	>50%
1120	Fair ride	Poor ride	Bad ride	PSL<10%	10%-30%	>30%
2101	CW<1/8"	1/8"-1"	>1"	CS>15'	10'-15'	<10'
2102	CW<1/8"	1/8"-1"	>1"	<50'/ST	50'-100'	>100'
2104	Little	Moderate	Severe	PA<20%	20%-50%	>50%
2108	Fair ride	Poor ride	Bad ride	PSL<10%	10%-30%	>30%
2109	De<1"& A<1 yr^2	(De<1"& A>1 yr^2) or (De>1"& A<1yr^2)	De>1"& A>1 yr^2	PSL<20%	20%-50%	>50%
2111	Stains around cracks	Stains around cracks	Fault.	PSL<10%	10%-25%	>25%

(*continued on next page*)

TABLE 2 (*continued*)

Dist.	Severity Weights			Extent Weights		
Code	Low	Medium	High	Occas.	Freq.	Extens.
2112	Noti-ceable	Noti-ceable	Very notic.	PA<10%	10%-30%	>30%
2114	Fair ride	Poor ride	Bad ride	<1/mile	2-4/mi.	>4/mi.
2116				PSL<20%	20%-50%	>50%
2117	De<1/2"	1/2"-1"	>1"	PSL<20%	20%-50%	>50%
2119	De<1/4"	1/4"-1"	>1"	PSL<20%	20%-50%	>50%
2120	Fair ride	Poor ride	Bad ride	PSL<10%	10%-30%	>30%
2121	Fair ride CW<1/8"	Poor ride 1/8"-1"	Bad ride >1"	<2/mile	2-5/mi.	>5/mi.
3101	CW<1/4"	1/4"-1"	>1"	CS>15'	10'-15'	<10'
3102	CW<1/4"	1/4"-1"	>1"	PA<5%	5%-20%	>20%
3108	Light	Moder.	Severe	PA<5%	5%-20%	>20%
3109	De<1/4"	1/4"-3/4"	>3/4"	PA<20%	20%-50%	>50%
3110				PSL<20%	20%-50%	>50%
3111	Stains around cracks	Stains around cracks	Faulting	PSL<10%	10%-25%	>25%
3113	De<1/4"	1/4"-1/2"	>1/2"	PSL<20%	20%-50%	>50%
3114	Fair ride	Poor ride	Bad ride	<1/mile	2-4/mi.	>4/mi.
3115	CW<2""	2"-4"	>4"	PSL<20%	20%-50%	>50%
3116				PSL<20%	20%-50%	>50%
3117				<1/mile	1-3/mi.	>3/mi.
3118	CW<1/4"	1/4"-1"	>1"	<1/mile	1-3/mi.	>3/mi.

Abbreviations:

CW:	Crack width
PSL:	% of occurrence in section length
PA:	% of occurrence in section area
Di:	Diameter
De:	Depth
CS:	Crack spacing
ST:	Station
A:	Area

icant differences in the image segmentation of asphalt concrete and portland cement concrete images and classification approaches were found from this work.

Thresholding techniques based on either one- or two-dimensional histograms applied to asphalt concrete pavement image segmentation are not adequate. An asphalt concrete pavement image is composed of mineral aggregate with a wide range of gray tones embedded in a bituminous mixture with dark gray intensity. Moreover, the image displays a gradual change in darkness along the transverse direction because of stains and rubber tire marks. Consequently, the foreground and background can have similar gray tones, and a threshold value is unable to separate the foreground from the background pixels.

Edge detector methods in asphalt concrete pavement image segmentation do not reproduce a fair distress border or an accurate segmentation because the perimeter of the defects in discontinuous and the aggregate particles can be mixed up with the actual distress types.

The VRS method (*2,3*) constitutes an adequate and accurate technique in asphalt concrete pavement image analysis. The connective zone considerably improves the image segmentation results, and the analysis of separate vertical zones takes into account the influence of the gradual change in darkness along the transverse direction. Although the method was implemented mainly for asphalt concrete pavement images, it can successfully be used for portland cement concrete pavement images.

The accuracy achieved with the rule-based classification approach is close to 90 percent, and the misclassifications result from objects with features similar to the groups analyzed. They can be identified by taking into account more parameters in the decision rules implemented in the classification procedure.

The results obtained with the initial implementation of the low-cost system for video image pavement distress recording and analysis proved that an accurate and reliable quantitative measurement of the pavement condition can be calculated. Furthermore, the system eliminates the subjectivity inherent in manual pavement distress analysis.

Distress classification including severity and extent level is currently limited to distress types that can be quantified by width, length, geometry, or area covered by the distress. The system is designed to consider distress types requiring depth measurements once proper measuring techniques are developed.

ACKNOWLEDGMENTS

This paper is based on research sponsored by the Ohio Department of Transportation (ODOT) under Grant OD-5945. The authors gratefully acknowledge the assistance of William F. Edwards and the engineers from the Research and Development Division at ODOT.

REFERENCES

1. J. Baker, B. Dahlstrom, K. Longenecker, and T. Buu. Video Image Distress Analysis Technique for Idaho Transportation Department Pavement Management System. In *Transportation Research Record 1117*, TRB, National Research Council, Washington, D.C., 1987.
2. J. A. Acosta. *Implementation of the Video Image Processing Technique for Evaluating Pavement Surface Distress*, M.S. thesis. Case Western Reserve University, Cleveland, Ohio, 1991.
3. J. A. Acosta, R. L. Mullen, and J. L. Figueroa. Automatic Surface Distress Identification in Asphalt Concrete Pavements Using the Vertical Region Segmentation Technique. *Journal of Transportation*, ASCE (in preparation).
4. K. Majidzadeh and M. S. Luther. *Development and Implementation of a System for Evaluation and Maintenance and Repair Needs and Priorities—Volume 2*. Report FHWA/OH-80/003. Resource International, Inc.; Ohio Department of Transportation, Columbus, 1980.
5. C. K. Chow, S. K. Hilal, and K. E. Niebuhr. X-Ray Image Subtraction by Digital Means. *Journal of Research and Development*, IBM, Vol. 17, 1973, pp. 206–218.
6. S. Inoue. Video Image Processing Greatly Enhances Contrast, Quality, and Speed in Polarization-Based Microscopy. *Journal of Cell Biology*, Vol. 89, 1981, pp. 346–356.
7. H. C. Andrews and B. R. Hunt. *Digital Image Restoration*. Prentice Hall, Englewood Cliffs, N.J., 1977.
8. T. S. Hung. *Picture Processing and Digital Filtering*. Springer-Verlag, Berlin, Germany, 1979.
9. W. K. Pratt. *Digital Image Processing*. John Wiley & Sons, New York, N.Y., 1978.
10. A. V. Oppenhiem. *Application of Digital Signal Processing*. Prentice Hall, Englewood Cliffs, N.J., 1978.
11. *IMAGER-AT Reference Manual*. Matrox Electronic Systems Ltd., Dorval, Quebec, Canada, 1987.
12. T. F. Knoll and E. J. Delp. Adaptive Gray Scale Mapping to Reduce Registration Noise in Difference Images. *Computer Vision, Graphics, and Image Processing*, Vol. 33, 1986, pp. 129–137.
13. B. K. Ghaffary. Image Matching Algorithms. *Digital Image Processing*, Society of Photo-Optical Instrumentation Engineers Volume 528, 1985, pp. 14–22.
14. A. Rosenfeld. Expert Vision Systems: Some Issues. *Computer Vision, Graphics, and Image Processing*, Vol. 34, 1986, pp. 99–117.
15. P. Suetens and A. Oosterlinck. Critical Review of Visual Inspection. *Digital Image Processing*, Society of Photo-Optical Instrumentation Engineers Volume 528, 1985, pp. 240–252.
16. T. Fukuhara et al. Automatic Pavement Distress Survey System. *Proc., 1st International Conference on Applications of Advanced Technology in Transportation Engineering*, ASCE, San Diego, Calif., 1989.
17. R. Kasturi and J. F. Walkup. Nonlinear Image Restoration. *Digital Image Processing*, Society of Photo-Optical Instrumentation Engineers Volume 528, 1985, pp. 43–60.
18. T. T. Victor. Adaptive Filter Techniques for Digital Image Enhancement, *Digital Image Processing*, Society of Photo-Optical Instrumentation Engineers Volume 528, 1985, pp. 29–42.
19. R. Hummel. Image Enhancement by Histogram Transformation. *Computer Vision, Graphics, and Image Processing*, Vol. 6, 1977.
20. I. Pitas and A. N. Venetsanopoulos. Nonlinear Order Statistic Filters for Image Filtering and Edge Detection. *Signal Processing*, Vol. 10, 1986, pp. 395–413.
21. J. Serra. *Image Analysis and Mathematical Morphology*. Academic Press, New York, N.Y., 1982.
22. M. J. Braun, N. Ida, C. Batur, B. Rose, R. C. Hendricks, and R. L. Mullen. A Non-Invasive Laser Based Method in Flow Visualization and Evaluation in Bearings. *Proc., International Conference in Tribology Friction, Lubrication and Wear Fifty Years On*. Institution of Mechanical Engineers, London, England, 1987.
23. S. G. Ritchie. Digital Imaging Concepts and Applications in Pavement Management. *Journal of Transportation Engineering*, ASCE, Vol. 116, No. 3, 1990, pp. 287–298.
24. A. S. Abutaleb. Automatic Thresholding of Gray-Level Pictures Using Two-Dimensional Entropy. *Computer Vision, Graphics, and Image Processing*, Vol. 47, 1989, pp. 22–32.
25. M. James. *Pattern Recognition*. John Wiley & Sons, New York, N.Y., 1988.

Publication of this paper sponsored by Committee on Pavement Monitoring, Evaluation, and Data Storage.